ASSESSMENT OF THE PERFORMANCE OF CALCINED CLAY AS A PARTIAL REPLACEMENT FOR CEMENT IN RAMMED EARTH FLOOR

KYUNGU WA N'SIMBA YANNICK

MASTER OF SCIENCE

(Environmental Engineering and Management)

JOMO KENYATTA UNIVERSITY

OF

AGRICULTURE AND TECHNOLOGY

2024

Assessment of the Performance of Calcined Clay as a Partial Replacement for Cement in Rammed Earth Floor

Kyungu Wa N'simba Yannick

A Thesis Submitted in Partial Fulfilment of the Requirements for the Degree of Master of Science in Environmental Engineering and Management of the Jomo Kenyatta University of Agriculture and Technology

2024

DECLARATION

This thesis is my original work and has not been presented for a degree in any other university.

Signature……………………………………… Date…………………………

Kyungu Wa N'simba Yannick

This thesis has been submitted for examination with our approval as University Supervisors.

Signature…………………………………….. Date……………………………

Prof. James Wambua Kaluli, PhD

JKUAT, Kenya

Signature…………………………… Date………………………………………

Dr. Hosea Munge Mwangi, PhD

JKUAT, Kenya

Signature…………………………… Date………………………………………

Prof. Benson Muchoki Mwangi, PhD

Murang'a University of Technology

DEDICATION

I dedicate this work to my father, N'simba Ngoie Georges, and my mother, N'sangu Zambote Maguy. You have held me on your shoulders so I could reach this far. I bless God daily for your presence in my life. I hope you find in these words an expression of my gratitude.

ACKNOWLEDGEMENT

First and foremost, I give thanks to the Almighty God for the life, good health, and provision which were crucial in completing this research. I sincerely thank my supervisors: Prof. James W. Kaluli, Dr. Hosea M. Mwangi, and Prof. Benson M. Mwangi who guided and supported me throughout the course of this research period. The completion of this research would have not been possible without your help. I am also very grateful to the lecturers in the School of Biosystems and Environmental Engineering for their inputs during the progress report presentations.

Further, I extend my thanks to the staff members, technicians and technologists of the departments of Horticulture, Civil Engineering, and Soil, Water and Environmental Engineering (SWEED) for their assistance during this research period. Specifically, Ms. Rose Nyaboke and Mr. Patrick Amaheno from the Horticulture Laboratory (JKUAT), and Mr. Wickliffe Juma from the soil laboratory (JKUAT) whose assistance helped me conduct my lab activities very smoothly. I also appreciate the support provided by my parents and my siblings (Landry, Jocelyne, Vincent, Kevin, Georges, Rebecca, and Emmanuella N'simba). Thanks to my friends for the laughter and wonderful moments we shared together. Special thanks to Blessing Lengwe for his technical assistance during this research period. Thanks to my colleagues at JKUAT. It was such a pleasure working together with such a group of ambitious and smart people. More importantly, I am grateful to my fiancé and wife-to-be, Kayumba Tegra. Your presence in my life has been a constant source of motivation and inspiration.

TABLE OF CONTENTS

LIST OF TABLES

LIST OF FIGURES

LIST OF APPENDICES

ACRONYMS AND ABBREVIATIONS

Al_2O_3	Alumina
ANOVA	Analysis of Variance
ASTM	American Society for Testing and Materials
BCONTENT	Binder Content
$Ca(OH)_2$	Calcium hydroxide
C-A-H	Calcium-Aluminate-Hydrate
CaO	Calcium Oxide
[CaO]	Concentration in calcium oxide
CaO Th.	Initial Concentration in Calcium Hydroxide
CO_2	Carbon Dioxide
C-S-H	Calcium Silicate Hydrate
CSRE	Cement Stabilized Rammed Earth
CSRE	Cement Stabilized Rammed Earth
CTIME	Curing Time
EC	Electrical Conductivity
EDGE	Excellence in Design for Greater Efficiencies
EDTA	Ethylenediaminetetraacetic Acid
FA	Fly Ash
FAO	Food and Agriculture Organization of the United Nations
Fe_2O_3	Ferric Oxide
GHG	Green House Gases
IISA	International Institute for Applied Systems Analysis
IPCC	the Intergovernmental Panel on Climate Change
K_2O	Potassium Oxide
LL	Liquid Limit
LOI	Loss on Ignition
LS	Linear Shrinkage
MDD	Maximum Dry Density
MgO	Magnesium Oxide
MICP	Microbially Induced Calcium Carbonate Precipitation

MK	Metakaolin
MKG	Metakaolin-Based Geopolymer
$Na_4P_2O_7.10H_2O$	Tetrasodium Pyrophosphate Decahydrate
[OH-]	Concentration in Ion hydroxide
OMC	Organic Matter Content
OPC	Ordinary Portland cement
PI	Plasticity Index
PL	Plastic Limit
RE	Rammed Earth
RRATE	Cement Replacement Rate
SAI	Strength Activity Index
SCM	Supplementary Cementitious Materials
SiO_2	Silicon Dioxide
SO_3	Sulphur Trioxide
STYPE	Soil Type
TiO_2	Titanium Dioxide
UCS	Unconfined Compressive Strength
USCS	Unified Soil Classification System
USDA	United States Department of Agriculture
XRF	X-Ray Fluorescence

ABSTRACT

Excessive dependence on cement for the stabilization of rammed earth in construction degrades the environment. Therefore, sustainable and easily available alternatives are needed. The aim of this study was to assess the performance of calcined clay as a partial replacement for cement in rammed earth floor construction for low-income housing. The pozzolanic activity of clay collected from selected wetlands in three sub-counties of Murang'a County, Kenya, (Kahuro, Kiharu and Maragua Sub-Counties) was analysed after thermal activation. Thermal treatment (calcination) was carried out in an electronic muffle furnace at 600, 700, and 800°C for a duration of 2 hours. Three methods (electrical conductivity (EC), Frattini test, and strength activity index (SAI)) were used to assess the pozzolanic activity of clay. Two soils were stabilized: murrum soil and black cotton soil. Each soil was stabilized by mixing it with a binder in accordance with BS 1377. The binder consisted of Portland cement and calcined clay mixed at various proportions. A decrease in the electrical conductivity of the lime-clay solution was observed over a 24-hour period. Results of the Frattini test showed that clay calcined at 600°C and 700°C reacted with Ordinary Portland Cement (OPC) - CEM-I and reduced CaO and OH^- concentrations to levels below the solubility curve of $Ca(OH)_2$. Calcination of clay from Kahuro and Maragua sub-counties, at 600°C and 800°C, respectively, increased the strength activity index of cement blocks from less than 0.75 to about 1 after 28 days. The temperature range of 600-800°C was considered effective for clay calcination and provided sufficient pozzolanic activity (EC reduction > 0.12 S/m in the first 2 minutes and SAI > 0.75). For general construction, the KS02-1070:1993 standard requires a minimum compressive strength of 2.5 MPa after 28 days. This performance was achieved with murrum soil stabilized with a binder content in the range of 10-15% and 25% cement replacement with calcined clay. For stabilized rammed murrum, cement replacement with 25% calcined clay did not lead to a substantial increase in capillary water absorption after 24 hours of contact with water (0.15 and 0.11 kg water/kg soil block for a binder content of 10% and 15%, respectively). On the other hand, a replacement beyond 25% presented undesirable water absorption. Moreover, stabilized black cotton soil presented excessive water absorption of 0.28 kg water/kg soil block (10% cement content). It was not possible to stabilize black cotton soil sufficiently to achieve the required compressive strength. With a 25% cement replacement with calcined clay, Murrum soil was sufficiently stabilized as long as the binder content was in the range of 10-15%. Thus, a blend of calcined clay and Portland cement can provide an adequate mix for use in rammed earth floor construction.

CHAPTER ONE

INTRODUCTION

1.1. Background Information

The ancient earth building technique known as rammed earth construction produces dense, load-bearing structures by dynamically compacting moist sub-soil between removable shuttering to create a monolithic on-site construction which is both strong and durable (Hall & Djerbib, 2006; Naeini et al., 2021). This building approach has been traditionally used in the construction of walls, floors, and roofs for thousands of years (Suresh & Anand, 2017). It is reported that a third of the world's population is still living in earthen buildings (Arooz & Halwatura, 2018). There has been, in the last decades, increasing interest in rammed earth construction as a sustainable construction approach (Indekeu et al., 2021; Thuysbaert, 2012; Walker et al., 2005). This building approach is endowed with advantages such as low-manufacturing impact, low-embodied energy, and natural beauty (Fernandes et al., 2019; Naeini et al., 2021; Suresh & Anand, 2017). In rammed earth construction, soil stabilization is done to improve soil strength and water resistance (Suresh & Anand, 2017). According to KS 02:1070:1993 standards, the required minimum compressive strength for stabilized soil after 28 days of curing is 2.5 MPa for general construction. Among the binders used, cement has been found to be effective. However, due to its increasing cost and environmental pollution, stabilization with cement alone is less preferred (Al-Swaidani et al., 2016).

Use of ordinary Portland cement (OPC) becomes unsustainable in the sense that the cement industry consumes approximately 7% of the global energy consumption each year (Cantini et al., 2021). Moreover, it is reported that cement production is responsible for the emission of approximately 5-8% of carbon dioxide (CO_2) (Marangu, 2020). It also contributes to the emissions of sulphur dioxide, nitrogen oxide, carbon monoxide and composition of lead, being responsible for the emission of 30% to 40% of these gases (Leitãoa et al., 2017; Marangu, 2020; Vignesh et al., 2020). It has been reported that cement stabilization of soil also increases the embodied energy of earthen buildings (Gomes et al., 2016). A study by Henry et al. (2014) reported that a cement block house expends at least 1.5 times more embodied energy and emits at least 1.7 times more embodied CO_2 than an earth or mud brick house in Cameroon. A comparative study conducted by Akbarnezhad and Xiao (2017) demonstrated that the embodied energy of a CSRE building (1.15 GJ/m2) was in the range of one third of a load bearing brickwork masonry building (3-4 GJ/m2) and less than one fourth of a reinforced concrete framework building (4-10 GJ/m2) with brick masonry. As a result, it is suggested that use of CSRE would cut back on carbon emission and embodied energy compared to conventional concrete (Adegun & Adedeji, 2017).

Due to the construction related carbon emissions, various high quality reactive pozzolana such as silica fume, fly ash (Bui et al., 2018), ground granulated blast furnace slag, bagasse ash, industrial by-products (Bumanis et al., 2020), and rice husk ash have been introduced as supplementary cementitious materials (SCMs) and are being used completely (Abdullah et al., 2012). Nevertheless, there is a shift in interest to search for alternative SCM sources due to supply-and-demand concerns in the future. One of the most promising alternative sources is clay. This material is abundant and widespread, which can lower the transportation cost, promote local acquisition of raw materials, and local production of calcined clay (Adegun & Adedeji, 2017; Amin, 2015; Hollanders et al., 2016). Furthermore, Zhou et al. (2017) reported that production of calcined clay consumed less energy than the production of cement clinker, and lowers carbon emissions due to an absence of carbonation stage during calcination. However, there is still limited research on the use of calcined clay, particularly sourced from wetlands, as a replacement of Portland cement in rammed earth floor construction. Therefore, this study aimed to assess the effect of calcined clay as a replacement for cement on the strength and water resistance properties of stabilized rammed earth for floor construction.

1.2. Problem Statement

Excessive dependence on cement for the stabilization of rammed earth in construction degrades the environment (Tironi et al., 2013). In Kenya for instance, Portland cement remains the most used binder for construction works. This material is made by inter-grinding calcareous and argillaceous materials that are then clinkered in a rotary furnace at a temperature exceeding 1300°C, fuelled by petroleum oil or coal (Nalobile et al., 2019). Its production results in emissions of approximately 866 kg CO_2/t of clinker (Hollanders et al., 2016). Furthermore, cement produced and consumed globally equals 4.2 billion tonnes per year (Faleschini et al., 2021). This makes the cement industry account for 5-8% of global anthropogenic CO_2 emissions, thus majorly responsible for global warming and climate change (Marangu, 2020). As a result, the resultant Portland cement is unsustainable.

In Kenya, counties such as Murang'a reported that around 60% of housing units have earthen floors (Murang'a County, 2018). For quality housing, rammed earth stabilization using cement is recommended as an effective flooring technology. However, environmental sustainability of the same remains a constraint. Several studies reported that use of calcined clay as a replacement for cement could reduce the carbon footprint associated with reliance on cement alone (Amin et al., 2015; Ciancio et al., 2013; Hollanders et al., 2016). Therefore, the purpose of this study was to characterize clay materials for potential application as supplementary cementitious materials. It also intended to determine the feasibility of using calcined clay as a partial replacement for cement in rammed earth floor construction.

1.3. Objectives

1.3.1. General Objective

To assess the performance of calcined clay as a partial replacement for cement in rammed earth floors.

1.3.2. Specific Objectives

- To determine the chemical and pozzolanic characteristics of calcined clay for potential application as an alternative material to cement.
- To evaluate the effect of calcined clay as a replacement for cement on the strength and water absorption of rammed earth for floor construction.

1.4. Research Questions

- What are the characteristics of calcined clay?
- What is the effect of cement replacement with calcined clay on the strength and water absorption of rammed earth for floor construction?

1.5. Justification of the Study

Several studies reported that clay minerals are widespread and easily available which lowers the cost associated with their transportation (Amin et al., 2015; Hollanders et al., 2016). In addition to reducing the significant carbon dioxide emissions from cement production, integration of calcined clay in concretes present acceptable mechanical properties and durability (Hollanders et al., 2016; Schulze & Rickert, 2019; Syagga et al., 2001; Tironi et al., 2013). This could reduce the reliance on cement alone, offering a sustainable alternative material for low-income housing. On the other hand, earthen floors are non-hygienic and can harbour harmful parasites, causing serious health conditions such as Tungiasis (Benjamin-Chung et al., 2021; Mwangi et al., 2015; Wambani, 2017; Wambani et al., 2018). Hence, this study aimed to assess the performance of calcined clay in changing the engineering properties of soil, with the ultimate goal of developing a strong and water-resistant rammed earth floor.

1.6. Scope and Limitations

1.6.1. Scope

The study evaluated the effectiveness of calcined clay in changing the engineering properties of natural soils for the development of a strong and water-resistant earthen floor. Stabilization tests were conducted on coarse-grained (murrum soil) and fine-grained soils (black cotton soil). Clay for calcination was sampled in wetlands of 3 sub-counties of Murang'a County. Research activities covered field work for soil sampling. Laboratory tests were conducted for the characterization of soils, evaluation of the pozzolanic activity of calcined clay and soil stabilization experiments. Field and laboratory activities, from soil sampling to statistical analysis covered a period of 12 months from March 2022 to March 2023.

1.6.2. Limitations

For economic reasons, the clay material was thermally and mechanically activated. This process relies on mechanical effort and thermal energy for particle size reduction and activation, respectively. It does not involve the use of chemicals which can be costly. This study did not cover field trial of constructed rammed earth floor, cost analysis and monitoring of its durability on the field.

CHAPTER TWO

LITERATURE REVIEW

2.1. Overview of Rammed Earth Construction

Various sources estimate that building with earth began between approximately 10,000 years ago by early agricultural societies (Burroughs, 2008; Thompson et al., 2022). It is reported that the first houses in the world were built in an improvised way by applying earth materials found in the immediate surroundings or obtained by digging basements, wells, or watering pits for cattle (Peric et al., 2021). Over the years, earth building approach has been successfully used to construct walls, floors, and roofs of advanced architectural design (Araujo et al., 2015; Makinde, 2012). To date, It is reported that a third of the world's population is still living in earthen buildings (Arooz & Halwatura, 2018). A study (Morel & Charef, 2019) reported that earth building techniques could be subdivided in blocks implemented with a mortar to build masonry structures (compressed earth blocks, cob or adobes) (Fernandes et al., 2019; Salim et al., 2014), and earth implemented in monolithic walls called rammed earth (Arrigoni et al., 2017; Indekeu et al., 2021; Marais et al., 2015; Thuysbaert, 2012). These techniques are also subdivided in dry manufacture process where the earth is compacted, and wet manufacture process where the earth is moulded or extruded or stacked. It is considered that rammed earth construction is one of the most important earth-building techniques both in traditional and modern earth architecture (Peric et al., 2021).

Building with rammed earth consists of pouring moistened soil in layers inside a wooden or metal formwork and compacting it by using a manual or pneumatic rammer to form walls (Figure 2.1) (Peric et al., 2021; Thompson et al., 2022). It is generally admitted that rammed earth includes clayey soil (usually less than 20% of clay by dry weight of soil) and is generally compacted with a water content varying with soils, but within the range of 8-20% by dry weight of soil ("dry" process). There has been, in the last decades, increasing interest in rammed earth as a sustainable construction material (Leitãoa et al., 2017). This fact is clearly illustrated by undertaken studies on stabilized rammed earth for housing (Arrigoni et al., 2017; Fernandes et al., 2019; Hall & Djerbib, 2004; Hall & Djerbib, 2006; Indekeu et al., 2021; Naeini et al., 2021; Suresh & Anand, 2017; Thuysbaert, 2012; Walker et al., 2005).

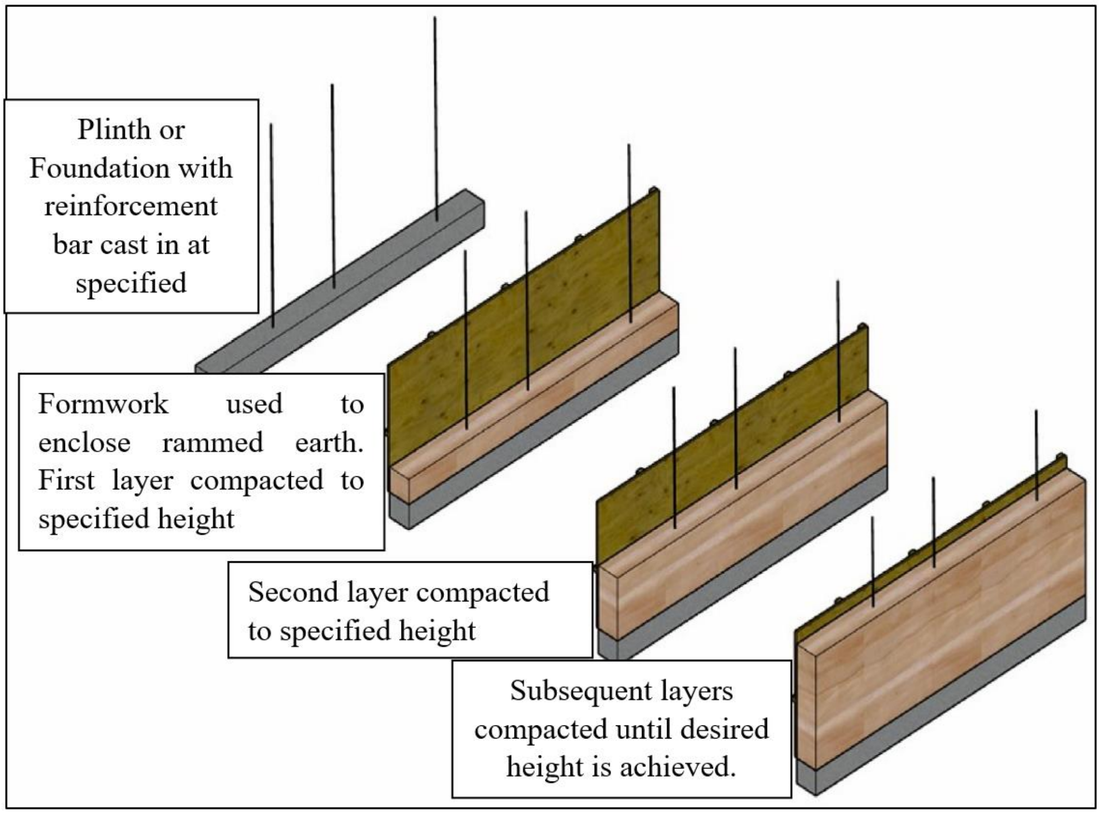

Figure 2.1: Rammed Earth Construction Process

Source: Thompson et al. (2022)

Many of the regions where earthen construction is most prominent include developing or low-income countries (Figure 2.2). In these regions, earthen construction (including rammed earth) is more common due to the ease and simplicity of the building technique, the possibility of sourcing unskilled labour force, reduced transportation and construction costs (Ciancio et al., 2013). In developed countries, on the other hand, rising public awareness concerning sustainable living, combined with better knowledge of thermal benefits, and durability of earth, and the lower energy inputs have brought renewed interest in earth as a green building approach (Burroughs, 2010; Thompson et al., 2022). Various rammed earth building techniques were used across the ancient world, including Europe, China, the Middle East, the Americas, and Africa (Burroughs, 2010; Indekeu et al., 2021; Maniatidis & Walker, 2003; Thompson et al., 2022). Rammed earth constructions can broadly be grouped into two categories: stabilized rammed earth and un-stabilized rammed earth (Reddy et al., 2014). The main shortcoming of un-stabilized rammed earth are low mechanical strength and durability of the final product (Kosarimovahhed & Toufigh, 2020).

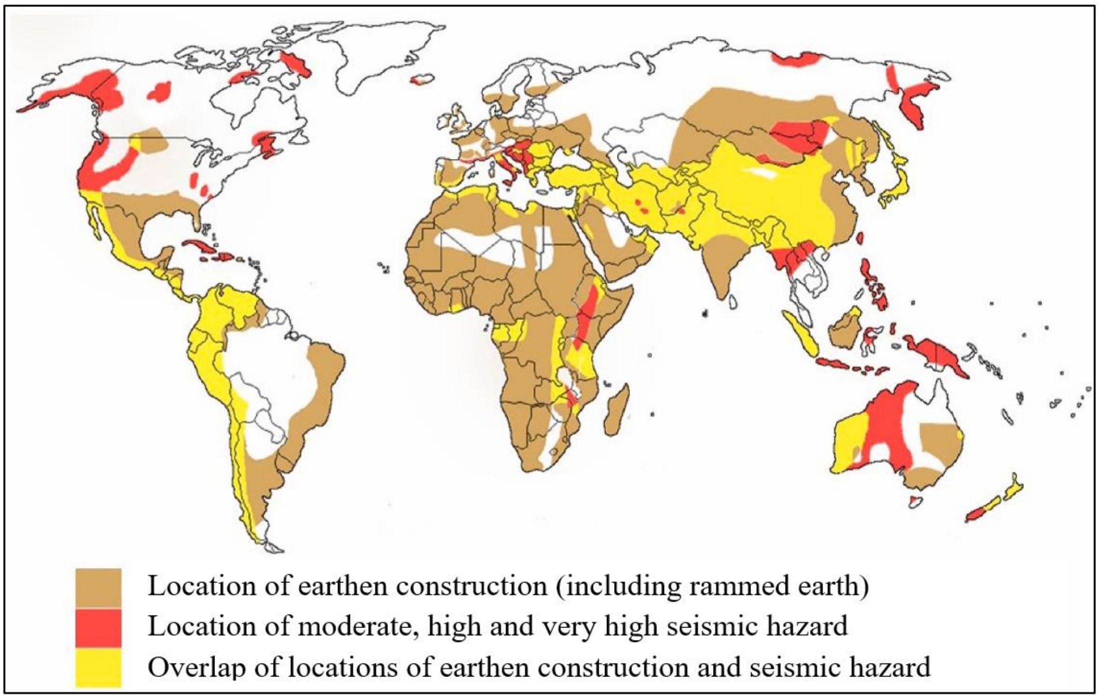

Figure 2.2: Locations of Earthen Construction and Seismic Hazards

Source: Thompson et al. (2022)

2.2. Rammed Earth Stabilization

Problems associated with un-stabilized rammed earth, including strength, permeability, volume stability, and durability can be improved through compaction or the addition of stabilizers in order to meet modern construction standards (Burroughs, 2010; Reddy et al., 2014). Here, the natural soil usually forms at least 85% of the volume of the mix (Kosarimovahhed & Toufigh, 2020). Soil stabilization can be achieved by several methods falling into two broad categories: mechanical and chemical stabilization, or a combination of both. Mechanical stabilization is achieved through a physical process by altering the physical nature of native soil particles by either induced vibration or compaction, or by incorporating other physical properties such as barriers and nailing. Chemical stabilization, on the other hand, depends on chemical reactions between the stabilizer and soil minerals to achieve the desired effect (Makusa, 2012). Soil stabilizers usually fall into two classes: those that materially increase strength and reduce moisture absorption; and those that reduce absorption and moisture movement but do not increase strength (Makusa, 2012; Maniatidis & Walker, 2003). Several studies have documented the effects of lime and cement on rammed earth stabilization (Al-Swaidani et al., 2019; Amiralian et al., 2012; Bagheri et al., 2014; Bryan, 1988; Gomes et al., 2016; Ikeagwuani et al., 2019; Muthakia et al., 2005;

Singh & Garg, 2006). In particular, cement stabilization has gained popularity due to higher and faster strength gain, durability, and ability to obtain acceptable properties with low cement content, especially with laterite soils (Kariyawasam & Jayasinghe, 2016).

2.2.1. Mechanism of Rammed Earth Cement Stabilization

Cement is the oldest binding agent since the invention of soil stabilization technology in 1915. It may be considered as a primary stabilizing agent or hydraulic binder because it can be used alone to bring about the stabilizing action required. Cement reaction is not dependent on soil minerals. Its reaction occurs with water that may be available in any soil. This is the reason why cement is used to stabilize a wide range of soils (Makusa, 2012). When water is mixed with cement, hydration occurs, meaning cementing compounds of calcium-silicate-hydrate (C-S-H) and calcium-aluminate-hydrate (C-A-H) are formed and excess calcium hydroxide ($Ca(OH)_2$) is released, approximately 31% by weight (Hamzah et al., 2015). Formation of C-S-H and C-A-H occurs when crystals begin forming a few hours after the water and cement are mixed; crystals will continue to form as long as unreacted cement particles and free water remain within the mixture (Firoozi et al., 2017). These hydration reactions are slow and proceed from the surface of the cement grains. In some occurrences, the centre of the grains may remain un-hydrated. The mechanisms of stabilization that utilize cement, lime, or fly ash were summarized as follows (Firoozi et al., 2017; Little, 1999):

- Cation exchange: sodium, magnesium, and other cations are replaced by the calcium cations from the available calcium hydroxide.
- Flocculation and agglomeration: flocculation of the clay particles increases the effective grain size and reduces plasticity, thus increasing the strength of the matrix.
- Pozzolanic reaction: the high pH environment created by the available calcium hydroxide solubilizes silicates and aluminates at the clay surface, which in turn react with calcium ions to form cementitious products that are composed primarily of calcium silicate hydrates or calcium aluminate hydrates, or both.
- Carbonate cementation: calcium oxide reacts with carbon dioxide from the atmosphere to form calcium carbonate precipitates, which cement the soil particles.

The chemical reactions during the hydration process include, but are not limited to, some of all the reactions listed below (Firoozi et al., 2017):

- $2\,C_2S + 6H_2O \rightarrow C_3S_2H_3 + 3Ca(OH)_2$ [2.1]
- $2C_2S + 4H_2O \rightarrow C_3S_2H_3 + Ca(OH)_2$ [2.2]
- $C_3A + 3(CaSO_4 2H_2O) \rightarrow 26H_2O \rightarrow C_3A.3CaSO_4.32H_2O$ [2.3]
- $2C_3A + C_3ACaSO_4 32H_2O \rightarrow 2[C_3ACaSO_4 12H_2O]$ [2.4]
- $C_3S + Ca(OH)_2 + 12H_2O \rightarrow C_3ACa(OH)_2 12H_2O$ [2.5]
- $C_4AF + 3(CaSO_4 2H_2O) + 27H_2O \rightarrow C_3(AF)3CaSO_4 32H_2O + Ca(OH)_2$ [2.6]
- $2C_4AF + C_3(AF)3CaSO_4 32H_2O + 6H_2O \rightarrow 3[C_3(AF)CaSO_4 12H_2O] + 2Ca(OH)_2$ [2.7]
- $C_4AF + 10H_2O + 2Ca(OH)_2 \rightarrow C_3AH_6 - C_3FH_6$ (Solid solution) [2.8]

There are many factors contributing to strength gain in soil-cement samples. These include ambient air temperature, relative humidity, type of cement used, cement content, impurities or foreign matters, water-to-cement ratio, presence of additives, and specific surface of the mixture. It is generally reported that faster wind speed, higher air temperature, lower relative humidity and longer delay in compaction commonly result in poor strength (Firoozi et al., 2017; Makusa, 2012).

Previous studies reported that cement reduces the plasticity of clay soils (Afrin, 2017). A review by Firoozi et al. (2017) indicated that cement treatment slightly increases the maximum dry density of sand and highly plastic clays but decreases the maximum dry density of silt. In contrast, cement increases the optimum water content and decreases the maximum dry density of sandy soils. Because of hardening of cement, shear strength and bearing capacity are also increased (Afrin, 2017). Cement stabilization increases plastic limit and reduces liquid limit, which mainly reduces the plasticity index (Firoozi et al., 2017). The other significant effects of soil-cement stabilization include reduction in shrinkage and swell potential, increase in strength, elastic modulus, resistance against the effect of moisture, freeze and thaw, and improvement in durability (Bagheri et al., 2014; Bryan, 1988; Firoozi et al., 2017; Kumar et al., 2015; Turkoz & Vural, 2013).

2.2.2. Stabilizing Agents

Cement is the most used stabilizer in rammed earth construction. However, cement increases the embodied energy of the final product. A possible solution to this problem is the replacement of an entire or a portion of cement with a sustainable stabilizer (Kosarimovahhed & Toufigh, 2020). A number of stabilizers such as fly ash (Amiralian et al., 2012; Kosarimovahhed & Toufigh, 2020; Kristiawan et al., 2017), blast furnace slags, silica fume (Khan & Khan, 2017; Oluremi et al., 2021), cow dung ash (Kumar et al., 2015; Ojedokun et al., 2014; Ramachandran et al., 2018; Venkatasubramanian et al., 2017), industrial by-products (Bumanis et al., 2020; Nalobile et al., 2019), polymer fibres, sugarcane bagasse ash, glass powder, rice husk ash, and Metakaolin (MK)(Donatello et al., 2010; Mehsas et al., 2021; Shihembetsa & Sabuni, 2002; Syagga et al., 2001) have attracted interests as non-conventional stabilizing materials (Bagheri et al., 2014; Dou et al., 2016; Krishna et al., 2016). These pozzolanic materials contain high proportions of silicon dioxide (SiO_2). SiO_2 is known to react with free lime released during the hydration of cement and form additional calcium silicate hydrate (C-S-H). The new hydration products are responsible for the development of the mechanical properties in rammed earth, mortars and concretes (Ganesan et al., 2007).

According to ASTM C125, a pozzolanic material is referred to as a siliceous and aluminous material which, in itself, possesses little to no cementitious value, but will, in a finely divided form and in the presence of moisture, chemically react with $Ca(OH)_2$ at ordinary temperatures to generate compounds possessing cementitious properties (Abdullah et al., 2012; Faleschini et al., 2021). The amount of pozzolanic material replacing cement varies from 5 to 40% wt.% of cement (Amin et al., 2015; Bumanis et al., 2020; Donatello et al., 2010; Jurić et al., 2020; Tironi et al., 2013). Pozzolanic materials mentioned above have been introduced as supplementary cementitious materials (SCMs) and are being used completely. Nevertheless, there is a shift in interest to search for alternative SCM sources due to supply-and-demand concerns in the future. One of the most promising alternative sources are calcined clays. These materials have not yet reached their full potential as cement replacement. Moreover, clay is abundant and widespread which can lower transportation cost (Amin et al., 2015; Hollanders et al., 2016).

2.2.3. Compressive Strength and Water Resistance Properties of Stabilized Rammed Earth

Rammed earth, as any other form of earth construction, has relatively good strength in compression but generally poor strength in shear and tension, especially when moist. Maniatidis and Walker (2003) reported that the compressive strength of a soil is very much dependent on the voids of the soil after ramming, cohesive strength of fines, aggregate strength, density of the soil and moisture condition during testing. It is generally reported that increasing cement content leads to an increase in compressive strength (Houben & Guillaud, 2008; Maniatidis & Walker, 2003). A study (Atzeni et al., 2008) reported that the use of Portland cement, hydrated lime and polymers could increase the compressive strength from 0.9 MPa (unstabilized sample) to 5.1 MPa (after stabilization). The authors noted that the same value (0.9 MPa) was improved to 4.5 MPa with an addition of 10% of cement and up to 6.5 MPa by adding 20% of cement (Bahar et al., 2004).

Several studies have been conducted on the mechanical properties of earth materials stabilized with alternative cementitious materials. Using fly ash (alkaline activated) as a replacement for cement, Kosarimovahhed and Toufigh (2020) found that a mix design including 2.5% cement and 5.0% of fly ash showed 112.9% increase in compressive strength, compared to the mix with 7.5% of cement alone. This suggested that, in appropriate dosages, fly ash could be a more effective stabilizer than cement. In contrast, a study conducted by Porter et al. (2018) explored the multifunctional performance of rammed earth blocks using crumb rubber as an addition to cement. It was indicated that stabilization with 6% cement using increasing amounts of crumb rubber (5%, 10% and 20%) corresponded to a decrease in strength. A study by Losini et al. (2022) attempted to replace cement with waste and recycled biopolymers for rammed earth applications. Results showed that the use of lignin sulfonate and tannin could increase the unconfined compressive strength (UCS) value by 38% and 13%, respectively to control samples. This suggested that alternative cementitious materials such as Lignin sulfonate could enhance earth block strength due to the higher density and reduced macro-porosity achieved after stabilization.

In Papua New Guinea for instance, raw earth was stabilized with local materials such as volcanic ash, finely ground natural lime, cement and their various combinations. The results reported a compressive strength in the range of 0.39 MPa to 3.1 MPa (Houben & Guillaud, 2008). On the other hand, it was reported that earth material stabilized with 15% Metakaolin could achieve a compressive strength >3 MPa (Thiviya et al., 2020). Similarly, Dabakuyo et al. (2022) investigated the performance of compressed earth blocks stabilized with a combination of Metakaolin-based Geopolymer (MKG) and sugarcane molasses (SM). Results showed that a combination of 5% MKG + 4% SM achieved a compressive strength of 4.163 MPa at 28 days. However, further increase in SM beyond 4% decreased the compressive strength. This suggested that the combination of cementitious materials such as MKG and SM could reduce the porosity, making stabilized blocks more compact and denser, thus having a higher strength.

Water absorption has an important influence on the durability of cement-based materials and its value is closely related to pore structure (Zhao et al., 2019). It is reported that water is the main cause of concrete physical and chemical deterioration, as it is the carrier of corrosive ions. Moreover, certain rammed earth materials are typically unstable as they liquefy and expand upon contact with water. Indekeu et al. (2021) reported that the capillary absorption pattern of rammed earth materials is typically ideal, showing a linear relation between the accumulated moisture and the square root of time in the first stage of the capillary absorption process. The capillary absorption coefficient of rammed earth ranged from about 0.2 to 0.4 $kg/(m^2s^{0.5})$. A study by Wang et al. (2022) found that a 30% to 40% rate of cement replacement with fly ash could decrease the water absorption of cement-based materials by 27.8% and 14.2%, respectively, compared to specimens stabilized with cement alone. This was attributed to an improvement in the microstructure and increase in the density of the pore structure when an appropriate dosage of fly ash was added. Similar values were reported by Hall and Djerbib (2006), who showed that the optimum level of binder content (cement) for moisture ingress performance appeared to be around 6% for very good and good soils, and 9% for poor soils. Similarly, Porter et al. (2018) also reported that rammed earth stabilization using 6% cement could achieve 20% lower water absorption than unstabilized samples.

2.3. Clay Material as a Replacement for Cement

2.3.1. Properties of Clay Minerals

Natural pozzolans such as raw clays are widely available and constitute a very promising source of supplementary cementitious materials to substitute cement in the construction industry for a more sustainable future (Danner et al., 2018). Clay minerals, specifically "planar hydrous phyllosilicates", are composed of repeated tetrahedral (T) and octahedral (O) two-dimensional sheets. The T-sheet is commonly occupied by corner-sharing tetrahedral cations by edge-sharing octahedral cations such as Al^{3+}, Mg^{3+}, Fe^{3+}, and Fe^{2+} arranged in a pseudo-hexagonal symmetry. Alumina (Al_2O_3) and silica (SiO_2) are the principal constituents in most naturally occurring clay minerals, which makes them potential candidates for cement replacement (Garg & Skibsted, 2014). Clays usually have a fixed lattice structure in their original state where the aluminate and silicate sites have minimal reactivity. While clay minerals such as Kaolin, Smectite, and Illite may sometimes exhibit pozzolanic activity in their raw state, it is well-known that thermal treatment can induce disorder in their structure and potentially lead to enhanced reactivity (Jaskulski et al., 2020).

2.3.2. Clay Calcination and Mechanism of Thermal Activation

Raw clays usually have a moderate or low pozzolanic activity. To increase it, there is need for activation (Jaskulski et al., 2020). Thermal activation involves the intervention of a temperature high enough to destroy the structure of the clay minerals. This produces a state of structural disorder that is a metastable state (Tole et al., 2019). As a result, clay minerals undergo processes of dehydroxylation and amorphization. Dehydroxylation is referred to as the endothermic phenomenon that occurs in some clay minerals (phyllosilicates), when hydroxyl groups disappear, leaving reactive cations of silica and alumina (Yanguatin et al., 2019). The process of dehydroxylation is often accompanied by partial or complete kaolinite transformation, from crystalline to amorphous phase. This is then followed by a change in coordination of Aluminium ions, and their greater reactivity, which is a basic condition for an exhibition of the pozzolanic activity in clay minerals. Similarly, Shvarzman et al. (2003) showed that both the amount and the type of the amorphous phase can influence the activity of additives, which covers the chemical activity (usually pozzolanic activity) and the micro-filler effect. Fernandez et al. (2011) conducted a comparative study on calcined kaolinite, Illite, and montmorillonite using X-ray diffraction (XRD) and nuclear magnetic resonance spectroscopy. It was demonstrated that kaolinite, due to the amount and location of OH groups in the crystal structure of the clay, undergoes a different structural decomposition process than Illite or montmorillonite. It was then suggested that the calcination temperature varies with clay type.

Clay calcination at temperatures between 600°C and 800°C leads to the formation of amorphous phases that react with the compounds in either soil or lime or both to form cementing compounds such as C-S-H and C-A-H (Fernandez et al., 2011). A study by Zhou et al. (2017) reported that the dehydroxylation of kaolinite happened between 350°C and 600°C, while montmorillonite and Illite dehydroxylation took place between 600°C and 950°C. A number of authors have also reported that clays could be transformed into SCMs when they are calcined between 600-900°C (Aramburo et al., 2020; Hollanders et al., 2016; Mehsas et al., 2021; Yanguatin et al., 2019; Zhou et al., 2017). On their other hand, Shvarzman et al. (2003) reported that clay minerals such as Kaolinite achieved relatively low-level of dehydroxylation degree (less than 0.18) at a calcination temperature below 450°C. However, in the range of 570-700°C, the kaolinite was fully dehydroxylated (0.95 to 1.00). It was indicated that their pozzolanic activity depended on the dehydroxylation degree and the available surface for reaction. A study by Garg & Skibsted (2014) also reported that clay minerals such as pure montmorillonite showed optimum reactivity when heated at 800°C, reflecting a high degree of dehydroxylation and the absence of any inert, condensed Q^4 type phases. However, when heating at high temperatures (1000-1100°C), the layer structure of the clay breaks down and forms stable crystalline phases, resulting in a decreased reactivity (Garg & Skibsted, 2014). Nevertheless, raw clays are usually polymineral materials which makes it difficult to find the optimum calcination temperature (Danner et al., 2018).

2.3.3. Effect of the Addition of Calcined Clay on Cement-based Materials

It is reported that the replacement of cement with calcined clay drastically changes the engineering characteristics of concrete and mortars. Singh & Garg (2006) reported that Metakaolin could be used up to 10% as a replacement to ordinary Portland cement in the cement mortars without any reduction in strength, rather compressive strength was improved over the OPC mortars. This was attributed to the increased amount of C_4AH_{13} and CSH (I) that can be responsible for higher strength development in OPC-Metakaolin mortars (90:10). Moreover, the higher reactivity of Metakaolin in OPC mortars was associated with the formation of gehlenite (C_2ASH_8) and the crystalline C_4AH_{13} phase. Similarly, Frıas, Rodriguez, Vegas, & Vigil (2008) reported that thermally activated clay waste (Metakaolin) could replace OPC up to 10% and react with calcium hydroxide, from cement hydration, producing hydrated phases with hydraulic properties. This was also observed with kaolin deposits (Adeniyi et al., 2020; Mehsas et al., 2021), uncalcined termite clay (Otieno et al., 2015), fired rejected clay bricks (Marangu, 2020), burnt clay waste (Shihembetsa & Sabuni, 2002; Syagga et al., 2001), and excavated waste clay (Zhou et al., 2017). The microstructure of the calcined-kaolinite-cement system showed the following features: a dense microstructure, the absence of visible calcium hydroxide clusters and no hydration rings around cement grains suggesting that there has been a strong chemical interaction between the pozzolana and cement from early ages. However, when microstructures of cement systems obtained with calcined Illite or calcined montmorillonite after 28 days are compared to reference cement paste, results indicate that these admixtures show low activity and no influence on the microstructural development is observed (Fernandez et al., 2011). For this reason, kaolinite remains a commonly recommended clay mineral for cement substitution in concrete or mortars.

2.3.4. Standards and Guidelines in Rammed Earth Construction

The minimum required compressive strength for rammed earth varies from one standard to another (Maniatidis & Walker, 2003). For instance, the New Mexico code requires a minimum compressive strength of 2.07 N/mm^2. On the other hand, the Zimbabwe standard code of practice for rammed earth structures requires at least 1.5 N/mm^2 compressive strength for one storey walls up to 400 mm thick and 2.0 N/mm^2 for two storey walls. Furthermore, Thuysbaert (2012) indicated that the minimum acceptable value of compressive was 1.0 N/mm^2 and 2 N/mm^2 for non-load and load bearing applications in rammed earth construction, respectively. In Kenya, however, there is limited information on a specific standard for rammed earth. For general construction, the KS02-1070:1993 standard requires a minimum compressive strength of 2.5 MPa.

2.4. Soil Selection Criteria for Cement Stabilized Rammed Earth

In selecting materials for rammed earth, Ciancio et al. (2013) stated that it is most sensible to use standard testing allowing for the classification of different soils. Some of these tests include the particle size distribution, the Atterberg limits, and the linear shrinkage.

2.4.1. Particle Size Distribution

The most suitable type of soil for rammed earth construction is a well-graded soil with a range of particle sizes (Burroughs, 2008; Thompson et al., 2022). Burroughs (2008) reported that use of textural properties is encouraged to better indicate the likelihood of stabilization success once the Linear Shrinkage (LS) and Plasticity Index (PI) are known. A classification study conducted by Burroughs (2008) on soil favourability for stabilization used a 2 MPa compressive strength criterion as the measure of stabilization success. The results (Table 2.1) recommended that the upper boundary for clay/silt was 35%, and the lower boundary was 21%. This table was useful in the sense that it provided three sets of values of soil properties: those that should actively be avoided ("poor"), those that should be actively sought ("good"), and those that are intermediate ("fair") and which could be used. Moreover, it also reported that samples with gravel content >13% seemed to produce stronger specimens by imparting frictional strength to the stabilized soil (Burroughs, 2008). In addition, the recommended sand levels were found to be between 30% and 70%, similar to Bryan (1988). Other studies also recommended that modal values of soil properties should range between 5-25% clay, <30-35% clay/silt (Table 2.2) (Bryan, 1988).

Table 2.1: Value Ranges of Soil Suitability for Stabilization

Source: Burroughs (2008)

	Good	**Fair**	**Poor**
Clay/silt (%)	21-35	36-45	≤ 20 or ≥ 45
Gravel (%)	13-62	<13	-
Sand (%)	30-70	-	>70
LL (%)	≤ 35	36-45	>45
PL (%)	16-19	<16 or >19	-
PI (%)	<15	15-30	<30
LS (%)	<6.0	6.0-11.0	>11.0
PI and LS (%)	<15 and <6	15-30 and 6.0-11.0	>30 and >11.0

2.4.2. Atterberg Limits and Linear Shrinkage

Plasticity index is the numerical difference between liquid and plastic limits. The plasticity index is indicative of clay content and/or active clay minerals and that higher shrinkage will occur when the earth dries. Atterberg limits zone suggested between a plasticity index of 0 to 22% and liquid limit of 7% to 39%. As reported by Maniatidis and Walker (2003), liquid limit for unstabilized soils should be between 25% and 50% (30-35% preferred) and the plastic limit between 10% and 25% (12-22% preferred). On the other hand, the plasticity index (PI) was limited to <15-20% plasticity index (Bryan, 1988). A study by Burroughs (2008) also recommended an upper boundary for the liquid limit and plastic limit (PL) equal to 35% and 15%, respectively. Soils unsuitable for treatment with any stabilizer include organic soils, clean gravels and sands, soils with excessive silts and highly plastic clays.

Table 2.2: Suggested Criteria for Suitability of Soil for Cement Stabilization

Source : Bryan (1988)

Particle size analysis	Plasticity indices	Other criteria suggested
Not more than 20% (American Standards, clay <0.005 mm)	Liquid limit 50% maximum (preferably 30% maximum) plasticity index 20% maximum.	Proctor optimum between 6-17%
At least 33% sand between 5-20% clay	Liquid limit less than 40% plasticity index 30% maximum	Optimum moisture content 10-14% (assumed proctor)
Clay content between 15-35%	Plasticity index less than 20%	
Less than 35% passing No. 200 sieve (equivalent 63 micron)		
At least 33% sand between 5-30% clay/silt		

The linear shrinkage (LS) has an important meaning on the shrinkage capacity of a stabilized soil. It is reported that lower shrinkage values are associated with less cracking of the earth material. It also indicates the tendency of internal tensile stresses to pull apart the material from within and thereby weakening it (Burroughs, 2008). The study conducted by Burroughs (2008) recommended a LS < 6.0 and plasticity index (PI) < 15, or with LS 6.0-11.0 and PI 15-30 and sand content <64%, when stabilized with quantities of cement and lime that averaged 4% and 2%, respectively. Other types of soils, with LS 6.0-11.0 and PI 15-30 and sand content ≥ 64%, or with LS > 11.0 and PI > 30, achieved low stabilization success rates (in the range 13-55%) and as such, are regarded as unfavourable for stabilization (Burroughs, 2008). Nevertheless, cement can be applied to stabilize any type of soil except soils with organic content greater than 2% or having a pH lower than 5.3. The recommended practical stepwise procedure for determining soil favorability for stabilization based on testing natural soil properties is presented in Figure 2.3 below.

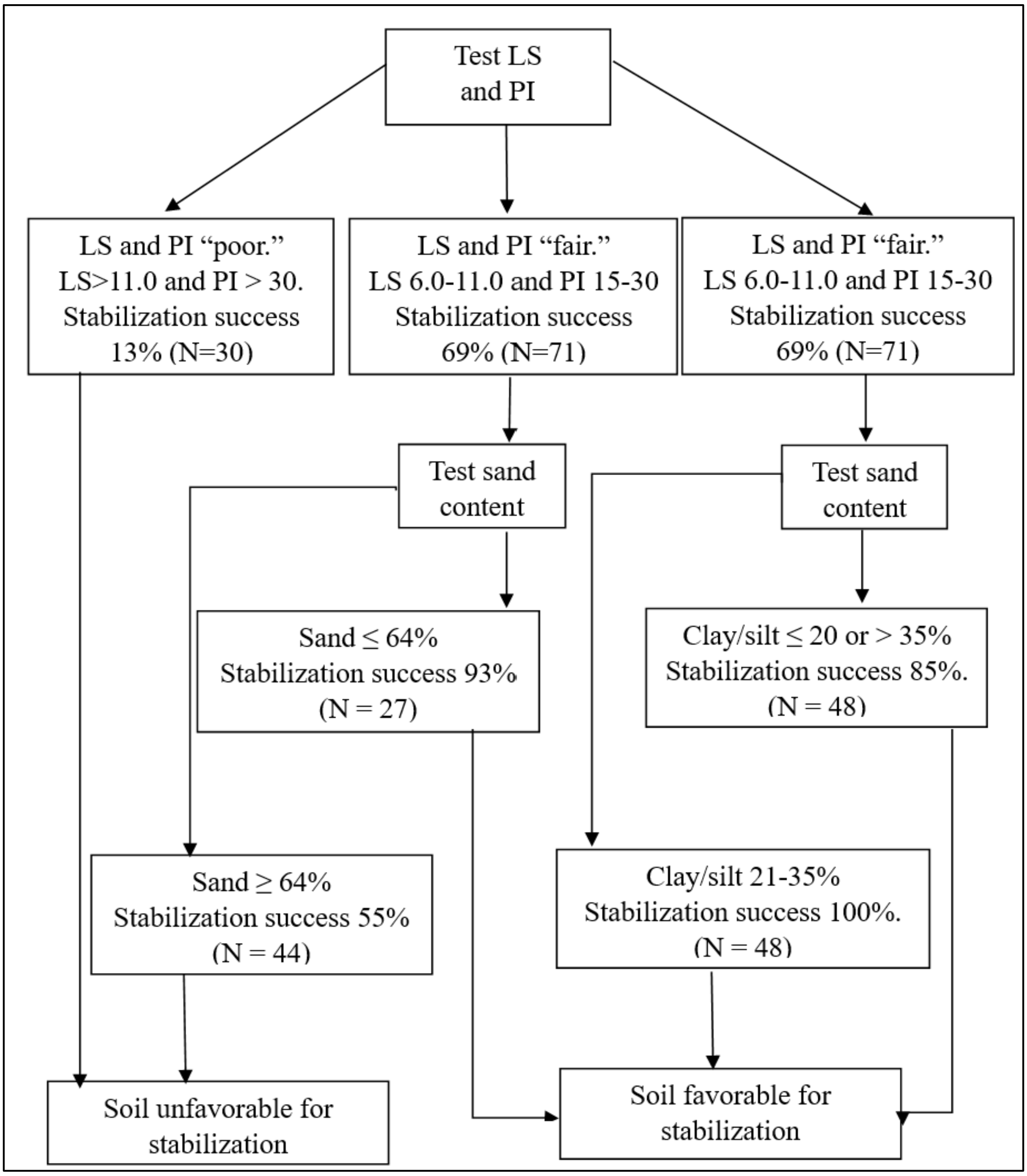

Figure 2. 3: Stepwise Procedure for Determining Soil Suitability for Stabilization based on testing soil properties. Source: Burroughs (2008)

2.5. Evaluation of Pozzolanic Activity

According to international regulations and literature, there is a consensus that the activity of most SCMs is linked to some main parameters: cement type, temperature, curing time, calcium hydroxide to pozzolana ratio, water-to-cement ratio and some pozzolana properties, particularly fineness, chemical, and mineralogical composition, dehydroxylation degree, amorphization rate and reactive silica and alumina content (Bumanis et al., 2020; Faleschini et al., 2021). X-Ray fluorescence (XRF) and X-ray diffraction (XRD) are instrumental test methods that give an initial idea about materials as potential pozzolans by the determination of silica and aluminium oxide composition (XRF) and by determination of amorphous phases (XRD). A higher surface area and smaller particle may ensure more rapid chemical reactions, which are important factors for pozzolans to exhibit their pozzolanic activity (Bumanis et al., 2020).

The pozzolanic activity of supplementary cementitious materials is evaluated using direct and indirect methods (Donatello et al., 2010; Faleschini et al., 2021). Direct methods evaluate the pozzolanic activity by measuring the concentration of Ca^{2+} and OH^- in a solution containing the pozzolanic material and saturated lime (saturated lime test); or a solution containing the pozzolanic material and Ordinary Portland Cement (OPC) CEM-I (Frattini test) (Donatello et al., 2010). On the other hand, indirect methods monitor physical properties (strength activity index or electrical conductivity) allowing to measure the material's pozzolanicity.

The Frattini test describes the dissolved Ca^{2+} and OH^- concentrations in a solution containing saturated lime and the test pozzolana, while the saturated lime test the amount of the dissolved Ca^{2+} and OH^- concentrations in a solution containing CEM I and the test pozzolana (Amin et al., 2015). The strength activity index measures the influence of the pozzolanic reaction on the densification of cementing matrix, and packing effect which improves the compressive strength (Amin et al., 2015). The electrical conductivity test, on the other hand, measures the change in electrical conductivity of pozzolanic material which is dispersed in a saturated solution of lime (Amin et al., 2015). However, direct and indirect methods do not always correlate with each other (Amin et al., 2015; Donatello et al., 2010; Faleschini et al., 2021; Tironi et al., 2013). Thus, Donatello et al. (2010) recommended using a combination of these tests to provide a robust evaluation of the pozzolanic activity.

2.6. Roadmap for Assessing the Suitability of a Pozzolanic Material for Cement Replacement

The roadmap for identifying if a material can be suitably used as a pozzolanic material is very complex, and often, or at least some indicators typically used for this characterization fail. Donatello, Tyrer, & Cheeseman (2010), who analysed comparatively the pozzolanic activity of incinerator sewage sludge ash, coal fly ash, Metakaolin, silica fume, and silica sand through both direct and indirect test methods, recommended using a combination of these tests to provide a robust evaluation of the reactivity of a potential pozzolanic material. Bumanis, et al. (2020) developed a roadmap to evaluate industrial by-product for use as a supplementary cementitious material (Figure 2.4).

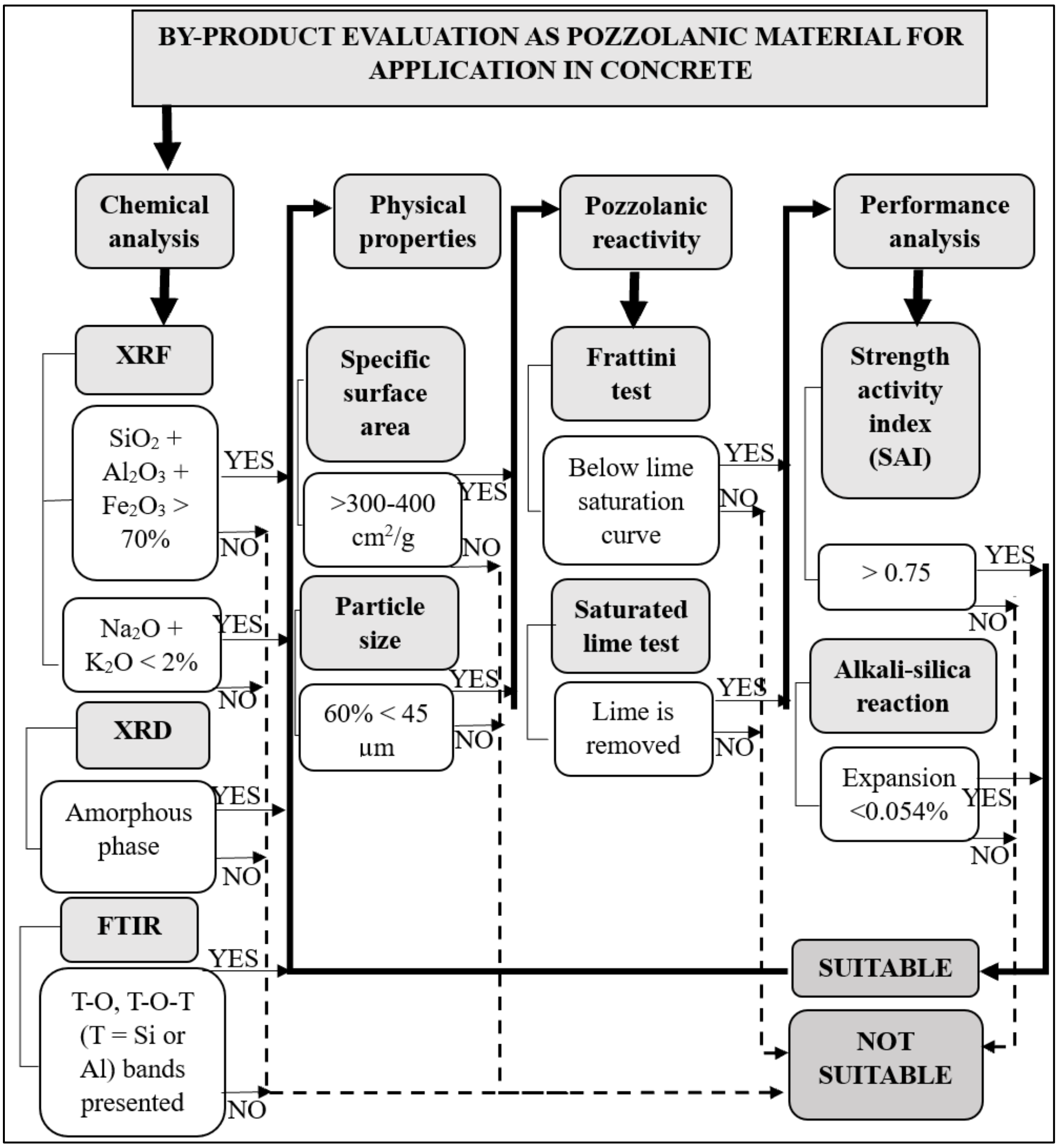

Figure 2.4: Roadmap for Material Evaluation as an Alternative to Cement

Source: Bumanis et al. (2020)

According to Bumanis, et al. (2020), the most basic test methods to start the assessment are associated with the material physical and chemical analysis. The chemical composition detected by XRF indicates the amounts of SiO_2, Al_2O_3, and Fe_2O_3, which are typically characteristic for pozzolanic materials. The mentioned compounds should be >70%, according to standard requirements given for Fly ash in EN450 (for class F fly ash). Mineral compound can also be in crystalline form, which can be indicated by the XRD. An alternative method of determining the fraction of the reactive phase of the starting materials is using selective chemical attack and titration, based on EN196-2, but this method is time consuming (Bumanis et al., 2020).

If the chemical composition falls between the requirements, the physical properties of the powder must be characterised, as fine-grained powder materials with fineness > 300 cm^2/g and more than 60 wt.% of particles <45 um are needed (described in EN450 for Fly Ash). It is reported that the appearance of pozzolans such as fineness can be adjusted by proper pre-treatment such as milling therefore this criterion could be easily adjusted (Bumanis et al., 2020). Further testing is associated with direct methods to describe the pozzolanic reactivity, which characterizes the possibility of attracting lime from a saturated lime solution or lime coming from cement hydration products. If a material attracts free lime, there is a possibility of pozzolanic reactions occurring in the concrete structure. Further testing is associated with performance analysis. Performance analysis provides quantitative results of strength gain during hardening. 20 wt.% replacement of cement by pozzolana should give > 75% strength than that of reference at 28 days and > 85% at 90 days, according to EN450 (Bumanis et al., 2020).

2.7. Environmental Sustainability of Rammed Earth Construction

2.7.1. Environmental Shortcomings of the Construction Industry

There are rising environmental concerns due to extensive exploitation of natural resources related to general construction and other housing development activities. According to Khadka (2020), 50% of all resources consumed across the planet are used in the construction sector, making it one of the least sustainable industries in the world. For instance, it is reported that 4.2 billion tonnes of cement is produced per year globally. This makes the cement industry alone responsible for 5-8% of global man-made CO_2 emissions (Marangu, 2020; Nalobile et al., 2019). Burroughs (2010) indicated that much of the discussion and analysis about the sustainability of building materials continues to surround energy consumption and CO_2 emissions involved in the life cycle of buildings.

Carbon dioxide emissions from the construction industry are estimated at 8.1 Gt of CO_2 emitted per year globally, induced by the over-exploitation of non-renewable resources, processing and transportation of raw materials and waste production. On the other hand, it also accounts for 25-40% of the energy consumption worldwide (Leitãoa et al., 2017). Khadka (2020) reported that building activities results in one-sixth of the world's freshwater withdrawals, one-quarter of its wood harvest, and two-fifths of its material and energy flows resulting in several massive side effects to the entire nature and its existence. Similarly, according to a report by the Intergovernmental Panel on Climate Change (2014) in 2010, buildings accounted for 32% of total global final energy use (equal to 117×10^{18} J), 19% of energy-related Green House Gases (GHG) emissions and 33% of black carbon emissions. This has led to the revitalization of alternative building technologies. Stabilized rammed earth has been identified as one such material which can optimize the resource usage while minimizing the carbon footprint (Kariyawasam & Jayasinghe, 2016).

2.7.2. Environmental Benefits of Rammed Earth Construction

Rammed earth is a construction technique that offers social, economic and environmental benefits (Ciancio et al., 2013). A rammed earth building can have a significantly lower embodied energy and carbon footprint than an equivalent building made of more conventional materials such as concrete, steel or masonry (Ciancio et al., 2013). In comparison with burnt clay bricks, Ciancio et al. (2013) found out that Cement Stabilized Rammed Earth (CSRE) achieved lower embodied energy which was in the range of 15-25% of burnt clay brick masonry (Reddy & Kumar, 2010). Another study was conducted by Reddy et al. (2014) on the design, construction and embodied energy consumption of three storey rammed earth load bearing school complex building. An analysis of the embodied energy demonstrated that the embodied energy of a CSRE building (1.15 GJ/m^2) was in the range of one third of a load bearing brickwork masonry building (3-4 GJ/m^2) and less than one fourth of a reinforced concrete framework building (4-10 GJ/m^2) with brick masonry. This study showed that reduction of carbon emissions in the construction sector through the use of low embodied energy materials such as CSRE walls and alternative floor/roof systems could be possible (Reddy et al., 2014).

Stabilized mud blocks were promoted as an alternative low-carbon material and it was estimated that 60-70% savings could be made on the embodied energy compared to clay bricks (Reddy & Kumar, 2010). On the other hand, Reddy and Kumar (2010) conducted a comparative study on the embodied energy consumption of CSRE and that of burnt clay brick masonry. It was reported that the embodied energy of a nonstabilized rammed wall could increase from 0.33-0.36 MJ/m^3 to 0.4-0.5 GJ/m^3 range when about 6-8% cement is added to stabilize soil. This increased further to 0.625 GJ/m^3 when cement content increased to 10% and the recorded embodied energy was 0.625 GJ/m^3. This suggested that the embodied carbon and embodied energy of stabilized rammed earth tends to increase proportionally with cement content (Akbarnezhad & Xiao, 2017). Thus, replacing cement with alternative sustainable materials could reduce the embodied carbon and energy of rammed earth buildings.

Another strategy to reduce the embodied carbon of buildings include increasing the content of recycled, waste or by-product materials in the mix design (Akbarnezhad & Xiao, 2017). A study by Morel and Charef (2019) conducted a comparative study between standard strip footings, cement stabilized earth footings and polymer stabilized earth footings. It was established that the concrete strip footings achieved a carbon footprint with a cube of concrete having between 100 to 300 kg of CO_2. The 2% cement stabilized earth would have a carbon footprint of 40 to 80 kg/m^3 with cement having a carbon footprint of 250 kg/m^3. The 5% polymer stabilized earth, on the other hand, had an estimated carbon footprint of 20 to 40 kg/m^3 with the main components being bitumen SS60 and urea with a carbon footprint for bitumen being 102 kg per tonne. This suggested that the use of alternative materials such as polymer stabilized earth foundations could achieve a reduction of 46% of CO_2 emissions compared to a cement concrete. Similar results were also reported by Meek and Elchalakani (2019) on industrial waste products (fly ash, ground granulated blast furnace slag, and silica fume) used as rammed earth stabilizers after alkaline activation. Using life-cycle analysis, it was estimated that the use of rammed earth mixes stabilized with aluminosilicates by-products and NaOH would reduce the global warming potential by 60% compared to cavity bricks for the same unit of external wall and by 40% compared to brick veneer.

2.8. Application and Cost of Rammed Earth Construction

Rammed earth has been successfully used in Kenya (Oyawa et al., 2015), and in many other countries for different applications (Maniatidis & Walker, 2003; Oyawa et al., 2015; Reddy & Kumar, 2010; Rosicki & Piotr, 2022; Suresh & Anand, 2017; Thompson et al., 2022; Thuysbaert, 2012; Walker et al., 2005). Several studies have been conducted on the application of rammed earth for wall construction (Burroughs, 2010; Reddy & Kumar, 2010; Suresh & Anand, 2017). In Sri Lanka for example, CSRE was used in external application of residential buildings in the form of boundary walls where tropical climatic conditions prevail. In this project, a full-scale formwork with plywood sheets as shuttering was used in the construction (Figure 2.5). Cement content was limited to 10% and sandy laterite soil was collected locally. Another challenging application of CSRE was road pavement construction (Figure 2.6). This driveway was constructed as an access road to a factory building where heavy container traffic travels daily to transport finished products. In this project, the laterite soil obtained from the site itself was mixed with 6-8 mm chips stabilized with 10-12% cement for road construction (Reddy et al., 2014). A study by Oyawa et al. (2015) reported that eco-blocks made of stabilized murrum soil and quarry dust achieved comparable or higher strength than conventional dressed stone blocks used in Kenya. This demonstrated the viability of constructing eco-building in Kenya employing sustainable construction materials (Oyawa et al., 2015).

Figure 2.5: CSRE Boundary Wall in a Residential Building

Source: Reddy et al. (2014)

Figure 2.6: Driveway Completed with CSRE

Source: Reddy et al. (2014)

It is reported that the cost of CSRE construction varies with cement content used, availability of soil at site and the type of formwork used. Reddy et al. (2014) reported that the cost of CSRE construction of a 150 mm thick wall using 8% cement and soil extracted from the site was in the range of \$10-11 per m^2 with slip from moulds and \$7-\$8 per m^2 with timber formwork. For load bearing wall construction for instance, Kandamby (2012) reported that a cost reduction in the range of 50% could be achieved with CSRE compared to that of brickwork. Kosarimovahhed and Toufigh (2020), on the other hand, demonstrated that rammed stabilized with 7.5% cement could cost 11.25\$ for 1 ton, while using a mix design of 5% fly ash (with alkaline activation) and 2.5% cement as stabilizing agents could only cost 10.47\$. The highlighted successful applications of CSRE such as boundary walls, load bearing walls of buildings, retaining walls, and road pavement construction have demonstrated CSRE as a cost-effective construction material (Kandamby, 2012; Reddy & Kumar, 2010; Reddy et al., 2014). In their study on the control of Tungiasis, Elson et al. (2017) mentioned Earthenable (www.earthenable.org), an organization in Rwanda, that attempted to apply rammed earth in their search to develop a multi-layer floor sealed with linseed oil. However, there is still limited published work on the application of rammed earth in house floor construction for low-income housing.

2.9. Design Considerations for the Proposed Rammed Earth Floor

The durability of earthen structures is mainly related to the action of water on the walls. This action is manifested primarily by increase of water content and erosion of earthen walls. The first problem is mainly due to capillary flow (from ground to surface). The second comes from incident rainfall (Morel, 2012). In the context of a rammed earth floor, the durability is mainly influenced by capillary flow from ground and surface. In addition to decreasing water absorption through the addition of a binder, use of damp-proof membranes is often provided along the interface between the footing and the base for earthen walls (Morel, 2012). This could also be adopted in earthen floors, especially in areas with excess moisture and having high water table. However, the damp-proofing membrane or material should be capable of withstanding ramming without damage and an impermeable floor-finish could be laid on the surface (Morel, 2012). On the other hand, as similarly reported by Hall and Djerbib (2004), when the mass of the binder fraction in a suitable soil is less than 10% of the total soil mass, it would appear that the rate of moisture ingress in rammed earth is significantly increased, due to capillary suction. In addition, during the 28-day curing period, it is essential to maintain a relative humidity level exceeding 95% for the newly constructed floor. Achieving this level of humidity is accomplished by regularly spraying the surface with water. This accelerated curing process is crucial to ensure that the floor attains a compressive strength that meets or exceeds the minimum requirement specified in accordance with KS02-1070:1993 standards, which is greater than 2.5 MPa.

2.10. Summary of the Review and Research Gap

From the above literature, it is clear that extensive studies explored the use of alternative materials to cement (Assumptor et al., 2020; Danner et al., 2018; Dhanya & Santhanam, 2017; Ganesan et al., 2007; Jaskulski et al., 2020; Justice, 2005; Khan et al., 2022; Mehsas et al., 2021; Okumu Mary Assumptor 1, 2020; Schulze & Rickert, 2018, 2019; Senhadji et al., 2012; Zhou et al., 2017). These included fly ash, cow dung ash, blast furnace slags, silica fume, rice husk ash, polymer fibres, waste and industrial by-products (Amiralian et al., 2012; Bumanis et al., 2020; Khan & Khan, 2017; Kosarimovahhed & Toufigh, 2020; Kristiawan et al., 2017; Oluremi et al., 2021). The literature also reviewed the properties of calcined clay, especially Metakaolin, as a potential replacement for cement (Bich et al., 2009; Dabakuyo et al., 2022; Ibrahim et al., 2018; Justice, 2005; Mehsas et al., 2021; Thiviya et al., 2020; Trusilewicz et al., 2012; Wang et al., 2018). In addition, studies were also conducted on strength improvement of cement stabilized rammed earth for the construction of walls, earth blocks, and road pavement (Hall & Djerbib, 2004; Hall & Djerbib, 2006; Indekeu et al., 2021; Kandamby, 2012; Kariyawasam & Jayasinghe, 2016; Kosarimovahhed & Toufigh, 2020; Marais et al., 2015; Naeini et al., 2021; Porter et al., 2018; Raj et al., 2018; Reddy & Kumar, 2010; Reddy, 2010; Suresh & Anand, 2017; Thiviya et al., 2020; Walker et al., 2005). Nevertheless, there is still limited existing research regarding the incorporation of calcined clay as a partial replacement for cement in stabilized rammed earth, with the ultimate goal of developing a strong and water-resistant floor. It is on this basis that this study aimed to assess the performance of calcined clay as a replacement for cement for potential use in the construction of earthen floors for low-income housing.

2.11. Conceptual Framework

Using the background information backed by evidence in the literature review, the study's paradigm on the performance of calcined clay as a partial replacement for cement in rammed earth floors was developed. It mainly consists in the effects of independent variables on the study's variables of interest (compressive strength and capillary water absorption). As illustrated on figure 2.7, independent variables included raw clay characteristics, pozzolanic activity of calcined clay, mix design, and soil type on the strength and water absorption properties of rammed earth floors as illustrated in Figure 2.7.

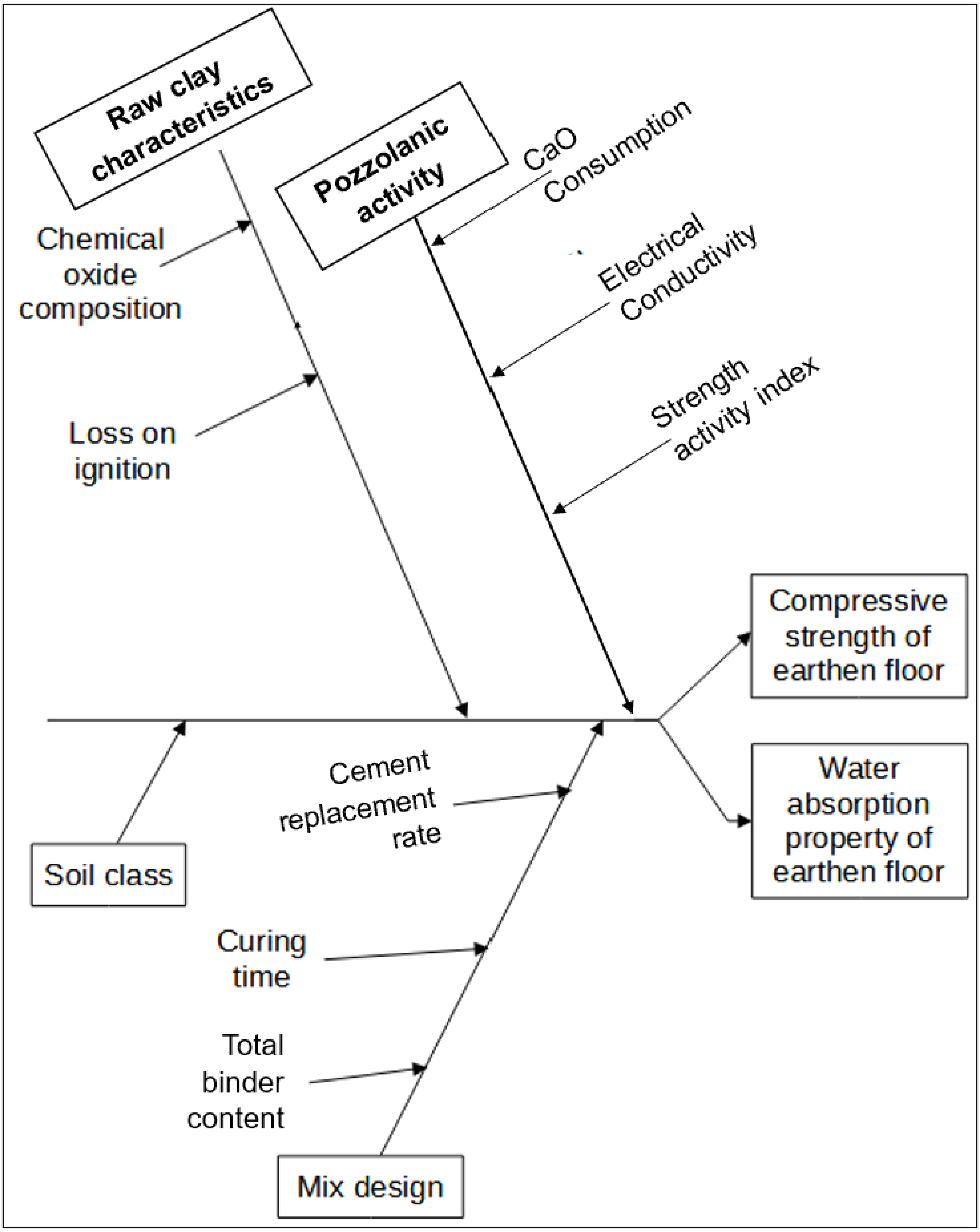

Figure 2.7: Conceptual Framework

CHAPTER THREE

RESEARCH METHODOLOGY

In this chapter, laboratory experiments conducted for the determination of the effect of calcined clay as a partial replacement for cement in rammed earth floor construction are described. The procedures used in soil sampling, assessment of the pozzolanic activity of calcined clay, and rammed earth stabilization using cement and calcined clay are presented. Sampling of clay for calcination and the evaluation of pozzolanic activity were conducted from March 2022 to September 2022. Soil stabilization experiments were conducted from November 2022 to March 2023.

4. Study Area

Murang'a County is one of the counties of Kenya's former Central Province. The county (Figure 3.1) covers 0.4% of Kenya's total land mass. It is bordered by the counties of Nyeri to the North, Kiambu to the South, Nyandarua to the West and Kirinyaga to the North-East, Embu to the East and Machakos to the South-East. It lies between latitudes 0°45'S-37°7'E and has a density of 3.7 people per household (Kamau et al., 2018). The county has a population of 942,581 people and it is host to 2.4% of the total population in Kenya based on the 2009 census. It is divided into eight sub-counties: Kiharu, Kahuro, Kangema, Gatanga, Mathioya, Kigumo, Kandara, Maragua (Murang'a County, 2018). The geology of the county consists of volcanic rock structure and most of the soil has developed from the volcanic activities. The soils are generally fertile and have good drainage. These soils include Humic Nitisols, Rhodic ferralsols, ferralic cambisols, umbric Andosols and some patches of vertisols which are poorly drained (Batjes & Gicheru, 2004). According to Murang'a Country Integrated Development Plan (Murang'a County, 2018), more than 40% of the households live in stone/brick walled houses, less than 58% in mud/wood walled houses while about 2% live in grass straw/tin walled houses. Most housing units in the county are roofed with corrugated iron sheets (about 95%), while Makuti and grass roof constitute 0.18% of the households. Majority of these housing units have earthen floors (60%), followed by cement floors at 39% (SGS Kenya Limited, 2018).

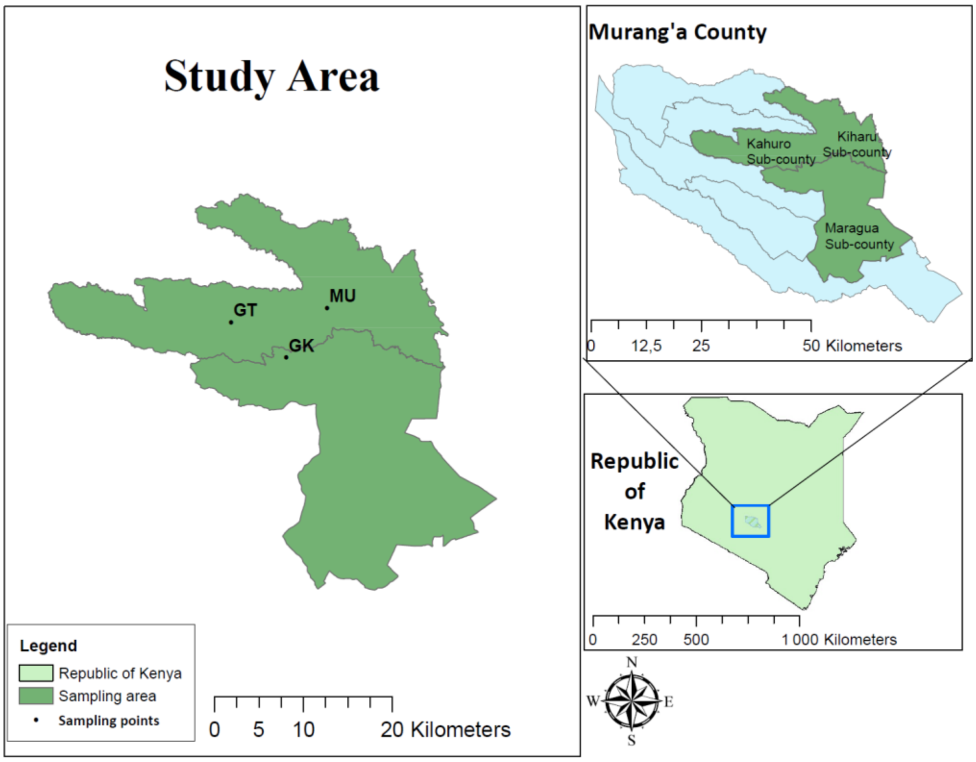

Figure 3.1: Map of Study Area Showing the Sampling Sites GT (Gatundu), GK (Gakoigo), and MU (Murang'a town)

5. Characterization of Clay Material and Evaluation of Pozzolanic Activity

3.5.1. Sampling of Clay Material

Natural clays (collected in triplicates) were obtained from Gathima wetland in Gatundu village, Kahuro sub-county; Murari wetland in Murang'a town, Kiharu sub-county; and Kaingiro wetland in Gakoigo town, Maragua sub-county (Figure 3.1). In each site, the three replicates, weighing 5 kgs each, were randomly sampled at a depth of 60 cm. The samples were coded as GT1, GT2, and GT3 for Gatundu; MU1, MU2, and MU3 for Murang'a Town; and GK1, GK2, and GK3 for Gakoigo (Table 3.1). Undesirable components such as roots, leaves of trees and plants were removed from the samples before use. The samples were then dried at 105°C to a constant weight using an EYELA windy oven (Model WFO – 1000ND, Rikakikai Co. Ltd, Tokyo, Japan). The samples were then crushed using a ball mill and sieved through a 75 micron sieve (Njoka et al., 2015). The soil group was determined using the Harmonized World Soil Database (HWSD) version 2.0 developed in 2008 by the

International Institute for Applied Systems Analysis (IIASA) and the Food and Agriculture Organization of the United Nations (FAO).

Table 3.1: GPS Coordinates of Sampling Locations

Sub-County	Wetland Name	Texture Class	Code	Longitude	Latitude	Elevation	Soil group
Kahuro	Gathima Wetland	Clay	GT1	37.05157	-0.74284	1530 m	Nitisols
			GT2	37.05188	-0.74269	1515 m	
			GT3	37.0485	-0.74299	1548 m	
Murang'a East	Murari Wetland	Clay	MU1	37.14867	-0.72816	1297 m	Nitisols
			MU2	37.14995	-0.72795	1296 m	
			MU3	37.15067	-0.72739	1295 m	
Murang'a South	Kaingiro Gakoigo Wetland	Clay	GK1	37.10715	-0.77855	1378 m	Nitisols
			GK2	37.10737	-0.77832	1377 m	
			GK3	37.10785	-0.77767	1379 m	

3.5.2. Characterization of Raw Clay Material

3.5.2.1. Determination of soil texture

Soil texture was evaluated using the hydrometer method in accordance with BS 1377:part 2, 1990 (British Standard Institute, 1990). A stock dispersing solution was prepared weekly from tetrasodium pyrophosphate decahydrate ($Na_4P_2O_7.10H_2O$, 500 g) made up to 10 L in deionized water. Clay was dried in a current of warm air (45°C) and pulverized to pass a 2-mm sieve. A subsample (50 g) was treated in a 1 L plastic cup with 100 mL of the stock solution. The mixture was made up to about 250 mL, and left overnight (16 h). It was then transferred to a metal cup with indentations (milk-shake cup), mixed with a high-speed blender for 5 minutes and rinsed into a measuring cylinder. The suspension was made up exactly to the 1000 mL mark with deionized water from a large stock at room temperature.

Homogenizing the suspension was made by raking the suspension from top to bottom with a plunger. After mixing, a standard ASTM type 152H hydrometer was carefully inserted 20 seconds ahead of the reading time. The stem scale was read at the top of the meniscus. The stem of the hydrometer was kept free of grease so that a meniscus forms properly. Readings were estimated at 40 seconds (R_{40s}) to the nearest 0.5 g/L, and the later, at 6 hours (R_{6h}), after mixing, to the nearest 0.1 g/L under good light with the aid of a magnifying glass. The soil texture was evaluated using Equations [3.1], [3.2], [3.3]. The results of the soil texture analysis were plotted on the USDA soil texture triangle using R software.

$$\% \text{ clay} = \frac{100}{w} \times (R_{6h} - R_L) \quad [3.1]$$

$$\% \text{ sand} = 100 - \left(\frac{100}{w}\right) \times (R_{40s} - R_L) \quad [3.2]$$

$$\% \text{ silt} = 100 - \%\, sand - \%\, clay \quad [3.3]$$

Where:

w was the weight (g) of dry soil in 1000 mL of suspension.

%clay, %sand, %silt represent the percentage of clay, sand, and silt in the soil sample, respectively.

The blank readings R_L in equations [3.1] and [3.2] were actual readings, which will not have the same value if the suspension temperature drifts.

3.5.2.2. Determination of loss on ignition (LOI)

This test was conducted to estimate the amount of organic matter. Organic matter reduces the pozzolanic activity if present in amounts higher than 10% (Arum et al., 2013). To determine the loss on ignition (LOI), 1 g of the sample was dried in an EYELA windy oven (Model WFO – 1000ND, Rikakikai Co. Ltd, Tokyo, Japan) at 105°C for 24 hours. The sample was then weighed to determine the moisture content and thereafter calcined at 500°C for 24 hours using an electronic muffle furnace (Advantec KL-420, Japan) (Figure 3.2) (Jensen et al., 2018; Konare et al., 2010). The analysis was done in triplicates for each sample. The LOI value was calculated using Equation [3.4]:

$$\text{LOI}\,\% = \left(\frac{\text{A}}{\text{B}}\right) \times 100 \quad [3.4]$$

Where A is the loss in mass between 105°C and 500°C, B is the mass of moisture-free sample. Calculations were made to the nearest 0.01%.

(a) (b)

Figure 3.2: a) Clay Samples Before Ignition and b) Clay Samples after Ignition

3.5.2.3. Determination of chemical oxide composition

The chemical composition analysis was conducted to determine the percentage of oxides present in clay samples using X-ray Fluorescence using a handheld XRF analyser (S1 TITAN Handheld XRF Analyser – Bruker) (Adeniyi et al., 2020; Schulze & Rickert, 2019; Zayed et al., 2018). According to ASTM C618, a material can be considered pozzolanic if the percentage of MgO and SO_3 is lower than 4% each, and the sum of SiO_2, Al_2O_3, and Fe_2O_3 exceeds 70% in the chemical composition (Arum et al., 2013; Bumanis et al., 2020). The analysis was conducted at the Mines and geological department, at the ministry of Petroleum and Mining in Nairobi, Kenya. Each analysis was done in 3 replicates.

3.5.3. Clay Calcination

The calcination was carried out to transform clay into an amorphous material (Arum et al., 2013). Crushed clay samples were sieved through a 75-micron sieve. An electronic muffle furnace (Advantec KL-420, Japan) was used for calcination. Clays were calcined at 600°C, 700°C and 800°C following the protocol suggested by Moodi et al. (2011). The heating rate was 25°C per minute and the time of residence at maximum temperature was fixed at 2 hours. Samples without thermal treatment were referred to as raw clay. The calcined clays were allowed to cool down to room temperature in the furnace overnight. After calcination, the material was gently ground by hand using a mortar and a pestle according to the protocol suggested by Ibrahim et al. (2018).

3.5.4. Evaluation of the Pozzolanic Activity

The pozzolanic activity of clay was measured using the electrical conductivity test, Frattini test and the compressive strength test.

3.5.4.1. Electrical conductivity test

The electrical conductivity test (EC) assessed the pozzolanic activity by monitoring the electrical conductivity of a saturated solution of $Ca(OH)_2$ at 40 ± 1°C after the addition of clay (Tironi et al., 2013). This test was conducted following the procedure described in Musyimi et al. (2016) and John (2013). In this test, 200 cm^3 of distilled water was heated on a hot magnetic plate (Polymix PX-MST) at 40 ± 1°C. Some 5.0 g of clay was added to the solution at 40 ± 1°C, and the mixture was continuously stirred using a magnetic stirrer for two minutes. The electrical conductivity of the resulting solution was measured after 2, 30, 60, 120, 240, 1200, and 1440 minutes (Figure 3.3). A pozzolanic reaction leads to a reduction of free Ca^{2+} and OH^- ions (Jurić et al., 2020). As a result, the EC value gradually decreases with time when the added material is reactive due to the consumption of Ca^{2+} ions (Tironi et al., 2013). The process was repeated three times.

(a) (b)

Figure 3.3: a) Solution of Calcined Clay and $Ca(OH)_2$ and b) Electrical Conductivity of the Solution Measured

3.5.4.2. Frattini test

The Frattini test evaluated the amount of dissolved Ca^{2+} and OH^- in a solution containing OPC CEM-I and the pozzolanic material after a curing period of 8 and 15 days (Donatello et al., 2010). This was conducted on the principle that a pozzolanic reaction consists in a fixation of $Ca(OH)_2$ by the pozzolanic material. Hence, the lower the resulting quantity of calcium hydroxide, the higher the pozzolanicity. The procedure specified in EN 196-5 was used. Portland cement, OPC-CEM-I, (16 g) and the clay (4g) were mixed with 100 ml of distilled water. The chemical composition of Portland cement is presented in Table 3.2. After mixing the three components, samples were left for 8 and 15 days in sealed plastic bottles in a water bath at 40°C. After curing, the samples were vacuum filtered through a 2.5 µm nominal pore size filter paper (Whatman No. 42) and allowed to cool down to ambient temperature in sealed Buchner funnels. The filtrate was analysed for [OH^-] and [Ca^{2+}] by titration against dilute HCl (0.1 mol/l) and Ethylenediaminetetraacetic acid (0.03 mol/l) (EDTA), respectively (Figure 3.4) (John, 2013). Results were presented as a graph showing CaO (mmol/l) on the y-axis against [OH^-] (mmol/l) on the x-axis. Test results below the Portlandite saturation curve indicate the removal of Ca^{2+} from the aqueous solution (the solution becomes under-saturated in Portlandite), which is then attributed to the pozzolanic activity of the material added to cement. Results lying on the line indicate zero pozzolanic activity, while the results above the line correspond to no pozzolanic activity. It should be noted that this procedure assumes that no other source of calcium is present in the system, since leaching would invalidate this approach (Jurić et al., 2020).

(a)

(b)

Figure 3.4: a) Setup for The Determination of Ca^{2+} and $[OH]^-$ by Titration and b) Titrated Solution after Frattini Test

Table 3.2: Chemical Composition of the Ordinary Portland Cement (OPC) CEM-I Used

Oxides	SiO_2 (%)	Al_2O_3 (%)	Fe_2O_3 (%)	CaO (%)	SO_3 (%)	K_2O (%)	TiO_2 (%)	Others (%)
Composition	25.38	4.75	2.91	63.00	2.32	0.79	0.25	0.6

3.5.4.3. Compressive strength test

This test involved the determination of the strength developed by mortar specimens following the procedure described in ASTM C109. Cement mortars containing clay replacing OPC CEM-I at 20% were tested. The control sample was prepared using 450 g of OPC CEM-I, 1350 g of graded sand and 225 ml of water. The test mixture was prepared with 360 g of OPC, 90 g of pozzolanic material, 1350 g of graded sand, and 225 ml of water. 40 mm ×40 mm ×160 mm square prisms were cast and kept in the moulds for 24 hours. The prisms were demoulded and cured in saturated lime water for 7, 14, and 28 days. After the respective curing time, the square prims were removed from the lime saturated water, surface-dried in an oven and cut using a concrete cutting machine to obtain 40 mm cubes (Figure 3.5). The uniaxial compressive strength was measured using a compressive strength testing machine (MATEST S.p.A TREVIOLO 24048 ITALY). The results were plotted from the average of three specimens. The strength activity index (SAI) was evaluated using equation [3.5] (Altwair et al., 2011):

$$SAI = \frac{CS_1}{CS_2} \qquad [3.5]$$

Where CS_1 is the compressive strength of cement block made with blended cement (MPa), and CS_2 is the compressive strength of cement block made with cement alone (MPa) (control sample).

Figure 3.5: Cement Block Cured for the Determination of Strength Activity Index of Calcined Clay

6. Evaluation of the Effect of Calcined Clay as a Replacement for Cement on the Strength and Water Absorption of Rammed Earth for Floor Construction

3.6.1. Sampling of Experimental Soils for Stabilization

Soils used for stabilization were collected in Juja town, Kiambu County, Kenya. In this study, the performance of calcined clay was studied on coarse-grained and fine-grained soils. Murrum soil was selected as the coarse-grained soil, while Black cotton soil was selected as the fine-grained soil. Murrum soil was collected at latitude 1°5'24" S and longitude 37°0'32" E. Black cotton soil, on the other hand, was collected at latitude 1°5'28" S and longitude 37°0'50" E (Figure 3.6). At each sampling site, soils were sampled at a depth of 1 m after scraping off the topsoil. This was consistent with the protocol suggested by Al-Swaidani et al. (2016). Soils were packed in plastic bags and transported to the geotechnical laboratory, at the Jomo Kenyatta University of Agriculture and Technology. Experimental soils were sun-dried for 2 weeks, crushed and sieved through a 4.75 mm sieve.

(a) (b)

Figure 3.6: Soils Used for Stabilization Experiments : a) Black Cotton Soil and b) Murrum Soil.

3.6.2. Characterization of Experimental Soils

3.6.2.1. Determination of Particle Size Distribution

The hydrometer test was used to determine the soil texture of murrum and black cotton soils in accordance with the BS 1377:part 2, 1990 (British Standard Institute, 1990). 50 g of the soil sample was mixed with a 100 mL soil dispersant (tetrasodium pyrophosphate decahydrate). The suspension was washed on a 75-µm sieve using a jet of distilled water. The material retained on the 75 µm was oven dried, and re-sieved on relevant sieves down to 75 µm. The suspension that passed through the sieve was transferred to a 1 L measuring cylinder and used for the sedimentation analysis. After thoroughly mixing, a hydrometer was immersed and the hydrometer readings taken at ½ min, 1 min, 2 min and 4 min, 8 min, 15 min, 30 min, 1h, 2h, 4h, and 24h from the start of sedimentation. The temperature was recorded during the first 15 minutes and after each subsequent reading. The proportion of soil retained on each sieve was calculated as a percentage of the dry mass of soil used, m (in g), and the cumulative percentages by mass passing each of the sieves from the general relationship. The percentage by mass of particles smaller than the corresponding equivalent particle diameter was also evaluated.

3.6.2.2. Determination of Atterberg Limits

The Atterberg limits test was conducted to describe the transitions of the soil material from semi-solid, to plastic, to fluid. The Atterberg limits are important properties of fine-grained soils, and are used in identifying and classifying soils (Burroughs, 2001). This test was carried out according to the BS 1377: part 2:1990. The liquid limit (LL) and plastic limit (PL) tests were analysed on soil material passing a 425 µm sieve. The liquid limit was determined using the cone penetrometer method (British Standard Institute, 1990). Some 400 g soil sample was mixed with distilled water such that the first cone penetrometer reading was about 15 mm. A portion of the mixed soil was pushed into a metal cup. The dial gauge was lowered to contact the cone shaft and the reading of the dial gauge recorded to the nearest 0.1 mm. The cone was released for a period of 5 ± 1 sec. After locking the cone in position, the dial gauge was lowered to contact the cone shaft and record the reading of the dial gauge to the nearest 0.1 mm. The difference between the readings was recorded as the “cone penetration”. Some 20 g mixed soil was collected from the area penetrated by the cone to determine moisture content.

The penetration test was repeated three more times using the same sample of soil to which further increments of water had been added. The amount of water was added such that a range of penetration values of approximately 15 mm to 25 mm was covered by the four test runs. The relationship between the moisture content and cone penetration was plotted with the moisture content as the abscissae and the cone penetration as ordinates, both one linear scale. The Liquid Limit (LL) of the soil sample is the moisture content corresponding to a cone penetration of 20 mm and was expressed to the nearest whole number. The moisture content of each specimen was expressed using equation [3.6]:

$$\mathrm{LL} = \frac{\mathrm{m}_2 - \mathrm{m}_3}{\mathrm{m}_3 - \mathrm{m}_1} \times 100\ (\%) \qquad [3.6]$$

Where:

m_1 is the mass of the container (in g)

m_2 is the mass of the container and wet soil (in g)

m_3 is the mass of the container and dry soil (in g)

Plastic limit test determined the moisture content at which a soil becomes too dry to be plastic. A 40 g soil paste sample was partially dried until it became plastic enough to be shaped into a ball. The ball was moulded between the fingers and rolled between the palms of the hands until the heat of the hands had dried the soil sufficiently for slight cracks to appear on its surface. The sample was divided into 2 sub-samples of about 20 g each for a separate determination on each portion. The soil was formed into a thread and rolled to reduce to a diameter of about 3 mm until the thread shears both longitudinally and transversally when rolled to about 3 mm diameter. The first crumbling point was the plastic limit. The moisture content of the pieces of crumbled soil was determined. The moisture content was expressed and the value expressed to the nearest whole number. This was the Plastic Limit (PL). The Plasticity Index (PI) was defined as the difference between the Liquid Limit (LL) and the Plastic Limit (PL), and was calculated from equation [3.7]:

$$\mathrm{PI} = \mathrm{LL} - \mathrm{PL} \qquad [3.7]$$

The linear shrinkage was evaluated using BS 1377:1990 (British Standard Institute, 1990). Some 150 g soil paste sample at approximately the Liquid Limit was placed in a mould and levelled along the top with a palette knife. The mould was air-dried for 1-2 days and then at 105°C. The mean length of the soil bar was measured (L_D) and the linear shrinkage of the soil was calculated as the percentage of the original length of the specimen, L_o (in mm), from equation [3.8]:

$$\mathrm{LS}\ (\%) = \left(1 - \frac{L_D}{L_0}\right) \times 100 \qquad [3.8]$$

3.6.2.3. Determination of specific gravity

The specific gravity was determined using ASTM D854. A dry pycnometer was weighed to the nearest 0.01 gram (m_1). Oven-dried soil sample was added to the pycnometer and the weight was measured (m_2). Distilled water was added to the pycnometer until about two thirds full and the mixture agitated. Then, water was added to the volume mark, and the mixture weighed (m_3). The procedure was repeated in three replicates. The pycnometer was filled with water to its calibration mark and the weight was determined (m_4). The specific gravity was measured using equation [3.9]:

$$G_s = \frac{m_2 - m_1}{(m_4 - m_1) - (m_3 - m_2)} \qquad [3.9]$$

3.6.2.4. Determination of Optimum Moisture Content and Maximum Dry Density

The optimum moisture content (OMC) and maximum dry density (MDD) of the soil samples were determined using the British standard light compaction method (BS 1377:part 2, 1990). The compaction effort was obtained using a 2.5 kg rammer falling freely through 30 cm onto the soil. Compaction was done in three layers, each receiving 27 uniformly distributed blows. A mould of 1000 cm^3 was used (Ikeagwuani et al., 2019).

3.6.3. Stabilization Experiments

The raw materials for soil stabilization included black cotton and murrum soil, ordinary Portland cement (OPC CEM I 42.5 N), calcined clay, and water (Table 3.3). The binder content (Portland cement + calcined clay) varied at 5%, 10% and 15% of the binder-soil mixture in reference to Adekitan and Ayininuola (2018). Calcined clay was used as a replacement for Portland cement. The replacement rates were as follows: 0% (control specimens), 25%, 50%, and 75%, respectively, in reference to Adekitan and Ayininuola (2018) (Table 3.3). Unstabilized soil was referred to as soil rammed with 100% soil.

Before compaction, soil was mixed thoroughly with water and the binder (Table 3.3). Water content was informed by the optimum moisture content obtained during the compaction test. The stabilized rammed earth was cast by compacting the mixed material in a 1000 cm^3 cylindrical mould in accordance with BS 1377. The specimens were compacted in 3 equal layers using a 2.5 kg rammer. Each layer received a compaction effort of 27 blows (Figure 3.7). The specimens were kept on smooth and flat plates in a curing room at room temperature and a relative humidity > 95% (Wang et al., 2022; Zhang et al., 2019). After curing for 14 and 28 days, the specimens were removed from the curing room and tested for strength and capillary water absorption.

(a) (b)

Figure 3.7: Rammed Earth Stabilization Procedure : A) Mixing of Soil, Portland Cement, Calcined Clay and Water Before Compaction and B) Compaction of the Mix into a Block Using a 2.5 Kg Rammer

Table 3.3: Mix Proportions of Stabilized Rammed Earth

Soil material	Soil (%)	Binder: Portland Cement (PC) + Calcined Clay (CC)	Calcined Clay (CC) (in the binder)
Black Cotton Soil	100%	-	-
	95%	5%	0%
	95%	5%	25%
	95%	5%	50%
	95%	5%	75%
	90%	10%	0%
	90%	10%	25%
	90%	10%	50%
	90%	10%	75%
	85%	15%	0%
	85%	15%	25%
	85%	15%	50%
	85%	15%	75%
Murrum Soil	100%	-	-
	95%	5%	0%
	95%	5%	25%
	95%	5%	50%
	95%	5%	75%
	90%	10%	0%
	90%	10%	25%
	90%	10%	50%
	90%	10%	75%
	85%	15%	0%
	85%	15%	25%
	85%	15%	50%
	85%	15%	75%

3.6.4. Testing of Stabilized Rammed Earth

3.6.4.1. Determination of Unconfined Compressive Strength

The unconfined compressive strength (UCS) was measured using a compressive strength testing machine (MATEST S.p.A TREVIOLO 24048 ITALY). The procedure adopted in this study was based on ASTM D2166. After the curing period, the specimen was placed in the loading device of the testing machine, ensuring proper alignment and load transfer (Figure 3.8). An axial load was applied gradually until the specimen failed. The unconfined compressive strength was obtained by dividing the maximum load at failure by the cross-sectional area of the specimen. Tests were conducted in 3 replicates. The results were subjected to a graphical representation of the average and standard deviation (Altwair et al., 2011). UCS results at 28 days were compared against KS 02:1070:1993 standards for cement stabilized rammed earth.

Figure 3.8: Stabilized Blocks Prepared for Compressive Strength Test

3.6.4.2. Determination of Capillary Water Absorption

Capillary water absorption tests of cement-based materials usually apply the weighing method, which includes the upwards, side, and downwards suction methods. The most used method is the downwards suction method (Figure 3.9) (Wang et al., 2022). This test was conducted on blocks cured for 14 days in reference to Węgliński (2021) and Wang et al. (2022). In this study, specimens were dried in an oven for 24 hours at 105°C, weighed with an accuracy of 0.1 g ($m_{dry,s}$), and then coated with adhesive paper on the side, to ensure unidirectional transport of water (Wang et al., 2022). The samples were then immersed in water at a depth of 5 ± 1 mm (Figure 3.9). Increase in weight ($m_{so,s}$) as a result of water absorption was monitored after 1, 2, 4, and 24 hours. Prior to every measurement, specimens were wiped with a cloth. Each test was conducted in 3 replicates. In this study, capillary water absorption was expressed in kg water/kg soil block, and calculated using equation [3.10]:

$$C_{ws} = \frac{m_{so,s} - m_{dry,s}}{m_{dry,s}} \qquad [3.10]$$

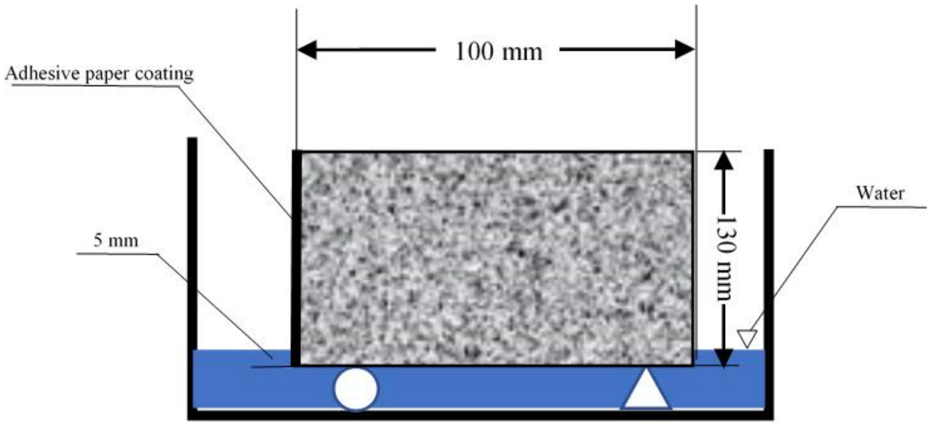

Figure 3.9: Capillary Water Absorption Test

Where: $m_{dry,s}$ is a sample weight after drying [g], $m_{so,s}$ is mass of the soaked sample at time t [g], C_{ws} is capillary water absorption [kg water/kg soil block].

7. Data analysis

The design for this objective was a full factorial design. For the first objective, factors included the sampling sites (Gatundu, Gakoigo, and Murang'a town), calcination temperature (Raw, 600°C, 700°C, and 800°C) and time. For the second objective, factors included soil type, the binder content, cement replacement rate with calcined clay, and curing time. The results were subjected to a graphical representation of the mean and the standard deviation. The data were further subjected to an ANOVA to evaluate the association between independent variables and their interactions using R-software.

Results for strength activity index at 7, 14 and 28 days were subjected to a comparison with ASTM C618 standards. Frattini test results were compared to the solubility curve of $Ca(OH)_2$ based on the EN 196-5 standards. Based on the findings of this objective, the optimum clay type and calcination temperature were used in the evaluation of the effects of calcined clays on the strength and water absorption of cement stabilized rammed earth. The 28-day compressive strength of stabilized rammed earth was subjected to a comparison with KS 02:1070:1993 standards for cement stabilized soil blocks for general construction.

CHAPTER FOUR

RESULTS AND DISCUSSION

4.1. Introduction

This chapter consists of two subsections presenting the results and discussion of the study. The first subsection focuses on the characterization of clay and the evaluation of its pozzolanic activity. The second subsection consists in the evaluation of the effect of cement replacement with calcined clay on the stabilization of murrum soil and black cotton soil for rammed earth floor construction.

4.2. Characteristics and Pozzolanic Activity of the Clay Material

4.2.1. Characteristics of the Clay Material

4.2.1.1. Soil Texture

The results of the soil texture analysis were plotted on the USDA soil texture triangle using R software (Figure 4.1). The results indicated average values of 40-50% of clay, 10-20% of silt and 30-40% sand for all the collected clays (GT, GK, and MU). In particular, samples from Gakoigo were the finest soil with a clay content of about 50%, and the least amount of silt and sand. This suggested that it is relatively more effective to extract the clay fraction from this soil than other samples. The wetland soils used in this study were classified as clay (CL) (see Appendix I).

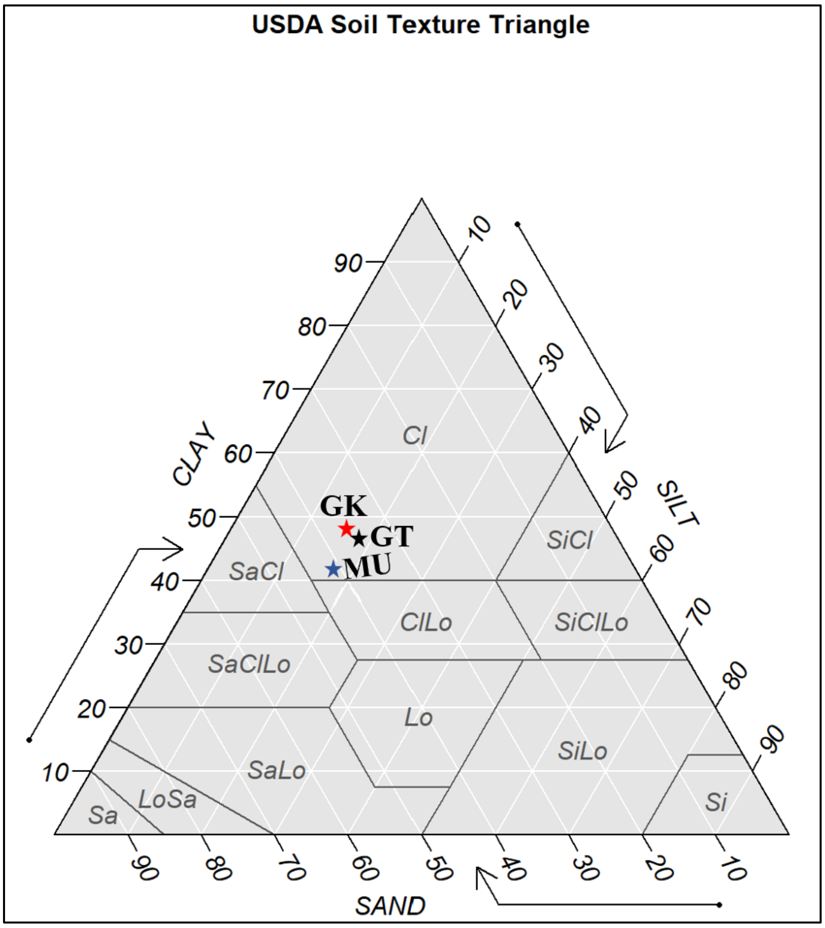

Figure 4.1: Standard Soil Texture Triangle Indicating Classification of Clay from Gatundu (GT), Murang'a Town (MU), Gakoigo (GK)

4.2.1.2. Loss on Ignition and Chemical Oxide Composition

It was observed that all raw clay samples conformed to the ASTM C618 chemical requirements for natural pozzolans (Table 4.1). The percentage of Magnesium oxide (MgO) and Sulphur trioxide (SO_3) was lower than 4% each, and the sum of Silicon dioxide (SiO_2), Aluminium oxide (Al_2O_3), and Ferric oxide (Fe_2O_3) exceeded 70% in the chemical composition. The large presence of pozzolanic oxides suggests that clay is likely to positively influence the strength development of cement blocks. SO_3 was present in trace quantities in all samples, suggesting a positive volumetric stability and hydration kinetics when clay replaces cement (Chelberg, 2019). On the other hand, MgO which if in excess of 4% would make the pozzolana unsound, was not detected (Arum et al., 2013). In contrast, LOI was higher than the 10% minimum required, suggesting a high content of unburnt carbon. This indicated that the adsorption of air entraining agents could be higher, which could inhibit the pozzolanic activity of raw clay (Arum et al., 2013; Chelberg, 2019). Thus, it was necessary to calcine the clay before its use as a replacement for cement.

Table 4.1: Chemical Composition and Loss On Ignition (LOI) of Raw Clay Samples

Sample	Parameters										
	SiO_2 (%)	Al_2O_3 (%)	Fe_2O_3 (%)	CaO (%)	MgO (%)	K_2O (%)	TiO_2 (%)	SO_3 (%)	Others (%)	SiO_2 $+Al_2O_3$ $+Fe_2O_3$ (%)	LOI (%)
GT1	44.57	30.38	19.63	0.38	undetected	0.25	4.17	undetected	0.61	94.59	14.11
GT2	45.26	28.50	20.12	0.55	undetected	0.32	4.69	undetected	0.56	93.88	11.76
GT3	41.11	34.11	19.31	0.24	undetected	0.18	4.23	undetected	0.83	94.52	13.03
MU1	52.77	26.53	15.63	0.86	undetected	0.41	2.43	undetected	1.37	94.93	14.40
MU2	50.47	29.26	15.18	0.72	undetected	0.76	2.32	undetected	1.27	94.92	12.33
MU3	48.57	30.36	15.42	0.93	undetected	1.06	2.44	undetected	1.22	94.35	13.45
GK1	43.91	33.91	17.20	0.44	undetected	0.25	3.15	undetected	1.14	95.02	12.84
GK2	44.06	34.36	16.99	0.33	undetected	0.24	3.26	undetected	0.76	95.41	13.97
GK3	44.06	33.86	17.28	0.41	undetected	0.28	3.23	undetected	0.88	95.21	13.84

4.2.2. Pozzolanic Activity of the Clay Material

4.2.2.1. Pozzolanic activity based on electrical conductivity

This test evaluated the reactivity of clay with calcium hydroxide. The results show the variation of the electrical conductivity (EC) of the lime-water solution after the addition of clay, as a function of calcination temperature and time (Figure 4.2, Figure 4.3, and Figure 4.4).

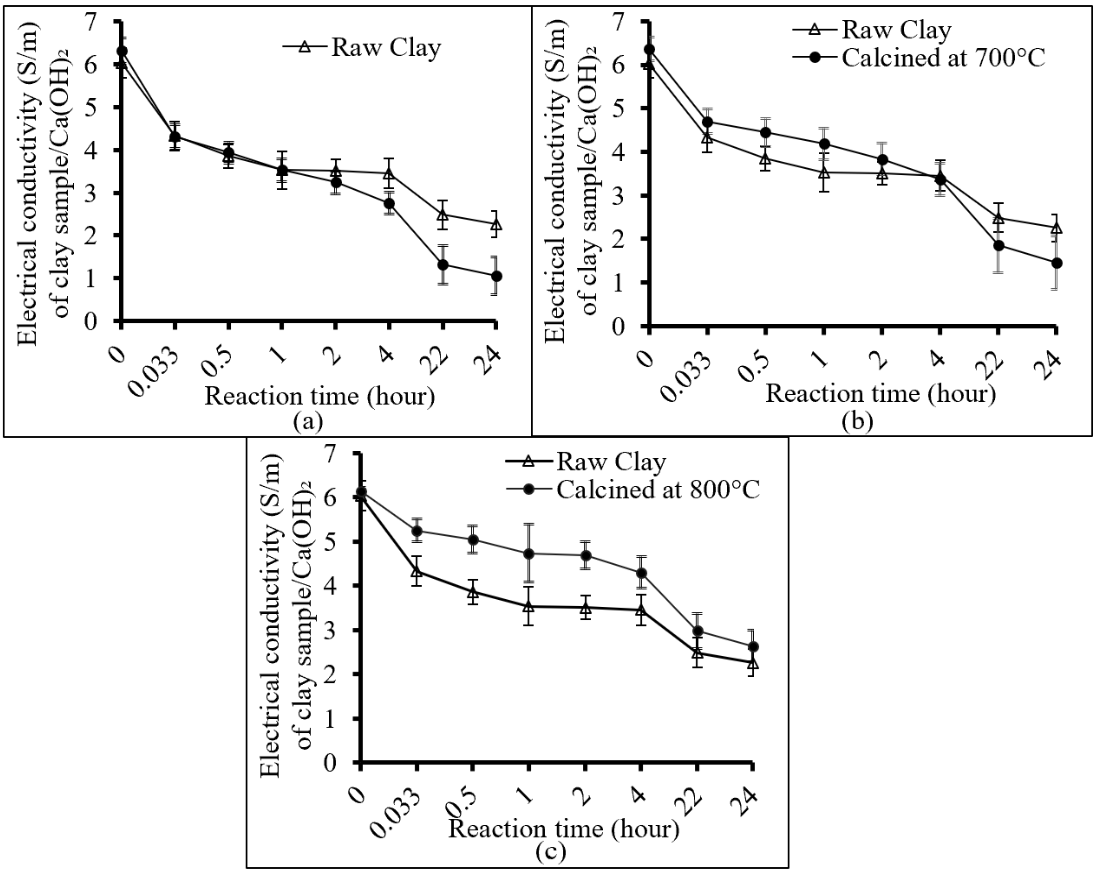

Figure 4.2: Electrical Conductivity (EC) of Aqueous Solutions of $Ca(OH)_2$ after the Addition of Clay from Gatundu (GT): (a) Clay Calcined at 600°C and Raw Clay, (b) Clay Calcined at 700°C and Raw Clay, (C) Clay Calcined at 800°C and Raw Clay.

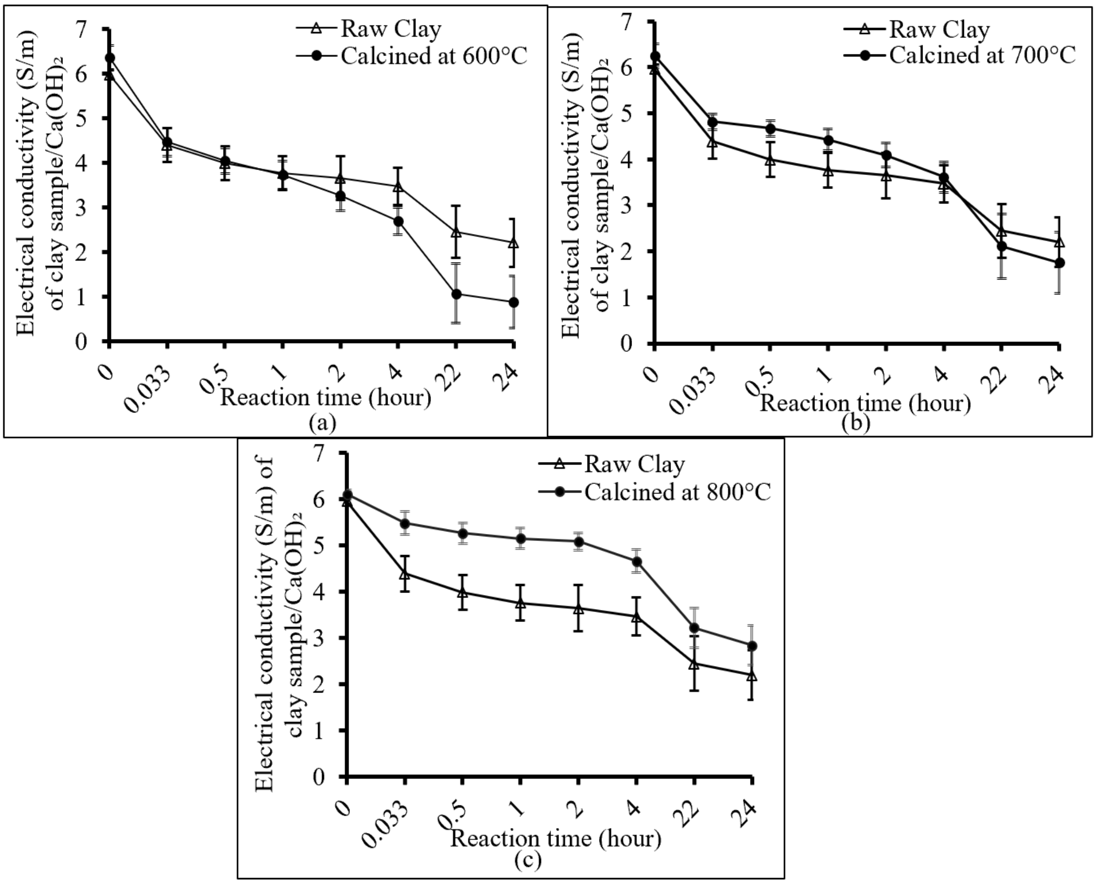

Figure 4.3: Electrical Conductivity (EC) of Aqueous Solutions of $Ca(OH)_2$ after the Addition of Clay from Murang'a Town (MU) : (a) Clay Calcined at 600°C and Raw Clay, (b) Clay Calcined at 700°C and Raw Clay, (c) Clay Calcined at 800°C and Raw Clay.

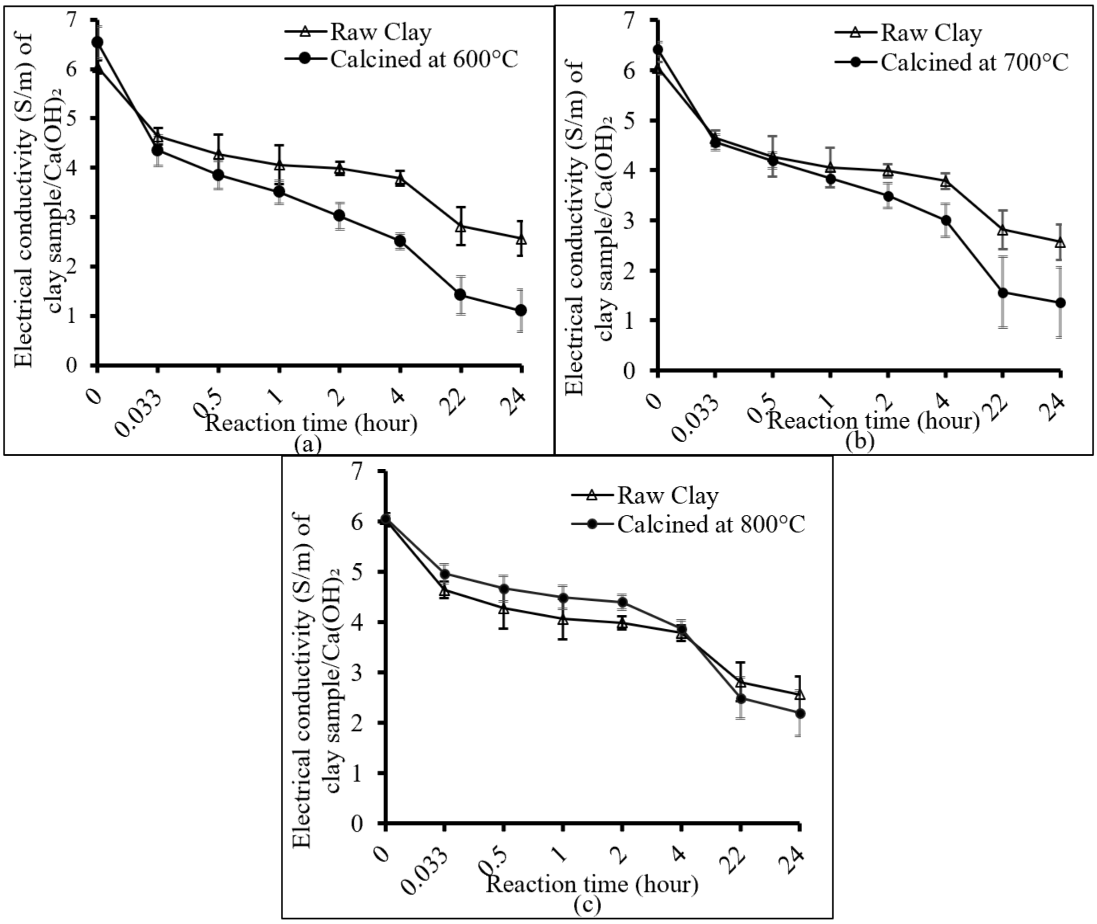

Figure 4.4: Electrical Conductivity (EC) of Aqueous Solutions of $Ca(OH)_2$ after the Addition of Clay from Gakoigo (GK) : (a) Clay Calcined at 600°C and Raw Clay, (b) Clay Calcined at 700°C and Raw Clay, (c) Clay Calcined at 800°C and Raw Clay.

In the first 2 minutes following the reaction of the saturated solution of $Ca(OH)_2$ and clay, a drastic drop of the electrical conductivity was observed (Figure 4.2, Figure 4.3, and Figure 4.4). Raw clay from Gatundu, Murang'a Town, and Gakoigo showed a 2-minute EC drop of 1.70, 1.57, and 1.40 S/m (Figure 4.2, Figure 4.3, Figure 4.4), respectively. When calcined at 600, 700, and 800°C, clay from Gatundu showed a 2-minute drop of 1.99, 1.65, and 0.88 S/m (Figure 4.2), respectively, compared to 1.89, 1.43, and 0.62 S/m for clay from Murang'a town (Figure 4.3), and 2.19, 1.85, and 1.10 S/m, respectively, for clay from Gakoigo (Figure 4.4). This significant drop in the initial stage was attributed to the high reduction rate of Ca^{2+} and OH^- ions, attributed to a fast fixation of the dissolved $Ca(OH)_2$ by calcined clay particles (Amin et al., 2015). As similarly reported by Tironi et al. (2013) and Walker and Pavía (2010), the EC later decreased slowly indicating a reduction in the content of chemically active components.

The maximum drop achieved for raw clay was 3.9 S/m after 24 hours for both Gatundu (GT) and Murang'a town (MU) clays (Figure 4.2a, and Figure 4.3a), compared to 3.6 S/m for GK clay (Figure 4.4a). However, after calcination, GK reactivity significantly increased with EC drops of 5.44, 5.07, and 3.95 S/m for clay calcined at 600°C (Figure 4.4a), 700°C (Figure 4.4b), and 800°C (Figure 4.4c), respectively, compared to 5.26, 5.48, 4.9 S/m (Figure 4.2a, Figure 4.2b, and Figure 4.2c, respectively), and 4.5, 3.56 and 3.33 S/m (Figure 4.3a, Figure 4.3b, and Figure 4.3c, respectively) for GT and MU, respectively, after 24 hours. The drop in electrical conductivity of clay calcined at 600°C (Figure 4.2a, Figure 4.3a, and Figure 4.4a) was generally greater than 700°C (Figure 4.2b, Figure 4.3b, and Figure 4.4b) and 800°C (Figure 4.2c, Figure 4.3c, and Figure 4.4c). This indicated that clays calcined at 600°C possess better pozzolanic reactivity, due to the presence of amorphous silica, which consumes the Portlandite phases to form additional C-S-H phases (Khan et al., 2022; Setina et al., 2013). Thus, the greater the drop in EC, the more reactive the material (Tironi et al., 2013). The low reactivity observed at 800°C could be explained by a recrystallization of mineral phases, oxidation of iron oxides and its transformation into hematite, which ultimately led to a decrease in the amorphous phases when the heating temperature increases to 800°C (Khan et al., 2022).

Results from the analysis of variance (see Appendix IV.a) (confidence level of 95%) showed that both clay type and calcination temperature had a significant effect on the electrical conductivity with p-values of $2.25e^{-05}$ and $< 2e^{-16}$, respectively. Moreover, an interaction between the clay type and the calcination temperature (p-value = $8.05e^{-13}$) was also observed. This could be due to the differences in the chemical and mineralogical compositions which affected the dehydroxylation degree of the clays (Donatello et al., 2010; Fernandez et al., 2011; Garcia-Valles et al., 2020; Schamban et al., 2002). A study by Shvarzman et al. (2003) reported that clay minerals such as Kaolinite achieved relatively low-level of dehydroxylation degree (less than 0.18) at a calcination temperature below 450°C. However, in the range of 570-700°C, the kaolinite was fully dehydroxylated (0.95 to 1.00). In addition, Bich et al. (2009) demonstrated that Metakaolin (calcined at 500°C) achieved a dehydroxylation degree of 0.50 and did not consume any calcium hydroxide during the pozzolanic reaction. However, the highest calcium hydroxide consumption (>90%) was achieved for samples with a degree of dehydroxylation > 0.95 (calcined at a temperature of 650°C). The individual comparison showed that there was no substantial difference between EC values for raw clay and clay calcined at 700°C (Figure 4.2b, Figure 4.3b, and Figure 4.4b), and raw clay and clay calcined at 800°C (Figure 4.2c, Figure 4.3c, and Figure 4.4c) at 24 hours. This closeness of the EC results showed the absence of a substantial effect when the calcination temperature excessively increases beyond 600°C (Khan et al., 2022). However, a substantial difference was observed between raw clay and clay calcined at 600°C. The results above suggested that the highest dehydroxylation degree was achieved at a calcination temperature of 600°C.

Based on the electrical conductivity test, calcined clay from Gakoigo showed higher reactivity compared to clay from Gatundu village and Murang'a town (see Appendix III.a, Appendix III.b, and Appendix III.c). A study by Walker and Pavía (2010) reported that the pozzolanic reaction is governed by the amount of active silica and alumina (SiO_2 + Al_2O_3), and the specific surface. From the chemical composition results above, it is apparent that there was no major difference between the aluminium oxide and silicon dioxide contents ($SiO_2 + Al_2O_3 \approx 78\%$) for the three investigated clays. Hence, the chemical composition could not be instrumental to explain the higher reactivity of Gakoigo clay as compared to the other analysed clays. However, not all the fraction of the clay structure is activated in the same degree and the dehydroxylated material contains amorphous, polycrystalline and crystalline fractions. Shvarzman et al. (2003) showed that both amount and type of the amorphous phase could influence the activity of additives, which covers the chemical activity (usually pozzolanic activity) and the micro-filler effect. In addition, Bich et al. (2009) demonstrated that the chemical activity is a linear function of the amorphous phase content in its range of 50-100%. In this study, the higher reactivity could be due to the amorphous phase content (SiO_2^{r-}+ $Al_2O_3^{r-}$) which could be more predominant in the Gakoigo clay than in the Gatundu and Murang'a town clays (Trusilewicz et al., 2012). This suggested that the amorphousness achieved after calcination determines the pozzolanic activity to a much greater extent than other pozzolan properties such as silica content (Walker & Pavía, 2010).

Pozzolanic reaction leads to a reduction of free Ca^{2+} and OH^- ions, which should lead to a decrease in electrical conductivity (Jurić et al., 2020). A study reported that when the variation of the electrical conductivity within the first 2 minutes exceeds 0.12 S/m, the material can be classified pozzolanic (Faleschini et al., 2021). This suggested that calcined clay possesses some pozzolanic properties. Similar observations were reported on the pozzolanic activity of clays calcined at different temperatures (Tironi et al., 2013). In contrast, Jurić et al. (2020) reported an increase in electrical conductivity with time for wood biomass fly ashes. The authors concluded that this method was not fully reliable for assessing the pozzolanic activity of fly ash due to the high content of soluble salts in the chemical composition, mostly Na_2SO_4, K_2SO_4 and $CaSO_4$, which increase the conductivity (Jurić et al., 2020). In the present study, the chemical composition reported no presence of CaO, MgO, Na_2O, and SO_3 in all clay samples. Thus, we might assume that there was no interference of soluble salts in the electrical conductivity values reported.

4.2.2.2. Pozzolanic activity based on Frattini test

The results of CaO and OH^- concentrations (mmol/l) from the Frattini test are reported (Figure 4.5, Figure 4.6, and Figure 4.7). Concentration values lying below the line (Portlandite saturation line) indicates removal of Ca^{2+} from the solution which is attributed to pozzolanic activity. Results lying on the line are indicative of zero pozzolanic activity and results above the line correspond to no pozzolanic activity (Donatello et al., 2010; Jurić et al., 2020).

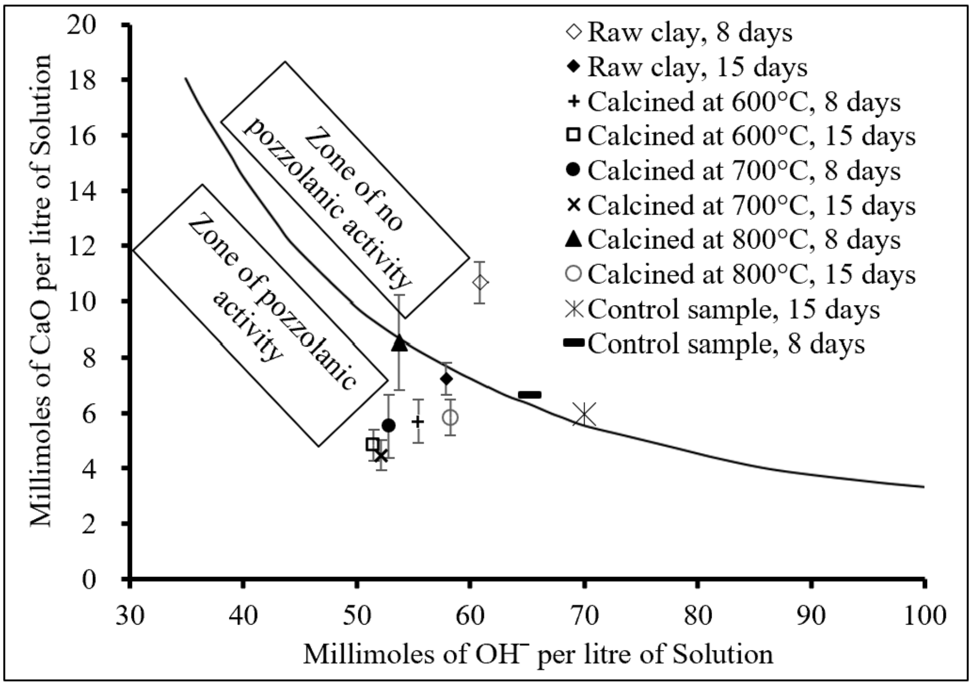

Figure 4.5: Frattini Test Results for Clay Material from Gatundu Tested after 8 and 15 Days.

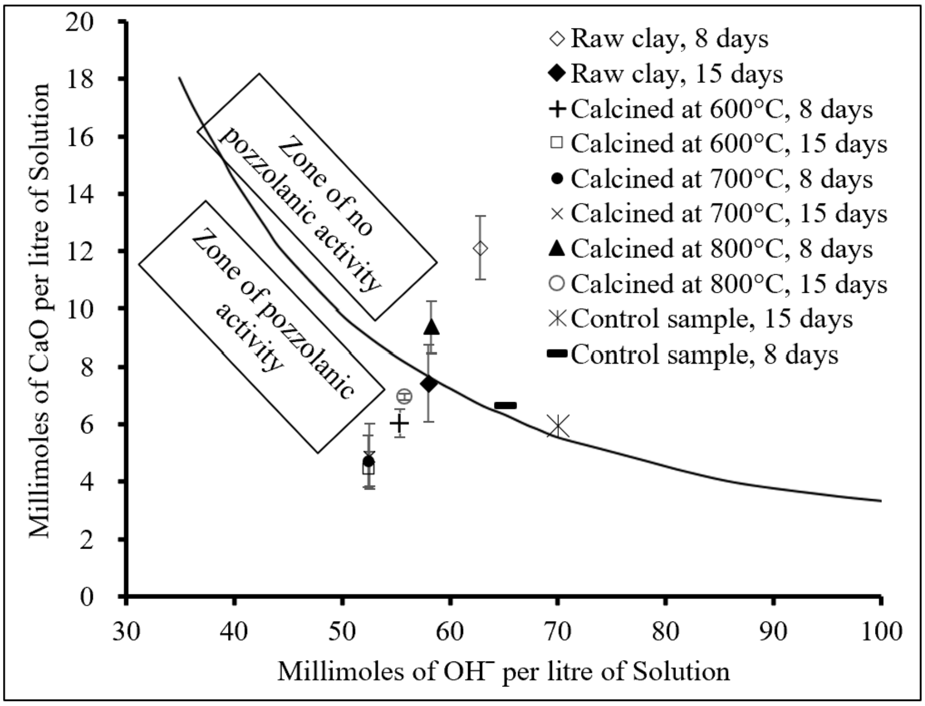

Figure 4.6: Frattini Test Results of Clay Material from Murang'a Town Tested after 8 and 15 Days.

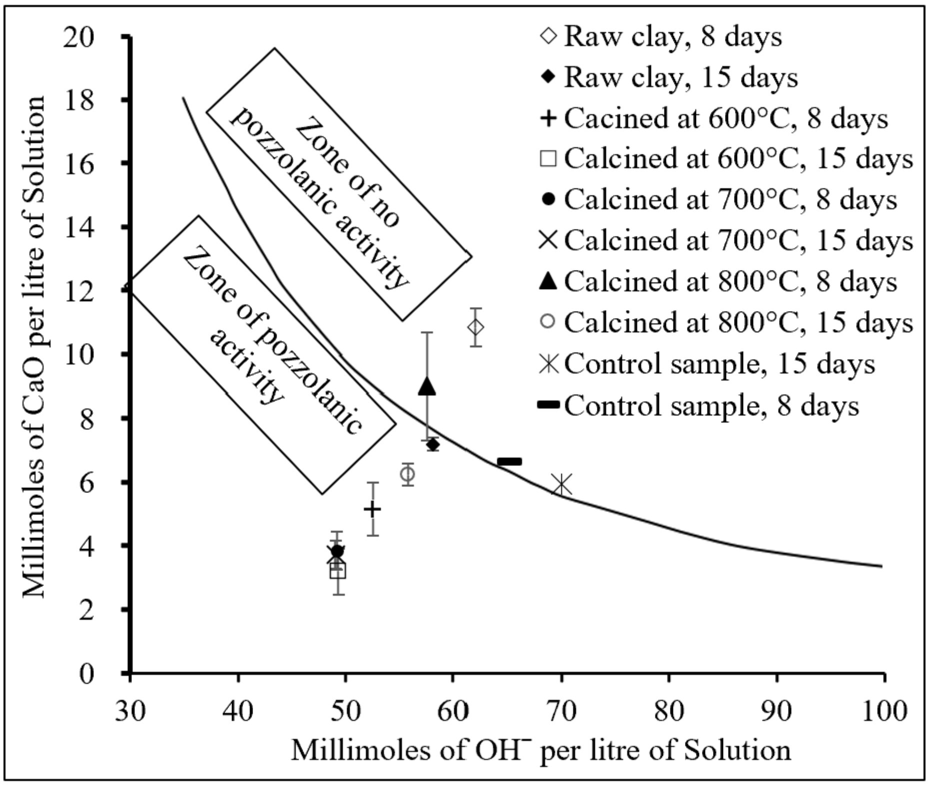

Figure 4.7: Frattini Test Results of Clay Material from Gakoigo Tested after 8 and 15 Days.

Raw clays from all sampling sites and clays calcined at 800°C showed a supersaturation in Portlandite at 8 days (concentration of $Ca(OH)_2$ above the normal saturation line at 40°C), and thus no pozzolanic activity. After 15 days, raw clay fell slightly below the Portlandite saturation line, indicating a slight positive pozzolanic activity (Jurić et al., 2020). On the other hand, the CaO and OH^- concentrations for samples calcined at 800°C shifted into the zone of pozzolanic activity at 15 days. This demonstrated the slow reactivity of this particular sample group at 15 days. This was also reported by Yanguatin et al. (2019) on excavated clay calcined at 550°C for 1 h. During calcination at high temperatures, the amorphous structure of clay breaks down and forms crystalline phases which are stable and less reactive (Garg & Skibsted, 2014). Thus, this could explain the lower pozzolanic activity achieved at 800°C (Khan et al., 2022).

Clays calcined at 600°C and 700°C showed higher pozzolanic activity than clays calcined at 800°C. At these temperatures, a significant undersaturation was observed with respect to Portlandite (Donatello et al., 2010; Jurić et al., 2020). This was due to a presence of large amorphous silica, which consumed the Portlandite phases to form C-S-H phases. A study reported that the temperature range of 600-900°C achieved the highest level of kaolin transformation to Metakaolin (Liu et al., 2017). Another study also reported that an almost complete dehydroxylation (0.99) could be achieved in the range of 700°C-800°C for Iranian kaolin (Souri et al., 2015). This suggested that the optimum temperature for dehydroxylation varied with clay type. This study found that calcination at 600°C and 700°C achieved better pozzolanic properties irrespective of the clay type. These results were in line with Jia et al. (2022) who revealed that alum sludge calcined at 600°C, 700°C, and 800°C showed positive pozzolanic activity at 15 days. These similar observations could be due to similar properties between calcined clay and calcined alum sludge. These properties included the particle size after calcination (< 75 µm) and the chemical composition (SiO_2 + Al_2O_3 + Fe_2O_3 equal to 83.7%) which was higher than 70% in accordance with ASTM C618 standards (Jia et al., 2022). The statistical analysis (see Appendix IV.b) at 95% confidence level showed that both the clay type (p-value = 0.02725) and the temperature (p-value < $2e^{-16}$) influenced the CaO consumption during the Frattini test. No interaction was observed between the clay type and the temperature (p-value = 0.28951) at 95% confidence level (see Appendix IV.b).

4.2.2.3. Pozzolanic activity based on compressive strength test

The results show the evolution of compressive strength (Figure 4.8, Figure 4.9, and Figure 4.10) and the strength activity index (SAI) (Figure 4.11) as a function of calcination temperature and curing time. In accordance with ASTM C618 standards, SAI values above 0.75 (represented by the dash line) qualify the clay as pozzolanic. The converse is that results lying below 0.75 correspond to an absence of pozzolanic activity.

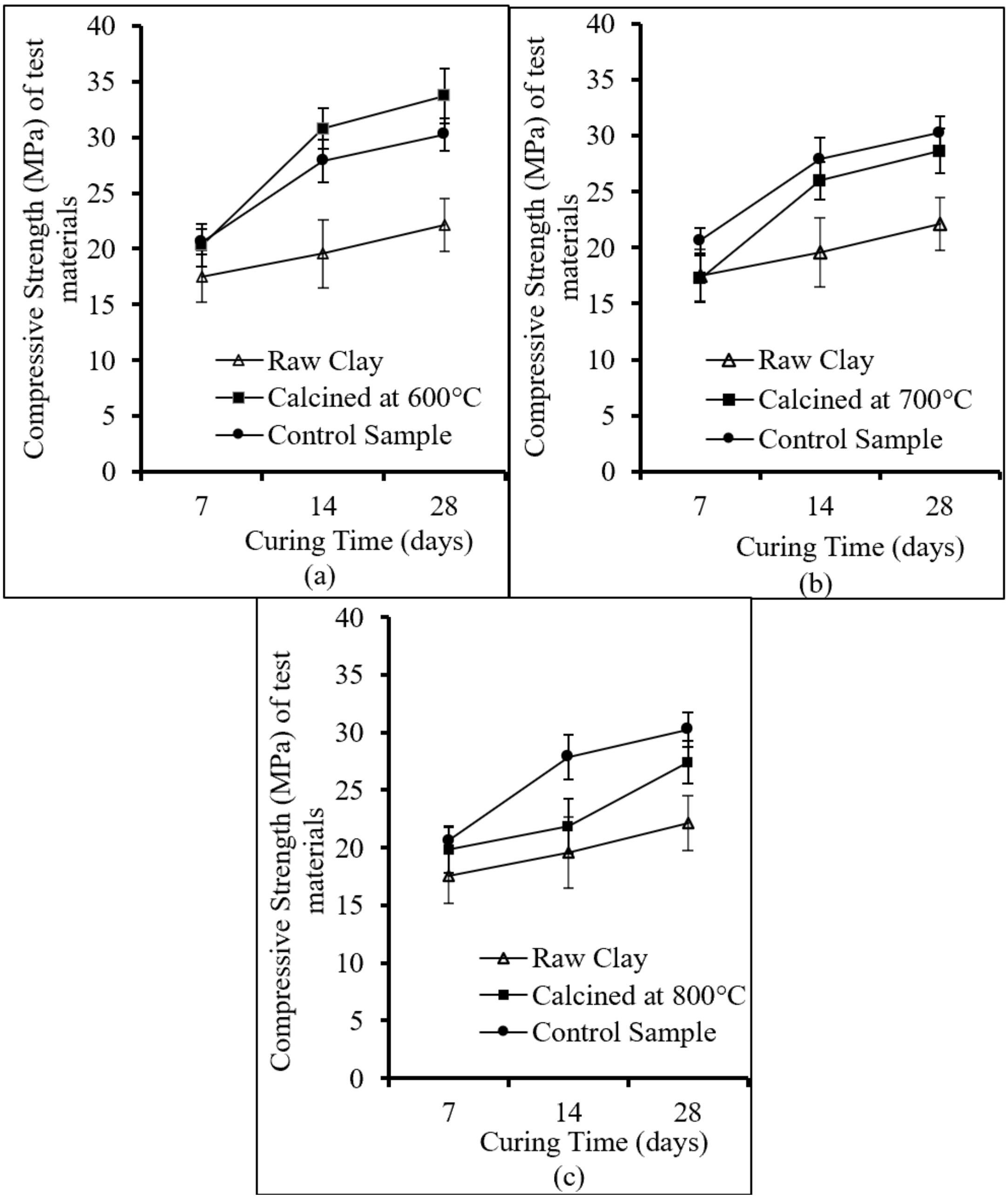

Figure 4.8: Compressive Strength of Blended Cement Blocks with 80% OPC and 20% Clay (GT) After 7, 14, and 28 Days: (a) Clay Calcined at 600°C, Raw Clay, and Control Sample, (b) Clay Calcined at 700°C, Raw Clay, and Control Sample, (c) Clay Calcined at 800°C, Raw Clay, and Control Sample.

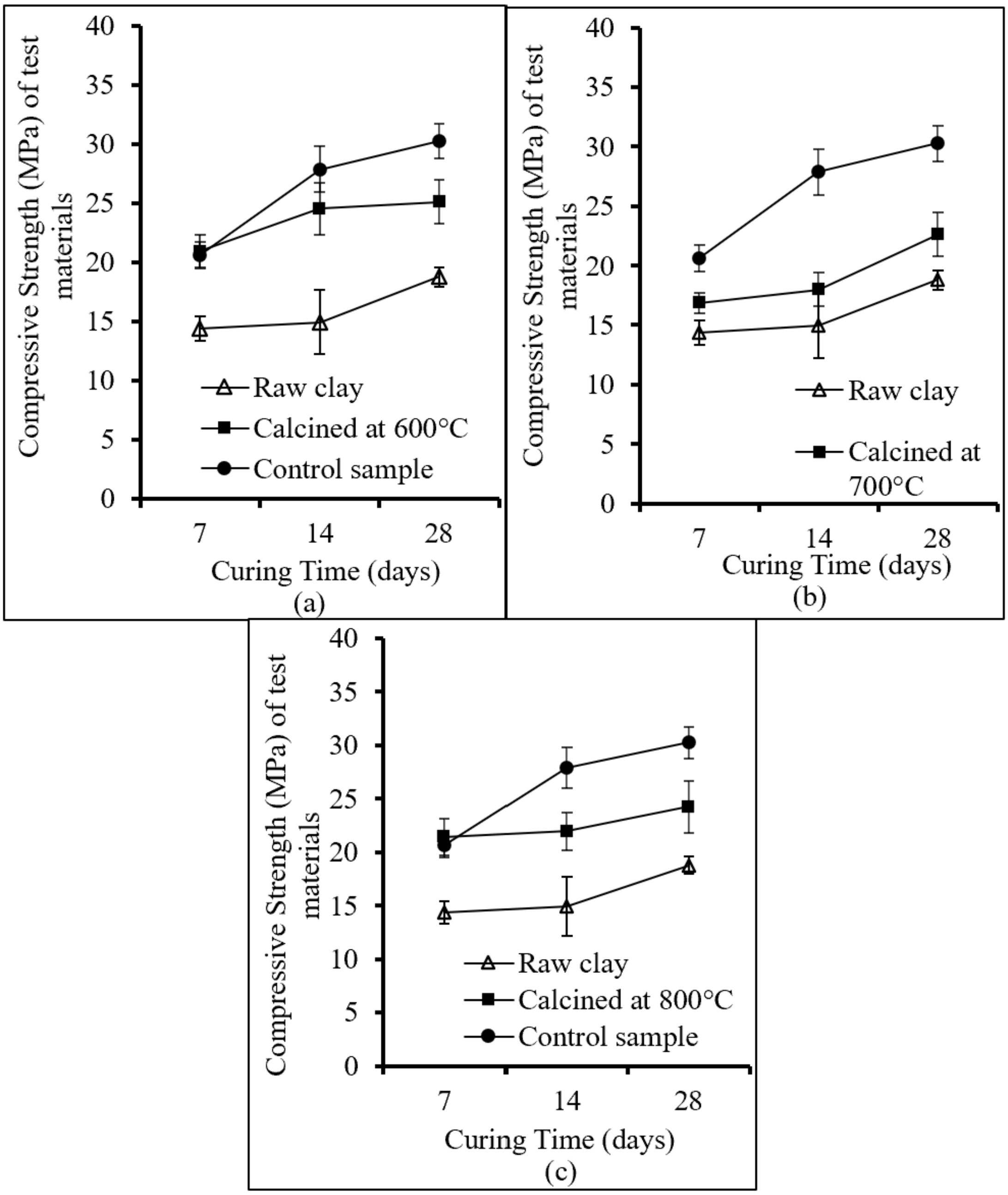

Figure 4.9: Compressive Strength of Cement Blocks with 80% OPC and 20% Clay (MU) after 7, 14, and 28 Days: (a) Clay Calcined at 600°C, Raw Clay, and Control Sample, (b) Clay Calcined at 700°C, Raw Clay, and Control Sample, (c) Clay Calcined at 800°C, Raw Clay, and Control Sample.

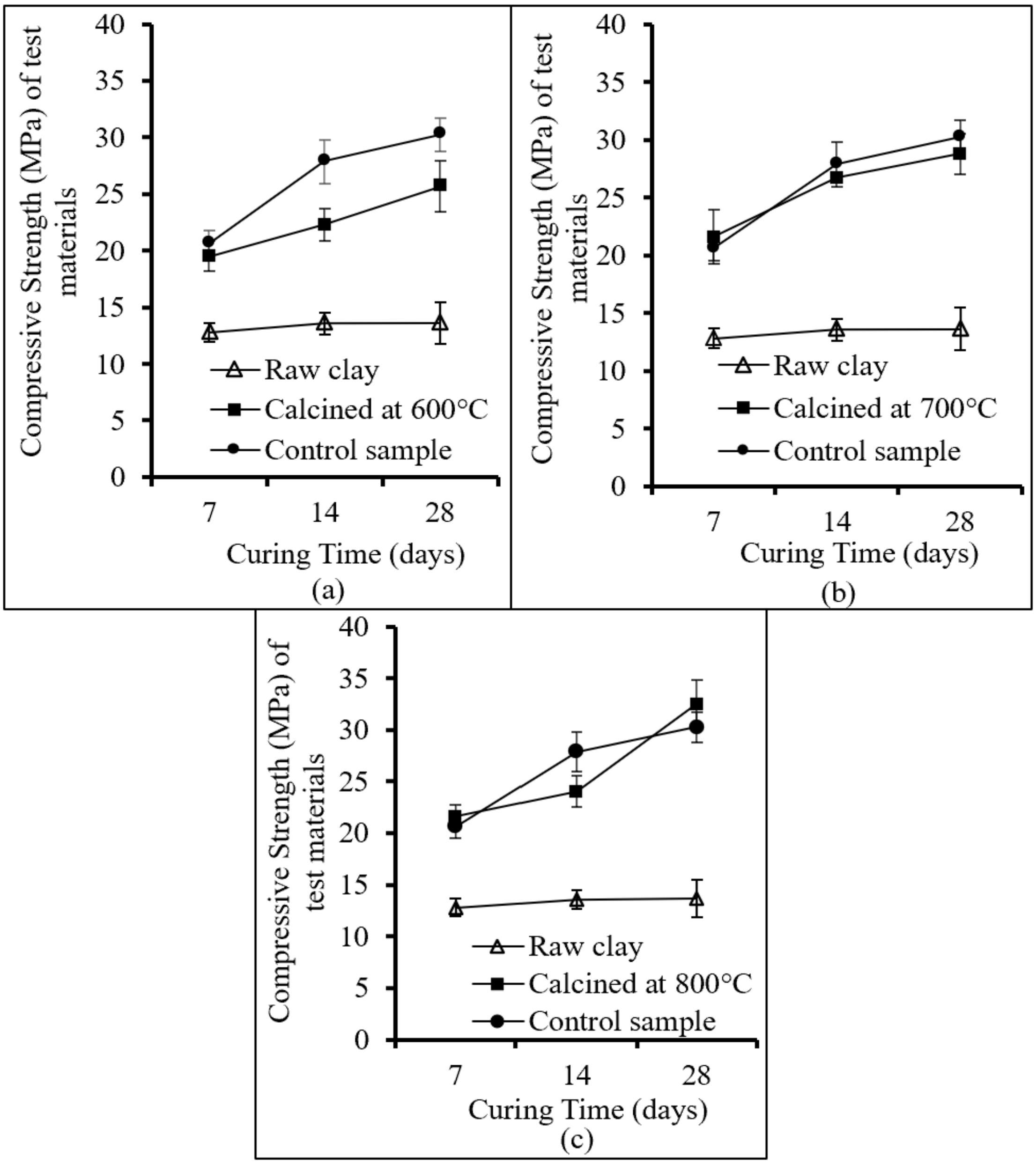

Figure 4.10: Compressive Strength of Cement Blocks with 80% OPC and 20% Clay (GK) after 7, 14, and 28 Days: (a) Clay Calcined at 600°C, Raw Clay, and Control Sample, (b) Clay Calcined at 700°C, Raw Clay, and Control Sample, (c) Clay Calcined at 800°C, Raw Clay, and Control Sample.

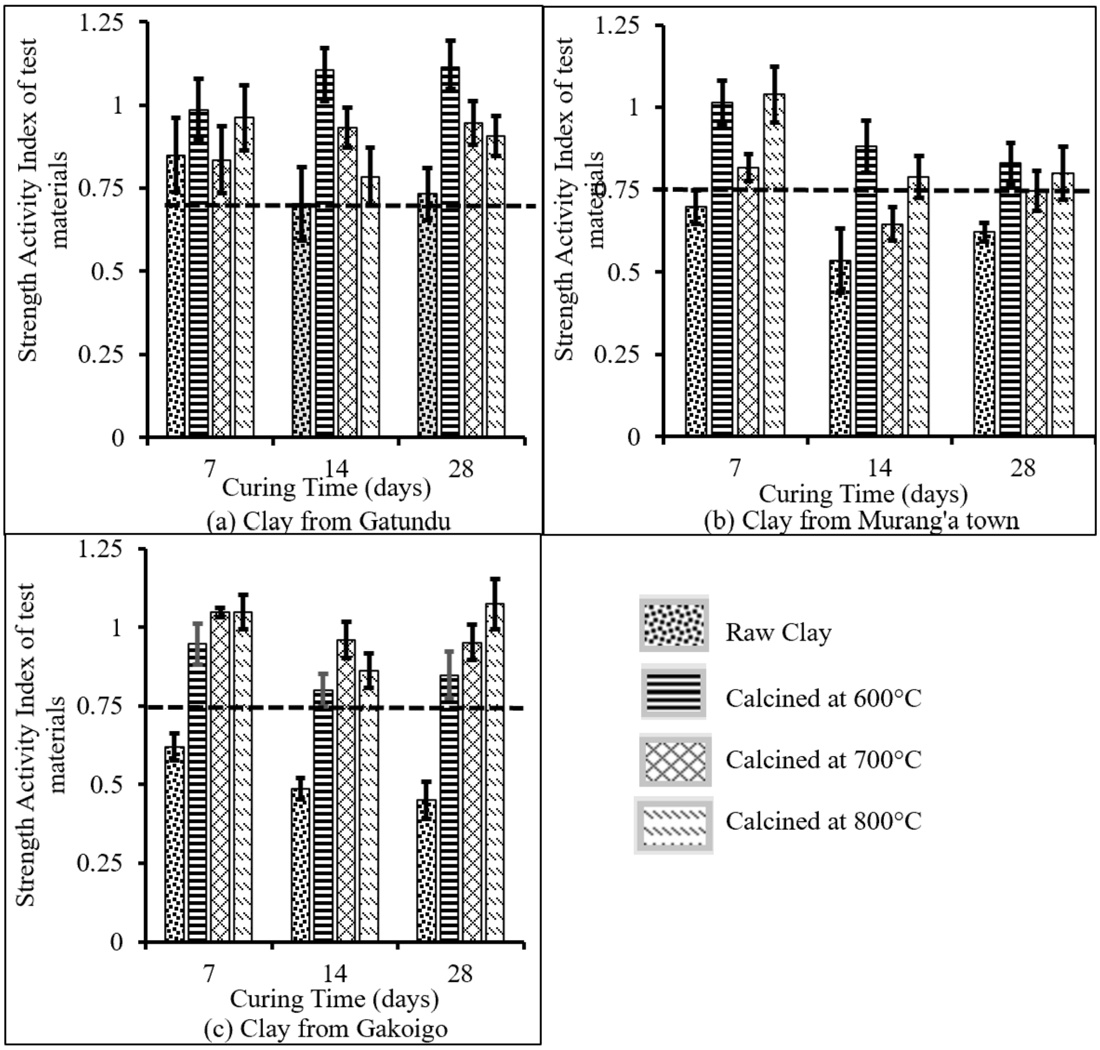

Figure 4.11: Strength Activity Index of Cement Blocks after 7, 14, And 28 Days

It was generally observed that the compressive strength increased with curing time (Figure 4.8, Figure 4.9, and Figure 4.10). However, after 14 days, a strength development rate of 37.95% (from 20.21 to 27.88 MPa) was observed for control samples. This rate was higher than that of blocks prepared with a blend of cement and clay, causing a general decrease in strength activity index at 14 days. Clay from Gakoigo (GK), calcined at 800°C, achieved a strength activity index (SAI) of 1.073 after 28 days (Figure 4.11c). This suggested that blended cement blocks made with 20% clay from Gakoigo (calcined at 800°C) increased the compressive strength by 7.3% compared to control samples (Figure 4.10c). Similarly, clay from Gatundu (GT), calcined at 600°C, maintained a SAI of 1 after 7 days, and increased to 1.11 (11% increase in compressive strength compared to control samples) after 28 days (Figure

4.11a). However, the SAI reduced to 0.90 when the calcination temperature increased to 800°C (Figure 4.11a), suggesting a 10% decrease in compressive in comparison to control samples (Figure 4.8c). All blended cement blocks made with 20% uncalcined clay decreased the compressive strength by more than 25% compared to control samples (Figure 4.8, Figure 4.9, and Figure 4.10), and presented an SAI below 0.75 (Figure 4.11). This suggested that clays could not be used as supplementary cementitious materials in their uncalcined state.

The process of dehydroxylation is often accompanied by partial or complete clay transformation, from crystalline to amorphous phase when the temperature increases, resulting in increased strength development (Yanguatin et al., 2019). This could explain the maximum strength activity index achieved by clay from Gakoigo, calcined at 800°C (Figure 4.10c and Figure 4.11c). However, depending on the clay type, the chemical and mineralogical composition, an excessive increase in the calcination temperature may lead to the recrystallization of mineral phases. This causes a decrease in the amorphous phases, and the compressive strength as a result. This could explain the lower performance of clay from Gatundu when the temperature increased from 600°C to 800°C (Figure 4.11a) (Khan et al., 2022). Compared to GK and GT, MU did not perform well at all temperatures.

The analysis of variance (see Appendix IV.c) at 95% confidence level showed that both temperature and clay type had a significant effect on the compressive strength, with p-values equal to $< 2e^{-16}$ and $3.09e^{-10}$, respectively. An interaction was also observed between the temperature and the clay type (p-value $1.94e^{-13}$). The individual comparison between raw and calcined clays (Figure 4.8, Figure 4.9, and Figure 4.10) showed that there was a significant difference between the compressive strength of the uncalcined and calcined clay at all ages. This study found that the temperature range of 600-800°C achieved a SAI > 0.75 at 7 and 28 days in line with ASTM C618 criteria (Figure 4.11).

Amin et al. (2015) have reported that a 30% replacement rate of cement with clay, calcined at 800°C, achieved a strength activity index of 1.02 (SAI > 0.75). On the other hand, a study achieved an optimum SAI of 0.9 for wood biomass fly ash at 28 days with a replacement of 15% (Jurić et al., 2020). In contrast, another study reported a SAI < 0.75 for alum sludge calcined at 600°C after 7 and 28 days, compared to 800°C which achieved a SAI of 1.14 at 28 days (Jia et al., 2022). In this study, the optimum temperature was 600°C. The difference with Jurić et al. (2020) could be due to the nature and quality of the clay. These factors affect the dehydroxylation degree and the content of amorphous phases after calcination (Tironi et al., 2013).

Several studies reported the strength performance of various pozzolanic materials. A study reported that the replacement of 50% lime with calcined clay achieved a mechanical index similar to ground granulated blast furnace slag (Walker & Pavía, 2010). The strength achieved was 69% higher than rice husk ash and micro-silica, and 89% higher than pulverised fly ash. In contrast, Faleschini et al. (2021) reported that a 50% cement replacement with municipal solid waste incinerator bottom ash (MSWI BA) caused about 50% strength loss in cement blocks. However, a 10% replacement led to a slight strength increase after 28 days of curing. The authors argued that replacing huge amounts of cement with pozzolanic materials induces severe strength loss due to the weaker nature of the ash (Faleschini et al., 2021). Another study reported that a 20% cement replacement with uncalcined ultrafine volcanic ash could achieve a SAI of 1.02 only after 91 days of curing (Khan et al., 2022). Similarly, Jurić et al. (2020) reported a SAI of 1 for cement blocks containing 15% wood biomass fly ashes after 365 days of curing. In contrast, this study found that calcination of clay increased the strength activity index of cement blocks from less than 0.75 to about 1 after 28 days of curing. Thus, compared to calcined clay, other pozzolanic materials demonstrated a delayed pozzolanic action (Khan et al., 2022).

To define the pozzolanic activity of calcined clays, various authors (Donatello et al., 2010; Tironi et al., 2013) recommended the use of a combination of the electrical conductivity, Frattini test, and the compressive strength test. The results obtained were summarized and compared with existing standards to evaluate the suitability of analysed clay for application as a pozzolanic material (Table 4.2). In this study, only uncalcined clays failed to meet the requirements for application as a replacement for cement. Hence, a thermal treatment 600-800°C produces enough dehydroxylation to transform the clays into supplementary cementitious materials. In particular, clay calcined at 600°C showed better pozzolanic activity for the electrical conductivity test, Frattini test and compressive strength test. Based on the results above, it is relatively efficient and cost-effective to calcine clay at 600°C. Furthermore, the soil texture analysis showed that clay from Gakoigo was the finest of all the samples collected. For this reason, clay from Gakoigo calcined at 600°C was considered for stabilization tests.

Table 4.2: Pozzolanic Activity of Analysed Clays Compared with the Standards (ASTM C618 and EN196-5)

Criteria & Standards		**Material evaluated**											
		Gatundu Clay				Murang'a Town Clay				Gakoigo Clay			
		Raw	600	700	800	Raw	600	700	800	Raw	600	700	800
XRF	> 70%	94	94	94	94	94	94	94	94	95	95	95	95
EC test	0.12	1.7	1.9	1.6	0.8	1.5	1.8	1.4	0.6	1.4	2.2	1.8	1.1
Frattini test	-	F	P	P	P	F	P	P	P	F	P	P	P
SAI	> 0.75	0.73	1.11	0.94	0.90	0.62	0.83	0.75	0.80	0.45	0.85	0.95	1.07

*P: Pass

*F: Fail

4.3. Effect of Calcined Clay as a Replacement for Cement on the Strength and Water Absorption of Rammed Earth for Floor Construction

4.3.1. Characteristics of Experimental Soils

The characterization results of black cotton soil and murrum soil are presented (Table 4.3). It was observed that black cotton soil had a clay content (69%) higher than murrum soil (28%). Black cotton soil had 0% gravel fraction compared to 44.2% for murrum soil (see Appendix V). The liquid limit of black cotton soil was 44% while the plasticity index was 22% (Table 4.3). The classification of the soils in terms of shrinkage limit (SL) showed that black cotton soil was of poor quality (SL = 14.4%), while murrum soil was classified as a medium soil (SL = 7.3%) (Ikeagwuani et al., 2019). In accordance with the Unified Soil Classification System, murrum soil was classified as a coarse-grained soil (clayey sand - SC) while black cotton soil was identified as a fine-grained soil (inorganic clay of low plasticity- CL). On the other hand, the optimum moisture content (OMC) and the maximum dry density (MDD) of black cotton soil were 28% and 1344 kg/m^3, while murrum soil showed an OMC and MDD of 22% and 1531 kg/m^3, respectively.

Table 4.3: Properties of Black Cotton Soil and Murrum Soil

Properties	Murrum Soil	Black Cotton Soil
Percentage passing through Sieve No. 200	49.24	99.28
Gravel fraction (%)	44.2	0.7
Sand fraction (%)	7.2	1.7
Silt (%)	20.7	27.7
Clay (%)	28.0	69.9
Specific gravity (Gs)	2.5	2.4
Liquid limit (LL) %	32	44
Plastic limit (PL) %	22	22
Plasticity index (PI) %	10	22
Linear Shrinkage (LS) %	7.3	14.4
Colour	Brown	Grey
UCS (MPa)	0.39	0.29
OMC (%)	21	26
MDD (kg/m^3)	1531	1344
USCS classification	SC	CL

4.3.2. Compressive Strength of Stabilized Rammed Earth

The unconfined compressive strength is one of the common parameters for expressing the strength of stabilized rammed earth. It demonstrates the effect of the binder on soil strength (Sheikh et al., 2022). In this study, the binder content varied at 5%, 10%, and 15% of the binder-soil mixture (Figure 4.12, Figure 4.13, and Figure 4.14).

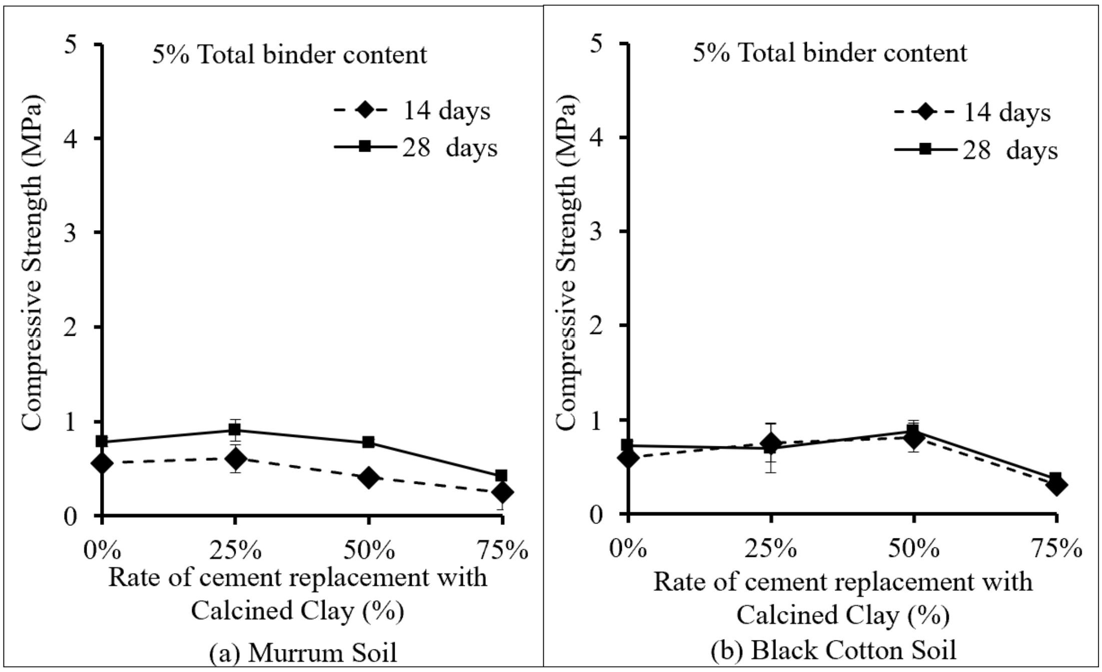

Figure 4.12: Compressive Strength of Murrum and Black Cotton Soils for 5% Binder Content

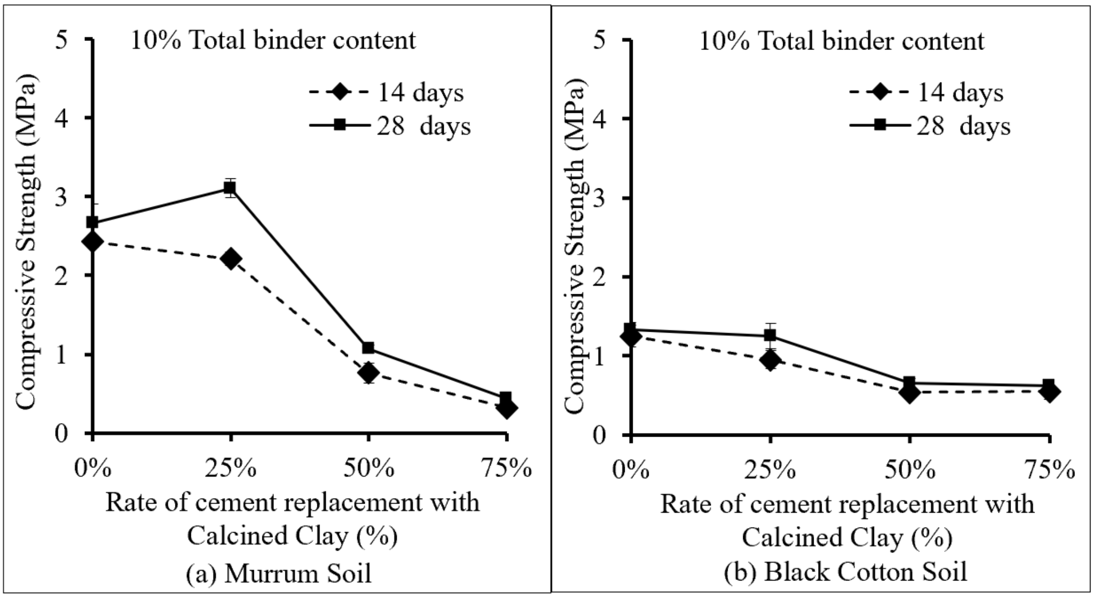

Figure 4. 13: Compressive Strength of Murrum and Black Cotton Soils for 10% Binder Content

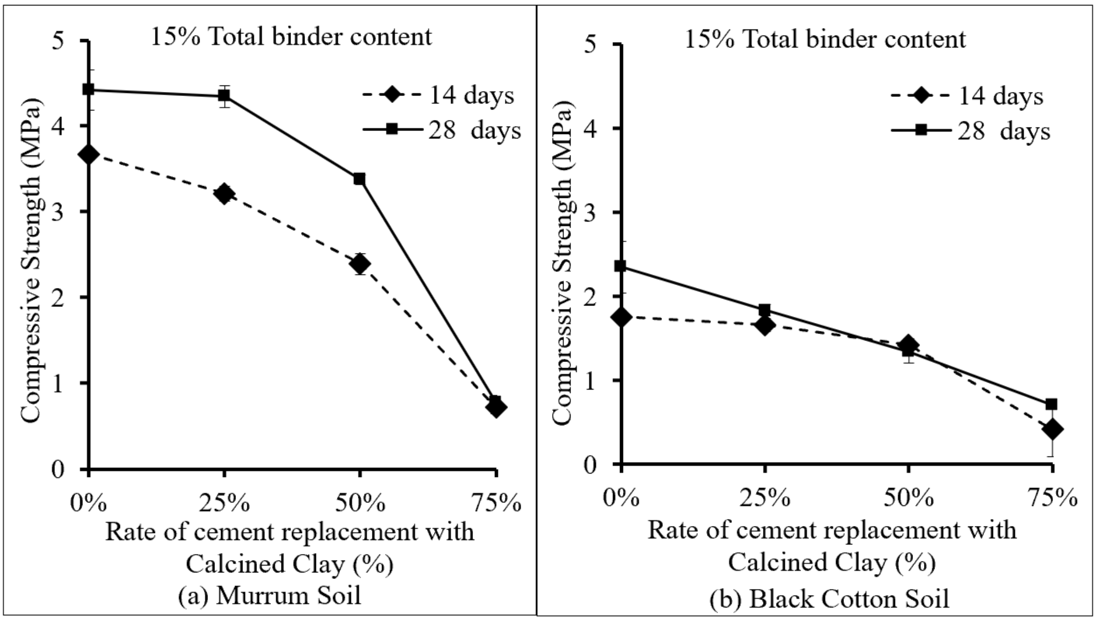

Figure 4.14: Compressive Strength of Murrum and Black Cotton Soils for 15% Binder Content

The compressive strength generally decreased with increasing rate of cement replacement with calcined clay (Figure 4.12a, Figure 4.12b, Figure 4.13a, Figure 4.13b, Figure 4.14a, and Figure 4.14b). For general construction, the target minimum compressive strength for stabilized soil after 28 days of curing should be 2.5 MPa (KS 02:1070:1993). The compressive strength achieved with 5% binder content did not meet the minimum strength requirement. The maximum strength achieved for stabilized rammed black cotton was 2.34 MPa for 15% cement content after 28 days (Figure 4.14b). As cement replacement with calcined clay increased to 25%, the compressive strength decreased to 1.83 MPa, still below the 2.5 MPa recommended threshold (Figure 4.14b). A study by Wang et al. (2018) reported that weakly cohesive soils, mainly composed of finer particles from 5-75 µm, need large amount of hydration products to bond the soil particles. As a result, hydration products resulting from the pozzolanic reactions between Portland cement and calcined clay were not enough to bond black cotton soil particles firmly. Thus, stabilized rammed black cotton did not meet KS 02:1070:1993 standards.

A study by Wang et al. (2018) demonstrated that strength development depended on the ratio of cement and the pozzolanic material in the binder mixture. This is responsible for the formation of calcium-silicate-hydrates (C-S-H) gels as a result of pozzolanic reactions. For rammed murrum stabilized with 10% binder content, this study found that a ratio of 75% cement and 25% calcined clay achieved a compressive strength of 3.10 MPa, compared to 2.65 MPa when cement is used alone (Figure 4.13a). For a 15% binder content, a ratio of 75% cement and 25% calcined clay achieved a compressive strength of 4.34 MPa, compared to 4.42 MPa when cement is used (Figure 4.14a). Beyond 25% cement replacement, the strength substantially decreased (see Appendix VII.a).

Similar results were reported by Wang et al. (2018), who showed that the 28-day compressive strength of cemented silty soil improved 1.22-1.83 times by incorporating 15-25% coal-bearing Metakaolin. Raj et al. (2018) also found that a compressive strength of 2.2 MPa could be achieved using 30% binder content (60:40 mix of Bagasse Ash and Fly ash) along with 6% cement as an activator, and 64% soil. These results were attributed to the formation of cementitious phases with distinct chemical composition and morphologies in the stabilized rammed earth (Naeini et al., 2021; Raj et al., 2018). Rammed murrum stabilized with a binder content of 15% and a 50% cement replacement also attained a strength of 3.37 MPa (>2.5 MPa) after 28 days (Figure 4.14a). However, the amount of Portland cement and calcined clay required to make this binder is higher than using 10% binder mixture for similar strength performances (> 2.5 MPa). To make a cost-effective rammed earth floor, 10% binder content with 25% calcined clay was an adequate mix.

Some other guideline reported by Thuysbaert (2012) indicated that an acceptable compressive strength of rammed earth for non-load bearing applications is 1 MPa. In contrast, KS 02:1070:1993 requires 2.5 MPa for stabilized soil. As earthen floors are particularly non-load bearing, it is assumed that applied live loads are lower compared to load-bearing structures. Thus, the threshold of 1 MPa could also be considered to qualify stabilized rammed earth for floor construction. This would therefore imply that rammed black cotton stabilized with 10-15% binder content and 25% calcined clay could be an adequate mix for non-load bearing applications (Figure 4.13b and Figure 4.14b). This would also be the case for rammed murrum stabilized with 10-15% binder content and up to 50% calcined clay (Figure 4.13a and Figure 4.14a).

4.3.3. Capillary Water Absorption of the Experimental Blocks

Capillary absorption of water mainly depends on the presence of medium and large pores (diameter > 2.5 µm) inside the stabilized soil (Ma & Liu, 2020). It was generally observed that an increase in cement replacement with calcined clay increased water absorption (Figure 4.15, Figure 4.16, and Figure 4.17). Similarly, as the contact time between water and the base surface of the rammed earth increased, the capillary water absorption increased for all the samples (see Appendix VI).

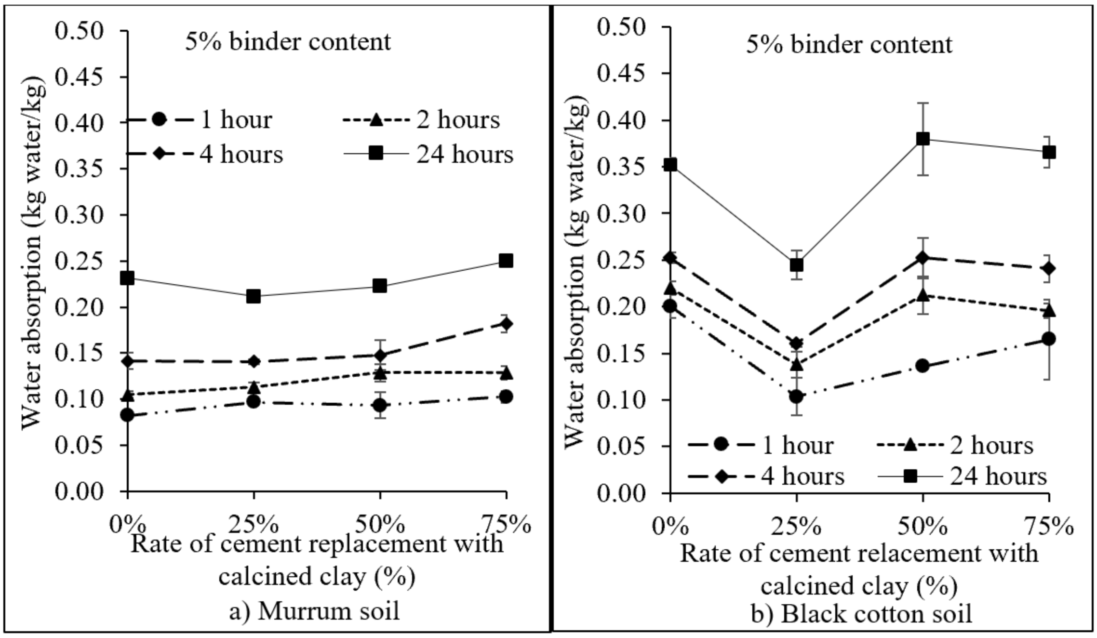

Figure 4.15: Water Absorption in Murrum and Black Cotton Soils for 5% Binder Content

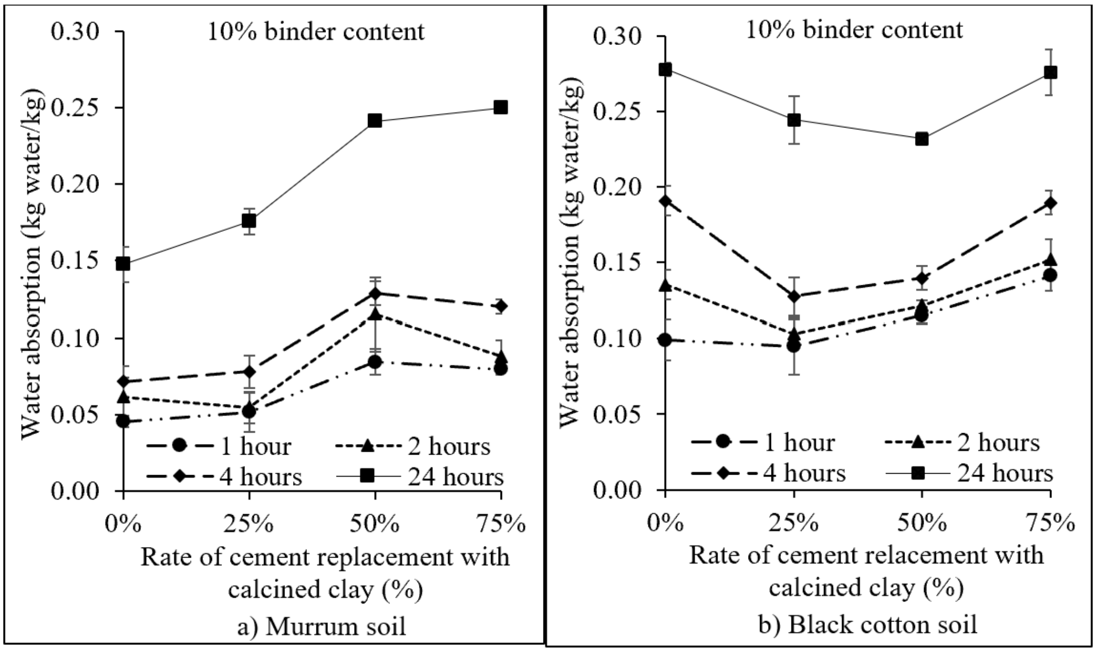

Figure 4.16: Water Absorption in Murrum and Black Cotton Soils for 10% Binder Content

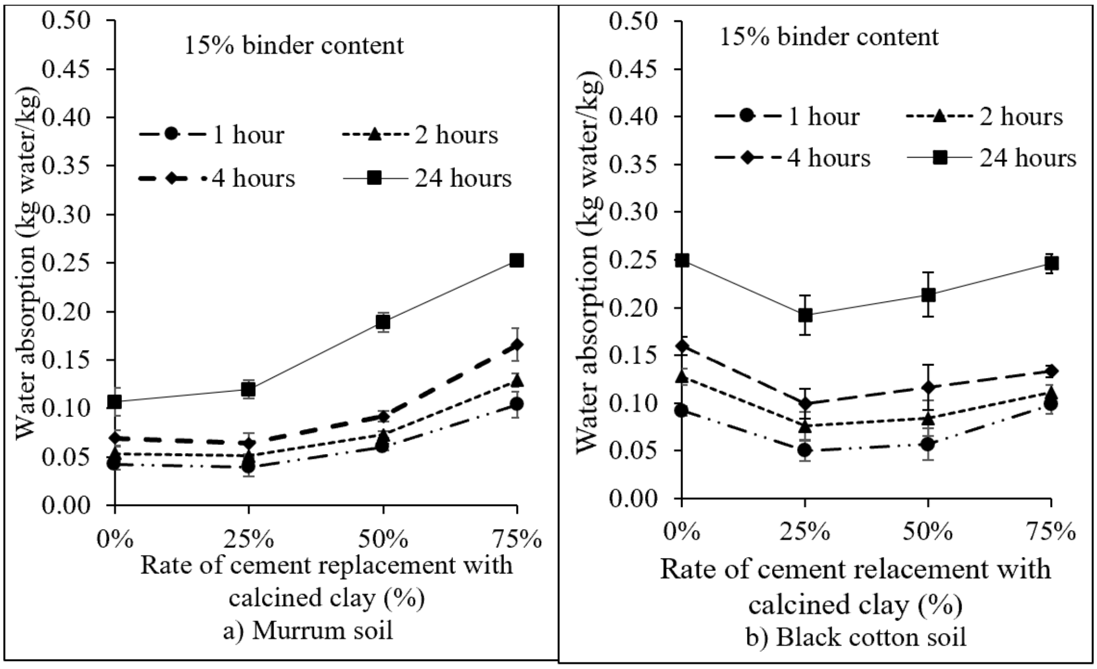

Figure 4.17: Water Absorption in Murrum and Black Cotton Soils for 15% Binder Content

For stabilized rammed murrum, the results showed that cement replacement with 25% calcined clay did not lead to a substantial increase in capillary water absorption (0.21, 0.18, and 0.12 kg water/kg soil block after 24 hours for a binder content of 5%, 10%, and 15%, respectively) (Figure 4.15a, Figure 4.16a, Figure 4.17a). The trend was similar to that of control specimens (0% cement replacement). Furthermore, the results were not substantially different after 24 hours of contact with water (0.23, 0.15, and 0.11 kg water/kg soil block for a cement content of 5%, 10%, and 15%, respectively) (Figure 4.15a, Figure 4.16a, Figure 4.17a). The soil texture results showed that calcined clay was finer than murrum soil. As a result, calcined clay might have filled the pores and reduced the total porosity, increasing seepage paths and blocking connected pores in the stabilized rammed earth (Wang et al., 2018). Owing to the effective filling effect, a 25% cement replacement achieved acceptable capillary water absorption (Wang et al., 2018). Beyond this critical value, capillary water absorption increased substantially (see Appendix VI.a).

This study found that capillary water absorption of stabilized rammed black cotton was minimized at 25% calcined clay. As reported by Wang et al. (2018), it could be possible that black cotton soil stabilized with cement alone had a loose structure and widely distributed macro-pores due to limited amounts of hydration products. This meant that the clayey soil particles could not be tightly bonded. However, due a replacement of 25% cement with calcined clay, hydration products were densely deposited and attached closely on the surface of the soil particles, and the soil particles became closely connected. As the cement replacement rate increased to 50% and 75%, the capillary water absorption substantially increased. This was in accordance with Wang et al. (2022) who observed that pozzolanic materials such as fly ash could minimize capillary water absorption of cement-based materials as long as the dosage did not exceed a critical value. Thus, beyond this critical value (25% cement replacement with calcined clay), there was a reduction of hydration products preventing the soil particles from being combined firmly (Ezreig et al., 2022). Compared to black cotton soil, murrum soil achieved the lowest capillary water absorption for all mix proportions. These results demonstrated the difficulty in stabilizing black cotton soil (see Appendix VI).

Water absorption has an important influence on the durability of cement-based materials and its value is closely related to pores structures (Zhao et al., 2019). Water is the main cause of concrete physical and chemical deterioration (Wang et al., 2022). This study found that 10-15% binder content and 25% calcined clay limited water absorption in both murrum soil and black cotton soil (Figure 4.15, Figure 4.16, and Figure 4.17). Similar results were reported by Wang et al. (2022) who observed that a 30% to 40% rate of cement replacement with fly ash could decrease the water absorption of cement-based materials by 27.8% and 14.2%, respectively, compared to specimens stabilized with cement alone. This was attributed to improvements in the microstructure and increase in the density of pore structures when an appropriate dosage of fly ash was added to cement-based materials. To minimize moisture ingress, a similar study reported that the optimum level of binder content could be fixed at 6% good soils, and 9% for poor soils (Hall & Djerbib, 2004; Hall & Djerbib, 2006).

The durability of earthen structures is mainly related to the action of water on the walls. The first problem is mainly due to capillary flow (from ground to surface). The second comes from incident rainfall (Morel, 2012). In the context of this study, the durability of earthen floors is mainly influenced by capillary flow from ground and surface. In addition to decreasing water absorption through the addition of a binder, use of a dam-proofing barrier is often provided along the interface between the footing and the base for earthen walls (Morel, 2012). This could also be adopted in earthen floors, but the dam-proofing material should be capable of withstanding ramming without damage and an impermeable floor-finish could be laid on the surface (Morel, 2012).

4.3.4. Environmental Implications of Cement-Calcined Clay Stabilized Rammed Earth

This study has found that building materials made of cement alone achieve high compressive strength. However, cement replacement could result in considerable energy saving and improve the environmental performance of earth buildings (Arrigoni et al., 2017; Gomes et al., 2016). In Cameroon for instance, a comparative study indicated that a cement block house expends at least 1.5 times more embodied energy and emits at least 1.7 times more embodied CO_2 than earth or mud brick houses (Henry et al., 2014). In particular, Chel and Tiwari (2009) observed that the embodied energy per unit floor area of a reinforced cement concrete and mud house were 3702.3 MJ/m^2 and 2298 MJ/m^2, respectively. On the other hand, a study (Fernandes et al.,

2019) reported that soil transportation represents more than 80% of all environmental impact categories in the making of compressed earth blocks. Although rammed earth construction has the potential to use zero transport energy (presuming that the soil available on the construction site is suitable), stabilizers must also be transported from the nearest batching plant to the construction site (Arrigoni et al., 2017). This will make the constructed rammed earth floor a low-embodied carbon and low-waste alternative to concrete. It is therefore recommended that a calcination plant be publicly funded by the government or any other agency for local production of calcined clay. Thus, cement replacement, local acquisition of raw materials, and local production of calcined clay could significantly cut back on carbon emissions and embodied energy in rammed earth floor construction (Adegun & Adedeji, 2017).

A report by the Excellence for Design and Greater Efficiencies (2018) reported the embodied energy for different structures. For instance, an in-situ reinforced concrete floor slab for homes with a default thickness of 0.300 m and a default reinforcement of 33 kg/m^2 would have an embodied energy of 1,148 MJ/m^2. The same structure with cement replaced at 25% with ground granulated blast-furnace slag (GGBS) decreases the embodied energy to 595 MJ/m^2. Similarly, a replacement with 30% pulverised fly ash achieves an embodied energy of 605 MJ/m^2. On the other hand, rammed earth stabilized with 6-8% cement content achieved an embodied energy of 400-500 MJ/m^2, respectively. However, this could increase further proportionally with cement content (Akbarnezhad & Xiao, 2017); this study recommends to maintain the binder content to 10%. Furthermore, Zhou et al. (2017) indicated that replacing 20-30% cement with calcined clay would produce a cementitious binder with 18-27% lower carbon emissions due to an absence of a carbonation stage during clay calcination. In this study, cement was replaced with 25% calcined clay in stabilized rammed earth. Thus, a similar reduction in carbon emission may be expected when cement is partially replaced with calcined clay in rammed earth floor as evaluated by Zhou et al. (2017).

A case study by Cabeza et al. (2021) indicated that for common concrete preparation coupled with cement production, high energy is required, increasing the embodied energy in concrete to 0.78-1 MJ/kg, compared to 0.60 MJ/kg for rammed earth. Moreover, a comparative study indicated that rammed earth achieved an embodied carbon of 0.023-0.025 kg CO_2/kg, while common concrete varies between 0.10-0.16

kg CO_2/kg (Hammond & Jones, 2011). This suggests that switching from a concrete slab to stabilized rammed earth floor will lower the overall embodied energy and carbon of the floor.

CHAPTER FIVE

CONCLUSIONS AND RECOMMENDATIONS

5.1. Conclusions

This study investigated the performance of calcined clay from Murang'a County as a partial replacement for cement in rammed earth floor construction for low-income housing. The following conclusions can be drawn from this study:

- Clay calcination at 600-800°C provides sufficient pozzolanic activity. The variation in the pozzolanic activity of clay from different wetlands in the study site was not substantial. Use of calcined clay as a pozzolanic material could therefore be more environmentally sustainable compared to the use of cement alone.
- It is possible to use calcined clay as a partial replacement for cement in rammed earth floor construction. The feasible replacement rate of cement in the binder is up to a maximum of 25% calcined clay. Murrum soil stabilized with a binder content of 10-15% attains a water absorption of 0.11-0.18 kg water/kg soil block, and a compressive strength above 2.5 MPa. For a cement replacement rate below 25%, the strength performance of stabilized rammed murrum falls within the requirements of KS 02:1070:1993 standards (minimum of 2.5 MPa) after 28 days of curing. However, the binder could not stabilize black cotton soil.

5.2. Recommendations

5.2.1. Applications

This study recommends that cement manufacturers could incorporate calcined clay as a partial substitute for clinker in blended cement manufacturing. A calcination temperature of 600°C is recommended for this purpose. Coarse-grained and well-graded soils like Murrum are recommended for rammed earth floor construction. It is advised to maintain a 10% binder content and a 25% cement replacement rate. Black cotton soil is discouraged for rammed earth floor construction.

5.2.2. Further studies

This study identified some key areas which require further investigations. It is therefore recommended that:

1. A quantitative analysis should be undertaken to establish the cost and environmental impacts of the use of calcined clay in construction for possible up-scaling and adoption by cement manufacturers.
2. Field trials be conducted to monitor the durability and performance of rammed earth floors in actual environmental conditions. There is need for other studies to evaluate the life cycle and cost analysis of rammed earth floors produced with a mixture of calcined clay and Portland cement.

REFERENCES

Abdullah, A., Jaafar, M. S., Taufiq-Yap, Y. H., Alhozaimy, A., Al-Negheimish, A., & Noorzaei, J. (2012). The effect of various chemical activators on pozzolanic reactivity: A review. *Scientific Research and Essays*, *7*(7), 719-729. https://doi.org/10.5897/SRE10.858

Adegun, O. B., & Adedeji, Y. M. (2017). Review of economic and environmental benefits of earthen materials for housing in Africa. *Frontiers of Architectural Research*, *6*(4), 519-528. https://doi.org/10.1016/j.foar.2017.08.003

Adekitan, O. A., & Ayininuola, G. M. (2018). Calcined Clay-Cement Stabilisation – Physicochemical Attributes and Stabilised Strengths of a-1-a and a-2-6 Soils. In F. Martirena, A. Favier, & K. Scrivener (Eds.), *Calcined Clays for Sustainable Concrete* (Vol. 16, pp. 1-7). RILEM Bookseries. https://doi.org/10.1007/978-94-024-1207-9_1

Adeniyi, F. I., Ogundiran, M. B., Hemalatha, T., & Hanumantrai, B. B. (2020). Characterization of raw and thermally treated Nigerian kaolinite-containing clays using instrumental techniques. *SN Applied Sciences*, *2*(821). https://doi.org/10.1007/s42452-020-2610-x

Afrin, H. (2017). A Review on Different Types Soil Stabilization Techniques. *International Journal of Transportation Engineering and Technology*, *3*(2), 19-24. https://doi.org/10.11648/j.ijtet.20170302.12

Akbarnezhad, A., & Xiao, J. (2017). Estimation and Minimization of Embodied Carbon of Buildings: A Review. *Buildings*, *7*(5). https://doi.org/10.3390/buildings7010005

Al-Swaidani, A., Hammoud, I., & Meziab, A. (2016). Effect of adding natural pozzolana on geotechnical properties of lime-stabilized clayey soil. *Journal of Rock Mechanics and Geotechnical Engineering*, *8*(5), 714-725. https://doi.org/https://doi.org/10.1016/j.jrmge.2016.04.002

Al-Swaidani, A. M., Hammoud, I., Alghoraibi, I., & Meziab, A. (2019). Effect of adding nano-calcined clay and nano-lime on the geotechnical properties of expansive clayey soil. IOP Conf. Series: Materials Science and Engineering: 7th International Conference on Euro Asia Civil Engineering Forum, Stuttgart, Germany.

Altwair, N. M., Johari, M. A. M., & Hashim, S. F. S. (2011). Strength Activity Index and Microstructural Characteristics of Treated Palm Oil Fuel Ash. *International Journal of Civil & Environmental Engineering IJCEE-IJENS, 11*(5), 85-92.

Amin, N., Alam, S., & Gul, S. (2015). Assessment of pozzolanic activity of thermally activated clay and its impact on strength development in cement mortar. *Royal Society of Chemistry*, *5*(8), 6079-6084. https://doi.org/10.1039/C4RA12237B

Amin, N. A., Sultan; Gul, Saeed. (2015). Assessment of pozzolanic activity of thermally activated clay and its impact on strength development in cement mortar. *Royal Society of Chemistry*, *5*, 6079-6084. https://doi.org/10.1039/c4ra12237b

Amiralian, S., Chegenizadeh, A., & Nikraz, H. (2012). A Review on The Lime and Fly ash Application in Soil Stabilization. *International Journal of Biological, Ecological and Environmental Sciences*, *1*(3), 124-126.

Aramburo, C. H., Pedrajas, C., & Talero, R. (2020). Portland Cements with High Content of Calcined Clay: Mechanical Strength Behaviour and Sulfate Durability. *Materials*, *13*(18, 4206), 1-15. https://doi.org/10.3390/ma13184206

Araujo, F., Scalize, P., Lima, J., Vieira, N., Albuquerque, A., & Santos, I. (2015). Soil-Cement Floor Produced with Alum Water Treatment Residues. *International Journal of Civil and Environmental Engineering*, *9*(3).

Arooz, F. R., & Halwatura, R. U. (2018). Mud-concrete block (MCB): mix design & durability characteristics. *Case Studies in Construction Materials*, *8*, 39-50. https://doi.org/10.1016/j.cscm.2017.12.004

Arrigoni, A., Beckett, C., Ciancio, D., & Dotelli, G. (2017). Life cycle analysis of environmental impact vs. durability of stabilised rammed earth. *Construction and Building Materials*, *142*, 128-136. https://doi.org/10.1016/j.conbuildmat.2017.03.066

Arum, C., Ikumapayi, C. M., & Aralepo, G. O. (2013). Ashes of Biogenic Wastes—Pozzolanicity, Prospects for Use, and Effects on Some Engineering Properties of Concrete. *Materials Science and Applications*, *4*, 521-527. https://doi.org/10.4236/msa.2013.49064

Assumptor, O. M., Masika, E., & Thiong'o, K. (2020). Probing Optimal Blends of Pozzolans to Develop Supplementary Cementing Material Within Busia County, Kenya. *IOSR Journal Of Applied Physics (IOSR-JAP)*, *12*(2), 59-69.

Atzeni, C., Pia, G., Sanna, U., & Spanu, N. (2008). Surface wear resistance of chemically or thermally stabilized earth-based materials. *Material structures*, *41*(4), 751-758. https://doi.org/10.1617/s11527-007-9278-1

Bagheri, Y., Ahmad, F., Ashraf, M., & Ismail, M. (2014). Strength and mechanical behavior of soil–cement–lime–rice husk ash (soil–CLR) mixture. *Materials and Structures*, *47*, 55-66. https://doi.org/10.1617/s11527-013-0044-2

Bahar, R., Benazzoug, M., & Kenai, S. (2004). Performance of compacted cement-stabilised soil. *Cement & Concrete Composites*, *26*, 811-820. https://doi.org/10.1016/j.cemconcomp.2004.01.003

Batjes, N. H., & Gicheru, P. (2004). Soil data derived from SOTER for studies of carbon stocks and change in Kenya (ver. 1.0: GEFSOC Project) (No. 2004/01). *ISRIC-World Soil Information*.

Benjamin-Chung, J., Crider, Y. S., Mertens, A., Ercumen, A., Pickering, A. J., & Lin, A. (2021). Household finished flooring and soil-transmitted helminth and Giardia infections among children in rural Bangladesh and Kenya: a prospective cohort study. *The Lancet Global Health*, *9*(3), e301-e308. https://doi.org/10.1016/S2214-109X(20)30523-4

Bich, C., Ambroise, J., & Péra, J. (2009). Influence of degree of dehydroxylation on the pozzolanic activity of metakaolin. *Applied Clay Science*, *44*, 194-200. https://doi.org/http://dx.doi.org/10.1016/j.clay.2009.01.014

British Standard Institute. (1990). Methods of testing soils for civil engineering purposes. In *Part 2*.

Bryan, A. J. (1988). Criteria for the Suitability of Soil for Cement Stabilization. *Building and Environment*, *23*(4), 309-319. https://doi.org/10.1016/0360-1323(88)90037-6

Bui, P. T., Ogawa, Y., & Kawai, K. (2018). Long-term pozzolanic reaction of fly ash in hardened cement-based paste internally activated by natural injection of saturated Ca(OH)2 solution. *Materials and Structures*, *51*(144), 1-14. https://doi.org/10.1617/s11527-018-1274-0

Bumanis, G., Vitola, L., Stipniece, L., Locs, J., Korjakins, A., & Bajare, D. (2020). Evaluation of Industrial by-products as pozzolans: A road map for use in concrete production. *Case study in construction materials*, *13*, 1-13. https://doi.org/10.1016/j.cscm.2020.e00424

Burroughs, S. (2008). Soil Property Criteria for Rammed Earth Stabilization. *Journal of Materials in Civil Engineering*, *20*(3). https://doi.org/10.1061/(ASCE)0899-1561(2008)20:3(264)

Burroughs, S. (2010). Recommendations for the selection, stabilization, and compaction of soil for rammed earth wall construction. *Journal of Green Building*, *5*(1), 101-114. https://doi.org/https://doi.org/10.3992/jgb.5.1.101

Burroughs, V. S. (2001). *Quantitative criteria for the selection and stabilisation of soils for rammed earth wall construction* University of New South Wales]. http://hdl.handle.net/1959.4/17861

Cabeza, L. F., Boquera, L., Chàfer, M., & Vérez, D. (2021). Embodied energy and embodied carbon of structural building materials: Worldwide progress and barriers through literature map analysis. *Energy and Buildings*, *231*(10), 110612. https://doi.org/10.1016/j.enbuild.2020.110612

Cantini, A., Leoni, L., De Carlo, F., Salvio, M., Martini, C., & Martini, F. (2021). Technological Energy Efficiency Improvements in Cement Industries. *Sustainability*, *13*(3819), 1-28. https://doi.org/https://doi.org/10.3390/su13073810

Chel, A., & Tiwari, G. N. (2009). Thermal performance and embodied energy analysis of a passive house-Case study of vault roof mud-house in India. *Applied Energy*, *86*(10), 1956-1969. https://doi.org/10.1016/j.apenergy.2008.12.033

Chelberg, M. (2019). *The Effect of Fly Ash Chemical Composition on Compressive Strength of Fly Ash Portland Cement Concrete* [MSc Thesis, The Ohio State University]. Columbus, USA.

Ciancio, D., Jaquin, P., & Walker, P. (2013). Advances on the assessment of soil suitability for rammed earth. *Construction and Building Materials*, *42*, 40-47. https://doi.org/10.1016/j.conbuildmat.2012.12.049

Dabakuyo, I., Mutuku, R. N. N., & Onchiri, R. O. (2022). Mechanical Properties of Compressed Earth Block Stabilized with Sugarcane Molasses and Metakaolin-Based Geopolymer *Civil Engineering Journal*, *8*(4). https://doi.org/10.28991/CEJ-2022-08-04-012

Danner, T., Norden, G., & Justnes, H. (2018). Characterisation of calcined raw clays suitable as supplementary cementitious materials. *Applied Clay Science*, *162*, 391-402. https://doi.org/10.1016/j.clay.2018.06.030

Dhanya, B. S., & Santhanam, M. (2017). Performance evaluation of rapid chloride permeability test in concretes with supplementary cementitious materials. *Materials and Structures, 50*(67). https://doi.org/10.1617/s11527-016-0940-3

Donatello, S., Tyrer, M., & Cheeseman, C. R. (2010). Comparison Of Test Methods To Assess Pozzolanic Activity. *Cement & Concrete Composites*, *32*, 121-127. https://doi.org/10.1016/j.cemconcomp.2009.10.008

Dou, F., Soriano, J., Tabien, R. E., & Chen, K. (2016). Soil Texture and Cultivar Effects on Rice (Oryza sativa, L.) Grain Yield, Yield Components and Water Productivity in Three Water Regimes. *PLoS ONE, 11*(3). https://doi.org/10.1371/journal.pone.0150549

Elson, L., Wright, K., Swift, J., & Feldmeier, H. (2017). Control of Tungiasis in Absence of a Roadmap: Grassroots and Global Approaches. *Tropical Medicine and Infectious Disease, 2*(3), 33. https://doi.org/10.3390/tropicalmed2030033

Excellence for Design and Greater Efficiencies. (2018). *EDGE Materials Reference Guide Version 2.1* https://edgebuildings.com/wp-content/uploads/2022/04/181203-EDGE-Materials-Reference-Guide-1.pdf

Ezreig, A. M. A., Ismail, M. A. M., & Ehwailat, K. I. A. (2022). Hydrophobic Effect of Soil Stabilization for a Sustainable Subgrade Soil Improvement. *Materials, 9*(15), 3087. https://doi.org/10.3390/ma15093087

Faleschini, F., Toska, K., Zanini, M. A., Andreose, F., Settimi, A. G., Brunelli, K., & Pellegrino, C. (2021). Assessment of a Municipal Solid Waste Incinerator Bottom Ash as a Candidate Pozzolanic Material: Comparison of Test Methods. *Sustainability*, *13*(16:8998). https://doi.org/10.3390/su1316899

Fernandes, J., Peixoto, M., Mateus, R., & Gervasio, H. (2019). Life cycle analysis of environmental impacts of earthen materials in the Portuguese context: Rammed earth and compressed earth blocks. *Journal of Cleaner Production*, *241*, 1-19. https://doi.org/10.1016/j.jclepro.2019.118286

Fernandez, R., Martirena, F., & Scrivener, K. L. (2011). The origin of the pozzolanic activity of calcined clay minerals: A comparison between kaolinite, illite and montmorillonite. *Cement and Concrete Research, 41*, 113-122. https://doi.org/10.1016/j.cemconres.2010.09.013

Firoozi, A. A., Olgun, C. G., Firoozi, A. A., & Baghini, M. S. (2017). Fundamentals of soil stabilization. *International Journal of Geo-Engineering*, *8*(26). https://doi.org/10.1186/s40703-017-0064-9

Ganesan, K., Rajagopal, K., & Thangavel, K. (2007). Evaluation of bagasse ash as supplementary cementitious material. *Cement & Concrete Composites, 29*, 515-524. https://doi.org/10.1016/j.cemconcomp.2007.03.001

Garcia-Valles, M., Alfonso, P., Martínez, S., & Roca, N. (2020). Mineralogical and Thermal Characterization of Kaolinitic Clays from Terra Alta (Catalonia, Spain). *Minerals*, *10*(2), 142. https://doi.org/10.3390/min10020142

Garg, N., & Skibsted, J. (2014). Thermal Activation of a Pure Montmorillonite Clay and Its Reactivity in Cementitious Systems. *The journal of physical chemistry*, *118*(21), 11464-11477. https://doi.org/10.1021/jp502529d

Gomes, M. I., Gonçalves, T. D., & Faria, P. (2016). Hydric Behavior of Earth Materials and the Effects of Their Stabilization with Cement or Lime: Study on Repair Mortars for Historical Rammed Earth Structures. *Journal of Materials in Civil Engineering*, *28*(7). https://doi.org/10.1061/(ASCE)MT.1943-5533.0001536

Hall, M., & Djerbib, Y. (2004). Moisture ingress in rammed earth: Part 1—the effect of soil particle-size distribution on the rate of capillary suction. *Construction and Building Materials, 18,* 269-280. https://doi.org/10.1016/j.conbuildmat.2003.11.002

Hall, M., & Djerbib, Y. (2006). Moisture ingress in rammed earth: Part 2 – The effect of soil particle-size distribution on the absorption of static pressure-driven water. *Construction and Building Materials*, *20*, 374-383. https://doi.org/10.1016/j.conbuildmat.2005.01.035

Hammond, G., & Jones, C. (2011). *Embodied carbon: the inventory of carbon and Energy*. University of Bath with BSRIA.

Hamzah, H. N., Abdullah, M. M. A. B., Yong, H. C., Zainol, M. R. R. A., & Hussin, K. (2015). Review of Soil Stabilization Techniques: Geopolymerization Method One of the New Technique. *Key Engineering Materials, 660*, 298-304. https://doi.org/10.4028/www.scientific.net/KEM.660.298

Henry, A. F., Elambo, N. G., Tah, J. H. M., Fabrice, O. E. N., & Blanche, M. M. (2014). Embodied Energy and CO2 Analyses of Mud-brick and Cement-block Houses. *AIMS Energy*, *2*(1), 18-40. https://doi.org/10.3934/energy.2014.1.18

Hollanders, S., Adriaens, R., Skibsted, J., Cizer, Ö., & Elsen, J. (2016). Pozzolanic reactivity of pure calcined clays. *Applied Clay Science*, *132-133*. https://doi.org/10.1016/j.clay.2016.08.003

Houben, H., & Guillaud, H. (2008). *Earth construction: a comprehensive guide. Intermediate Technology Development Group*.

Ibrahim, S. S., Hagrass, A. A., Boulos, T. R., Youssef, S. I., El-Hossiny, F. I., & Moharam, M. R. (2018). Metakaolin as an Active Pozzolan for Cement That Improves Its Properties and Reduces Its Pollution Hazard. *Journal of Minerals and Materials Characterization and Engineering*, *6*(1). https://doi.org/10.4236/jmmce.2018.61008

Ikeagwuani, C. C., Obeta, I. N., & Agunwamba, J. C. (2019). Stabilization of black cotton soil subgrade using sawdust ash and lime. *Soils and Foundations, 59*(1), 162-175. https://doi.org/10.1016/j.sandf.2018.10.004

Indekeu, M. L., Feng, C., Janssen, H., & Woloszyn, M. (2021). Experimental study on the capillary absorption characteristics of rammed earth. *Construction and Building Materials*, *283*. https://doi.org/10.1016/j.conbuildmat.2021.122689

Intergovernmental Panel on Climate Change. (2014). *Climate change 2014: Mitigation of climate change* Geneva.

Jaskulski, R., Józwiak-Niedzwiedzka, D., & Yakymechko, Y. (2020). Calcined Clay as Supplementary Cementitious Material. *Materials*, *13*(21), 4734. https://doi.org/10.3390/ma13214734

Jensen, J. L., Christensen, B. T., Schjonning, P., Watts, C. W., & Munkholm, L. J. (2018). Converting loss-on-ignition to organic carbon content in arable topsoil: pitfalls and proposed procedure. *European Journal of Soil Science*, *69*(4), 604–612. https://doi.org/10.1111/ejss.12558

Jia, Q., Zhuge, Y., Duan, W., Liu, Y., Yang, J., Youssf, O., & Lu, J. (2022). Valorisation of alum sludge to produce green and durable mortar. *Waste Disposal & Sustainable Energy*, *4*, 283–295. https://doi.org/10.1007/s42768-022-00113-3

John, L. K. (2013). *Pozzolana Cement Obtained by Calcining Raw Clays/Rice Husks Mixtures* [MSc. Thesis, Kenyatta University]. Nairobi, Kenya.

Jurić, K. K., Carević, I., Serdar, M., & Štirmer, N. (2020). Feasibility of using pozzolanicity tests to assess reactivity of wood biomass fly ashes. *Gradevinar, 72*(12), 1145-1153. https://doi.org/10.14256/JCE.2950.2020

Justice, J. M. (2005). *Evaluation of metakaolins for use as supplementary cementitious materials*.

Kamau, N. J., Margret, W. N., & Hillary, B. K. (2018). Structural Analysis of Social Networks Revealed by Small Holder Banana Farmers in Muranga County, Kenya. *Journal of Agricultural Science and Food Research*, *9*(2).

Kandamby, G. W. T. C. (2012). *Cement stabilized rammed earth for load bearing walls in two storey house* University of Moratuwa].

Kariyawasam, K. K. G. K. D., & Jayasinghe, C. (2016). Cement stabilized rammed earth as a sustainable construction material. *Construction and Building Materials*, *105*, 519-527. https://doi.org/10.1016/j.conbuildmat.2015.12.189

Khadka, B. (2020). Rammed earth, as a sustainable and structurally safe green building: a housing solution in the era of global warming and climate change. *Asian Journal of Civil Engineering*, *21*, 119–136. https://doi.org/10.1007/s42107-019-00202-5

Khan, A. G., & Khan, B. (2017). Effect of Partial Replacement of Cement by Mixture of Glass Powder and Silica Fume Upon Concrete Strength. *International Journal of Engineering Works*, *4*(7), 124-135. https://hal.science/hal-01569488

Khan, K., Amin, M. N., Usman, M., Imran, M., Al-Faiad, M. A., & Shalabi, F. I. (2022). Effect of Fineness and Heat Treatment on the Pozzolanic Activity of Natural Volcanic Ash for Its Utilization as Supplementary Cementitious Materials. *Crystals*, *12*(2), 302. https://doi.org/10.3390/cryst12020302

Konare, H., Yost, R. S., Doumbia, M., McCarty, G. W., Jarju, A., & Kablan, R. (2010). Loss on ignition: Measuring soil organic carbon in soils of the Sahel, West Africa. *African Journal of Agricultural Research*, *5*(22), 3088-3095.

Kosarimovahhed, M., & Toufigh, V. (2020). Sustainable usage of waste materials as stabilizer in rammed earth

structures. *Journal of Cleaner Production*, *277*, 123279. https://doi.org/10.1016/j.jclepro.2020.123279

Krishna, N. K., Sandeep, S., & Mini, K. M. (2016, 14–16 July 2016). *Study on concrete with partial replacement of cement by rice husk ash* International Conference on Advances in Materials and Manufacturing Applications (IConAMMA-2016), Bangalore, India.

Kristiawan, S. A., Sunarmasto, & Murti, A. Y. (2017). Porosity of Self-Compacting Concrete (SCC) incorporating high volume fly ash. International Conference on Advanced Materials for Better Future 2016,

Kumar, P. T., Reddy, R. H., & Bhagavanulu, D. (2015). A STUDY ON THE REPLACEMENT OF CEMENT IN CONRETE BY USING COW DUNG ASH. *International Journal of Scientific Engineering and Applied Science (IJSEAS)*, *1*(9), 314-327.

Leitãoa, D., Barbosa, J., Soares, E., Mirandab, T., & Cristelo, N. (2017). Thermal performance assessment of masonry made of ICEB's stabilised with alkali-activated fly ash. *Energy and Buildings*, *139*, 44e52. https://doi.org/https://doi.org/10.1016/J.ENBUILD.2016.12.068

Little, D. N. (1999). *Evaluation of structural properties of lime stabilized soils and aggregates. Prepared for the national lime association, vol 1, pp 1–89.*

Liu, Y., Lei, S., Lin, M., Li, Y., Ye, Z., & Fan, Y. (2017). Assessment of pozzolanic activity of calcined coal-series kaolin. *Applied Clay Science*, *143*, 159-167. https://doi.org/10.1016/j.clay.2017.03.038

Losini, A. E., Grillet, A.-C., Woloszyn, M., Lavrik, L., Moletti, C., Dotelli, G., & Caruso, M. (2022). Mechanical and Microstructural Characterization of Rammed Earth Stabilized with Five Biopolymers. *Materials*, *15*(9), 3136. https://doi.org/10.3390/ma15093136

Ma, Q., & Liu, S. (2020). Effect on Silt Capillary Water Absorption upon Addition of Sodium Methyl Silicate (SMS) and Microscopic Mechanism Analysis. *Coatings*, *10*(724), 1-12. https://doi.org/10.3390/coatings10080724

Makinde, O. O. (2012). Ecological and Sustainability Issues In Earth Construction. *IOSR Journal of Environmental Science, Toxicology and Food Technology (IOSR-JESTFT)*, *1*(4), 20-28. https://doi.org/10.9790/2402-0142028

Makusa, G. P. (2012). *Soil Stabilization Methods and Materials in Engineering Practice*.

Maniatidis, V., & Walker, P. (2003). *A Review of Rammed Earth Construction for DTi Partners in Innovation Project 'Developing Rammed Earth for UK Housing'* N. B. T. Group.

Marais, P., Littlewood, J., & Karani, G. (2015). The use of polymer stabilised earth foundations for rammed earth construction. Energy Procedia,

Marangu, J. M. (2020). Physico-chemical properties of Kenyan made calcined Clay - Limestone cement (LC3). *Case Studies in Construction Materials*, *12*, 1-13. https://doi.org/10.1016/j.cscm.2020.e00333

Meek, A. H., & Elchalakani, M. (2019). *Life cycle assessment of rammed earth made using alkaline activated industrial by-products* IOP Conf. Series: Earth and Environmental Science,

Mehsas, B., Siline, M., & Zeghichi, L. (2021). Development of supplementary cementitious materials from Algerian kaolin: elaboration of metakaolin and assessment of pozzolanicity. *Innovative Infrastructure Solutions*, *6*(50), 1-12. https://doi.org/10.1007/s41062-020-00444-2

Moodi, F., Ramezanianpour, A. A., & Safavizadeh, A. S. (2011). Evaluation of the optimal process of thermal activation of kaolins. *Scientia Iranica A*, *18*(4), 906-912. https://doi.org/10.1016/j.scient.2011.07.011

Morel, J. C. (2012). Weathering and durability of earthen material and structures. In M. R. L. Hall, R.; Krayenhoff, M. (Ed.), *Modern earth buildings. Materials, engineering, construction and applications* (pp. 282-303). Woodhead Publishing. https://doi.org/10.1533/9780857096166.2.282

Morel, J. C., & Charef, R. (2019). *What are the barriers affecting the use of earth as a modern construction material in the context of circular economy?* IOP Conf. Series: Earth and Environmental Science

Murang'a County. (2018). *Murang'a County Integrated Development Plan 2018-2022*. Unpublished

Musyimi, N. F., Karanja, T. J., Wachira, M. J., & Mulwa, M. O. (2016). Pozzolanicity and Compressive Strength Performance of Kibwezi. *IOSR Journal of Applied Chemistry (IOSR-JAC)*, *9*(2), 28-32. https://doi.org/10.9790/5736-09222832

Muthakia, G. K., Karanja, J. W., & Muthengia, J. W. (2005). Cement material from calcium carbide residue and broken bricks. *East African Journal of Physical Sciences*, *6*(1), 13-19.

Mwangi, J. N., Ozwara, H. S., & Gicheru, M. M. (2015). Epidemiology of tunga penetrans infestation in selected areas in Kiharu constituency, Murang'a County, Kenya. *Tropical Diseases, Travel Medicine and Vaccines*, *1*(13). https://doi.org/10.1186/s40794-015-0015-4

Naeini, A. A., Siddiqua, S., & Cherian, C. (2021). A novel stabilized rammed earth using pulp mill fly ash as alternative low carbon cementing material. *Construction and Building Materials*, *300*, 124003. https://doi.org/10.1016/j.conbuildmat.2021.124003

Nalobile, P., Wachira, J. M., Thiong'o, J. K., & Marangu, J. M. (2019). Pyroprocessing and the optimum mix ratio of rice husks, broken bricks and spent bleaching earth to make pozzolanic cement. *Heliyon*, *5*(9). https://doi.org/10.1016/j.heliyon.2019.e02443

Njoka, E. N., Ombaka, O., Gichumbi, J. M., Kibaara, D. I., & Nderi, O. M. (2015). Characterization Of Clays From Tharaka-Nithi County In Kenya For Industrial And Agricultural Application. *African Journal of Environmental Science and Technology*, *9*(3), 228-243. https://doi.org/10.5897/AJEST2014.1816

Ojedokun, O. Y., Adeniran, A. A., Raheem, S. B., & Aderinto, S. J. (2014). Cow Dung Ash (CDA) as Partial Replacement of Cementing Material in the Production of Concrete. *British Journal of Applied Science & Technology*, *4*(24), 3445-3454.

Okumu Mary Assumptor 1, E. M., Karanja Thiong'o. (2020). Probing Optimal Blends of Pozzolans to Develop Supplementary Cementing Material Within Busia County, Kenya. *IOSR Journal Of Applied Physics (IOSR-JAP)*, *12*(2), 59-69.

Oluremi, J. R., Elsaigh, W. A., Ikotun, B. D., Osuolale, O. M., Adedokun, S. I., Oyelakin, S. E., & Ayodele, O. P. (2021). Strength enhancement in high silica wood ash stabilized lateritic soil using sodium tetraoxosulphate VI (Na2SO4) as activator. *International Journal of Pavement Research and Technology*, *14*, 410–420. https://doi.org/10.1007/s42947-020-0087-2

Otieno, M. O., Kabubo, C. K., & Gariy, Z. A. (2015). A Study of Uncalcined Termite Clay Soil as Partial Replacement in Cement as a Sustainable Material for Roofing Tiles in Low Cost Housing Schemes in Kenya. *International Journal of Engineering and Advanced Technology (IJEAT)*, *4*(3), 56-59.

Oyawa, W. O., Manette, N., & Musiom, T. (2015). *Development of a two-storey model eco-house from rammed earth*, *QLD* International Conference on Performance-based and Life-cycle Structural Engineering, Brisbane, QLD, Australia.

Peric, A., Kraus, I., Kaluder, J., & Kraus, L. (2021). Experimental Campaigns on Mechanical Properties and Seismic Performance of Unstabilized Rammed Earth—A Literature Review. *Buildings*, *11*(367). https://doi.org/10.3390/buildings11080367

Porter, H., Blake, J., Dhami, N. K., & Mukherjee, A. (2018). Rammed earth blocks with improved multifunctional performance. *Cement and Concrete Composites*, *92*, 36-46. https://doi.org/10.1016/j.cemconcomp.2018.04.013

Raj, S. S., Sharma, A. K., & Anand, K. B. (2018). Performance Appraisal of Coal ash Stabilized Rammed Earth. *Journal of Building Engineering*, *18*, 51-57. https://doi.org/10.1016/j.jobe.2018.03.001

Ramachandran, D., Vinita, V., & Viswanathan, K. (2018). Detailed studies of cow dung ash modified concrete exposed in fresh water. *Journal of Building Engineering*, *20*, 173-178. https://doi.org/10.1016/j.jobe.2018.07.008

Reddy, B. V. V., & Kumar, P. P. (2010). Embodied energy in cement stabilised rammed earth walls. *Energy and Buildings*, *42*(3), 380-385. https://doi.org/10.1016/j.enbuild.2009.10.005

Reddy, B. V. V., Leuzinger, G., & Sreeram, V. S. (2014). Low embodied energy cement stabilised rammed earth building—A case study. *Energy and Buildings*, *68*(4), 541-546. https://doi.org/10.1016/j.enbuild.2013.09.051

Reddy, B. V. V. K., P. Prasanna (2010). Embodied energy in cement stabilised rammed earth walls. *Energy and Buildings*, *42*(3), 380-385. https://doi.org/10.1016/j.enbuild.2009.10.005

Rosicki, Ł., & Piotr, N. (2022). Studies on the Ageing of Cement Stabilized Rammed Earth Material in Different Exposure Conditions. *Sustainability in Construction and Building Materials*, *15*(3). https://doi.org/10.3390/ma15031090

Salim, R. W., Ndambuki, J. M., & Adedokun, D. A. (2014). Improving the Bearing Strength of Sandy Loam Soil Compressed Earth Block Bricks Using Sugercane Bagasse Ash. *Sustainability*, *6*, 3686-3696. https://doi.org/10.3390/su6063686

Schamban, I., Shter, G. E., Shvarzman, A., Grader, G. S., & Kovler, K. (2002). Influence of chemical and phase composition of mineral admixtures on their pozzolanic activity. *Advances in Cement Research*, *14*, 35-41. https://doi.org/10.1680/adcr.2002.14.1.35

Schulze, S. E., & Rickert, J. (2018). Suitability of natural calcined clays as supplementary cementitious material. *Cement and Concrete Composites*.

Schulze, S. E., & Rickert, J. (2019). Suitability of natural calcined clays as supplementary cementitious material. *Cement and Concrete Composites*, *95*, 92-97. https://doi.org/10.1016/j.cemconcomp.2018.07.006

Senhadji, Y., Escadeillasa, G., Khelafi, H., Mouli, M., & Benosman, A. S. (2012). Evaluation of natural pozzolan for use as supplementary. *European Journal of*

Environmental and Civil Engineering, *1*, 77-96. https://doi.org/10.1080/19648189.2012.667692

Setina, J., Gabrene, A., & Juhnevica, I. (2013). Effect of Pozzolanic Additives on Structure and Chemical Durability of Concrete. 11th International Conference on Modern Building Materials, Structures and Techniques, MBMST 2013,

SGS Kenya Limited. (2018). *Environmental and social impact assessment (ESIA) study report for the proposed mitubiri sanitary landfill in Murang'a County*.

Sheikh, A., Akbari, M., & Shafabakhsh, G. (2022). Laboratory Study of the Effect of Zeolite and Cement Compound on the Unconfined Compressive Strength of a Stabilized Base Layer of Road Pavement. *Materials*, *15*(22), 7981. https://doi.org/ 10.3390/ma15227981

Shihembetsa, L., & Sabuni, B. (2002). Burnt clay waste as a pozzolanic material in Kenya. *Journal of Civil Engineering, JKUAT*, *7*. https://doi.org/10.4314/jce.v7i1.18982

Shvarzman, A., Kovler, K., Grader, G. S., & Shter, G. E. (2003). The effect of dehydroxylation/amorphization degree on pozzolanic activity of kaolinite. *Cement and Concrete Research 33*, 405-416.

Singh, M., & Garg, M. (2006). Reactive pozzolana from Indian clays—their use in cement mortars. *Cement and Concrete Research*, *36*, 1903-1907. https://doi.org/10.1016/j.cemconres.2004.12.002

Souri, A., Golestani-Fard, F., Naghizadeh, R., & Veiseh, S. (2015). An investigation on pozzolanic activity of Iranian kaolins obtained by thermal treatment. *Applied Clay Science*, *103*, 34-39. https://doi.org/10.1016/j.clay.2014.11.001

Suresh, A., & Anand, K. B. (2017). Strength and Durability of Rammed Earth for Walling. *Journal of Architectural Engineering*, *23*(4), 06017004. https://doi.org/10.1061/(ASCE)AE.1943-5568.0000281

Syagga, P. M., Kamau, G. N., Sabuni, B., & Dulo, S. O. (2001). Potentials of using Waste Burnt Clay as a Pozzolanic Material in Kenya. *Discovery and Innovation*, *13*(3), 114-118.

Thiviya, S. K., Krishnan, A. G., Kalathuru, M., Sharma, A. K., & Kolathayar, S. (2020). Strength Behavior of Rammed Earth Stabilized with Metakaolin. In *Advances in Geotechnical and Transportation Engineering* (pp. 29-39). Springer Nature Singapore Pte Ltd. https://doi.org/10.1007/978-981-15-3662-5_4

Thompson, D., Augarde, C., & Osorio, J. P. (2022). A review of current construction guidelines to inform the design of rammed earth houses in seismically active zones. *Journal of Building Engineering*, *54*. https://doi.org/10.1016/j.jobe.2022.104666

Thuysbaert, J. (2012). *The suitability of rammed earth for construction in the Cape Town metropolitan area* University of Cape Town].

Tironi, A., Trezza, M. A., Scian, A. N., & Irassar, E. F. (2013). Assessment of pozzolanic activity of different calcined clays. *Cement and Concrete Composites*, *37*, 319-327. https://doi.org/10.1016/j.cemconcomp.2013.01.002

Tole, I., Cwirzen, K. H., & Cwirzen, A. (2019). Mechanochemical activation of natural clay minerals: an alternative to produce sustainable cementitious binders – review. *Mineralogy and Petrology*. https://doi.org/10.1007/s00710-019-00666-y

Trusilewicz, L., Martınez, F. F.-., Rahhal, V., & Talero, R. (2012). TEM and SAED Characterization of Metakaolin. Pozzolanic Activity. *Journal of the American Ceramic Society*, 1-8. https://doi.org/10.1111/j.1551-2916.2012.05325.x

Turkoz, M., & Vural, P. (2013). The effects of cement and natural zeolite additives on problematic clay soils. *Science and Engineering of Composite Materials*, *20*(4), 395-405. https://doi.org/10.1515/secm-2012-0104

Venkatasubramanian, C., Muthu, D., Aswini, G., Nandhini, G., & Muhilini, K. (2017). Experimental studies on effect of cow dung ash (pozzolanic binder) and coconut fiber on strengthproperties of concrete. International Conference on Civil Engineering and Infrastructural Issues in Emerging Economies (ICCIEE 2017) 17–18 March 2017,, Tirumalaisamudram, Thanjavur, India.

Vignesh, N. P., Mahendran, K., & Arunachelam, N. (2020). Effects of Industrial and Agricultural Wastes on Mud Blocks Using Geopolymer. *Advances in Civil Engineering*, 1-9. https://doi.org/10.1155/2020/1054176

Walker, P., Keable, R., Martin, J., & Maniatidis, V. (2005). *Rammed earth: design and construction guidelines: BRE Bookshop*. brebookshop.

Walker, R., & Pavía, S. (2010). Physical properties and reactivity of pozzolans, and their influence on the properties of lime–pozzolan pastes. *Material structures, 44*, 1139–1150. https://doi.org/10.1617/s11527-010-9689-2

Wambani, Z. (2017). *Tungiasis Risk Factors in Rural Community in Murang'a County, Kenya* [MSc Thesis, Kenyatta University]. Nairobi, Kenya. http://ir-library.ku.ac.ke/handle/123456789/18057

Wambani, Z., Nyamari, J., & Kimani, H. (2018). Environmental Factors Predisposing Rural Community Members To Tungiasis In Murang'A East Sub County, Murang'A County. *Journal of Health, Medicine and Nursing*, *3*(2), 90-97. https://ir-library.ku.ac.ke/handle/123456789/24963

Wang, L., Li, X., Cheng, Y., Zhang, Y., & Bai, X. (2018). Effects of coal-bearing metakaolin on the compressive strength and permeability of cemented silty soil and mechanisms. *Construction and Building Materials*, *186*, 174-181. https://doi.org/https://doi.org/10.1016/j.conbuildmat.2018.07.057

Wang, Y., Li, L., An, M., Sun, Y., Yu, Z., & Huang, H. (2022). Factors Influencing the Capillary Water Absorption Characteristics of Concrete and Their Relationship to Pore Structure. *Appl. Sci.*, *12*(4), 2211. https://doi.org/https://doi.org/10.3390/app12042211

Węgliński, S. (2021). Capillary water absorption in mixtures of cohesive soils stabilized with cement and hydrophobic agent. *Budownictwo i Architektura*, *20*(2), 15-28. https://doi.org/10.35784/bud-arch.2422

Yanguatin, H., Ramírez, J. H., Tironi, A., & Tobón, J. I. (2019). Effect of thermal treatment on pozzolanic activity of excavated waste clays. *Construction and Building Materials*, *211*, 814-823. https://doi.org/10.1016/j.conbuildmat.2019.03.300

Zayed, A., Shanahan, N., Sedaghat, A., Stetsko, Y., & Lorentz, B. (2018). *Development of Calcined Clays as Pozzolanic Additions in Portland Cement Concrete Mixtures* [Technical Report, University of South Florida]. Tallahassee, USA.

Zhao, H., Ding, J., Huang, Y., Tang, Y., Xu, W., & Huang, D. (2019). Experimental analysis on the relationship between pore structure and capillary water absorption characteristics of cement-based materials. *Structural Concrete, 20*(5), 1750-1762. https://doi.org/10.1002/suco.201900184

Zhou, D., Wang, R., Tyrer, M., Wong, H., & Cheeseman, C. (2017). Sustainable infrastructure development through use of calcined excavated waste clay as a supplementary cementitious material. *Journal of Cleaner Production*, *168*, 1180-1192. https://doi.org/10.1016/j.jclepro.2017.09.098

APPENDICES

Appendix I: Soil Texture of Raw Clay Samples

Samples	Weight (g)	Corrected R40s[d] (g/L)	Corrected R6h[e] (g/L)	Corrected RL6h[f] (g/L)	Sand (%)	Silt (%)	Clay (%)	Texture Class
GT1[a]	51.80	1037.37	1026.87	1003.26	34.10	20.26	45.64	Clay
GT2	52.63	1035.79	1025.99	1003.26	38.14	18.61	43.25	Clay
GT3	51.70	1036.37	1029.07	1003.26	35.88	14.04	50.07	Clay
MU1[b]	51.47	1033.22	1024.65	1003.26	41.78	16.63	41.59	Clay
MU2	50.00	1032.34	1023.77	1003.26	41.84	17.13	41.03	Clay
MU3	50.00	1033.28	1024.62	1003.26	39.96	17.32	42.72	Clay
GK1[c]	52.83	1037.49	1028.11	1003.26	35.25	17.71	47.03	Clay
GK2	52.07	1036.40	1029.05	1003.26	36.35	14.12	49.53	Clay
GK3	53.57	1037.15	1029.26	1003.26	36.71	14.74	48.56	Clay

[a] GT: Raw clay from Gatundu

[b]MU: Raw clay from Murang'a town

[c]GK: Raw clay from Gakoigo

[d]Corrected R40s: Corrected Hydrometer Reading after 40 seconds

[e]Corrected R6h: Corrected Hydrometer Reading after 6 hours

[f]Corrected RL6h: Corrected Hydrometer Reading after 6 hours (Blank)

Appendix II: Results of the Pozzolanic Activity of Calcined Clay

Appendix II.a: Frattini Results of Saturated OPC-Calcined Clay Solutions

	T (°C)	Time Days	Filtrate (ml)	HCl (ml)	EDTA (ml)	[OH-] (mmol/l)	[CaO] (mmol/l)	CaO Th. (mmol/l)	RCaO (%)
GT	Raw	8	25	15.2±0.52	8.9±0.62	60.8±2.08	10.68±0.75	7.641921	0
MU	Raw	8	25	15.7±0.17	10.1±0.92	62.8±0.69	12.12±1.1	7.322176	0
GK	Raw	8	25	15.5±0.36	9.03±0.5	62±1.44	10.84±0.6	7.446809	0
GT	600	8	25	12.87±0.75	4.03±0.65	55.4±3	5.7±0.78	8.663366	34.20571
MU	600	8	25	13.13±0.5	3.7±0.42	55.33±2.01	6.04±0.5	8.677686	30.39619
GK	600	8	25	12.33±0.61	2.67±0.69	52.53±2.44	5.16±0.83	9.325044	44.66514
GT	700	8	25	13.03±0.49	3.73±0.45	52.13±1.97	4.48±0.54	9.425494	52.46933
MU	700	8	25	13.13±1.91	4.07±0.95	52.53±7.66	4.88±1.14	9.325044	47.66781
GK	700	8	25	12.27±1.64	3.1±0.36	49.07±6.58	3.72±0.43	10.27397	63.792
GT	800	8	25	13.43±1.57	7.1±1.42	53.73±6.28	8.52±1.7	9.036145	5.712
MU	800	8	25	14.57±0.95	7.8±0.75	58.27±3.78	9.36±0.91	8.089368	0
GK	800	8	25	14.4±0.52	7.5±1.4	57.6±2.08	9±1.68	8.215962	0
GT	Raw	15	25	14.47±0.5	6.03±0.47	57.87±2.01	7.24±0.57	8.164852	11.32724
MU	Raw	15	25	14.5±0.36	6.17±1.11	58±1.44	7.4±1.33	8.139535	9.085714
GK	Raw	15	25	14.53±0.38	6±0.17	58.13±1.51	7.2±0.21	8.114374	11.26857
GT	600	15	25	13.85±0.6	4.75±0.47	51.47±2.41	4.84±0.57	9.597806	49.57181
MU	600	15	25	13.83±0.4	5.03±0.5	52.53±1.62	4.44±0.6	9.325044	52.38629
GK	600	15	25	13.13±0.55	4.3±0.6	49.33±2.2	3.2±0.72	10.19417	68.60952
GT	700	15	25	13.2±0.52	4.6±0.95	52.8±2.08	5.52±0.17	9.259259	40.384
MU	700	15	25	13.1±2.05	3.93±0.76	52.4±8.21	4.72±1.22	9.358289	49.56343
GK	700	15	25	12.3±0	3.2±0.5	49.2±0	3.84±0.15	10.23392	62.47771
GT	800	15	25	14.57±0.51	4.87±0.55	58.27±2.05	5.84±0.44	8.089368	27.80648
MU	800	15	25	13.95±0.45	5.8±0.1	55.8±1.8	6.96±0.49	8.578431	18.86629
GK	800	15	25	13.95±0.35	5.2±0.3	55.8±1.4	6.24±0.3	8.578431	27.25943

Appendix II.b: Average Compressive Strength Test Results and Strength Activity Index of Cement Mortars

Clay Sample	Temperature (°C)	Curing Time (Days)	Maximum Load (kN)	Compressive Strength (MPa)	Standard Deviation	Strength Activity Index
GT	Raw	7	28.027	17.51688	3.716836	0.866368
MU	Raw	7	23.01367	14.38354	3.374553	0.711396
GK	Raw	7	20.45967	12.78729	2.440893	0.632447
GT	600	7	32.5488	20.343	3.359814	1.006145
MU	600	7	33.49227	20.93267	1.387899	1.03531
GK	600	7	31.2496	19.531	1.353578	0.965985
GT	700	7	27.55967	17.22479	2.064511	0.851922
MU	700	7	26.999	16.87438	0.848039	0.83459
GK	700	7	34.58533	21.61583	4.108387	1.069098
GT	800	7	31.745	19.84063	2.003521	0.981298
MU	800	7	34.305	21.44063	1.735566	1.060433
GK	800	7	34.57587	21.60992	3.73589	1.068806
GT	Raw	14	31.29667	19.56042	2.777799	0.701541
MU	Raw	14	23.89733	14.93583	2.727175	0.535679
GK	Raw	14	21.721	13.57563	0.951592	0.486894
GT	600	14	49.271	30.79438	1.838982	1.10445
MU	600	14	39.28433	24.55271	5.309702	0.880591
GK	600	14	35.669	22.29313	1.46129	0.79955
GT	700	14	41.60267	26.00167	3.179482	0.932558
MU	700	14	28.793	17.99563	1.431134	0.645419
GK	700	14	42.747	26.71688	0.422268	0.958209
GT	800	14	34.99633	21.87271	6.033066	0.784472
MU	800	14	35.16433	21.97771	4.398797	0.788238
GK	800	14	38.462	24.03875	3.693465	0.862158
GT	Raw	28	35.43533	22.14708	4.3776	0.731687
MU	Raw	28	30.06367	18.78979	3.523643	0.62077
GK	Raw	28	21.805	13.62813	4.695584	0.450241
GT	600	28	53.948	33.7175	5.063339	1.113945
MU	600	28	40.20333	25.12708	4.317815	0.830139
GK	600	28	41.05933	25.66208	5.062226	0.847814
GT	700	28	45.806	28.62875	1.980143	0.945825
MU	700	28	36.20033	22.62521	1.826791	0.747483
GK	700	28	46.07433	28.79646	1.748145	0.951366
GT	800	28	43.881	27.42563	1.830645	0.906077
MU	800	28	38.77067	24.23167	2.448463	0.800556
GK	800	28	51.971	32.48188	6.061369	1.073123
Control	-	7	32.35	20.21875		
Control	-	14	44.611	27.88208		
Control	-	28	48.429	30.26854		

Appendix II.c: Electrical Conductivity of Saturated $Ca(OH)_2$ by Calcined Clay Pozzolana (s/m)

Incubation	**Raw Clays**			**Clays Calcined at 600°C**			**Clays Calcined at 700°C**			**Clays Calcined at 800°C**		
(min)	GT	MU	GK	GT	MU	GK	GT	MU	GK	GT	MU	GK
2	1.65±0.17	1.42±0.3	1.34±0.18	2±0.04	1.89±0.18	2.19±0.08	1.66±0.12	1.44±0.11	1.87±0.15	0.82±0.12	0.56±0.07	1.03±0.11
30	2.01±0.17	1.8±0.33	1.65±0.19	2.37±0.1	2.32±0.25	2.69±0.12	1.91±0.14	1.57±0.17	2.23±0.06	1.02±0.16	0.77±0.12	1.33±0.2
60	2.38±0.23	2.02±0.36	1.87±0.17	2.71±0.15	2.63±0.32	3.03±0.1	2.17±0.23	1.83±0.18	2.59±0.06	1.33±0.15	0.89±0.12	1.5±0.19
120	2.42±0.28	2.29±0.35	1.98±0.09	3.07±0.09	3.09±0.35	3.52±0.16	2.52±0.24	2.16±0.18	2.93±0.06	1.51±0.23	1.08±0.07	1.74±0.08
240	2.79±0.31	2.67±0.38	2.37±0.08	3.55±0.04	3.66±0.39	4.03±0.12	2.99±0.27	2.64±0.14	3.41±0.09	2.37±0.69	1.51±0.12	2.27±0.08
1320	3.74±0.28	3.68±0.55	3.35±0.31	4.99±0.21	5.29±0.54	5.12±0.39	4.5±0.51	4.14±0.3	4.86±0.17	3.22±0.27	2.95±0.24	3.65±0.28
1440	3.96±0.27	3.93±0.5	3.6±0.29	5.26±0.27	5.48±0.52	5.44±0.43	4.9±0.39	4.5±0.3	5.07±0.19	3.56±0.21	3.33±0.24	3.95±0.33

Appendix III: Electrical Conductivity (EC) of Aqueous Solutions of $Ca(OH)_2$ after the Addition of Clay

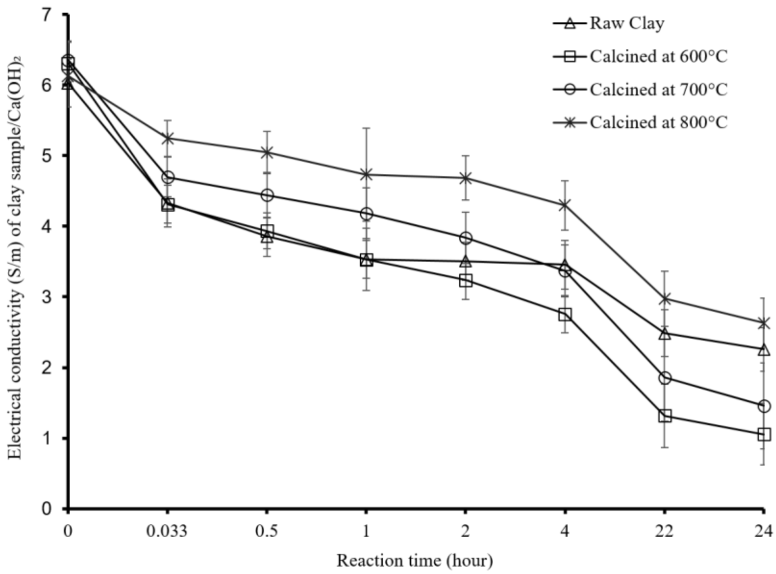

Appendix III.a: Electrical Conductivity (EC) of Aqueous Solutions of $Ca(OH)_2$ after the Addition of Clay from Gatundu (Raw Clay and Clay Calcined at 600°C, 700°C, And 800°C)

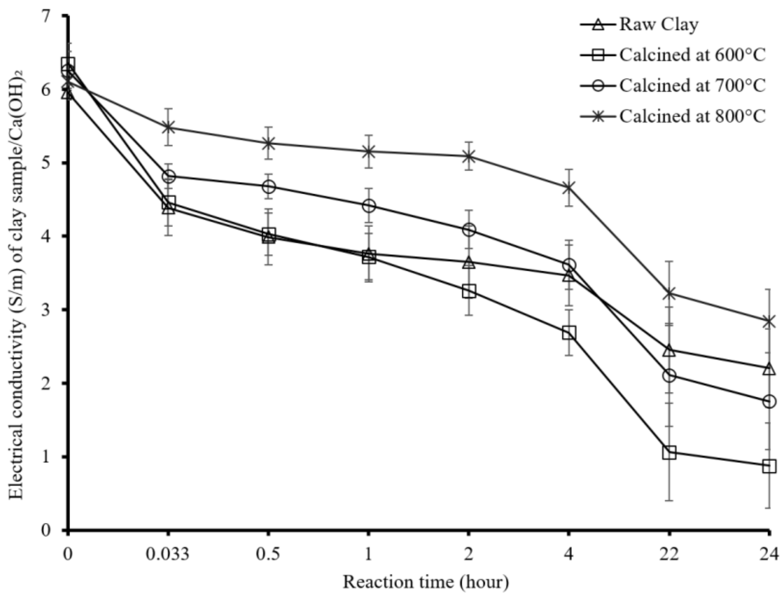

Appendix III.b: Electrical Conductivity (EC) of Aqueous Solutions of $Ca(OH)_2$ after the Addition of Clay from Murang'a Town (Raw Clay and Clay Calcined at 600°C, 700°C, and 800°C)

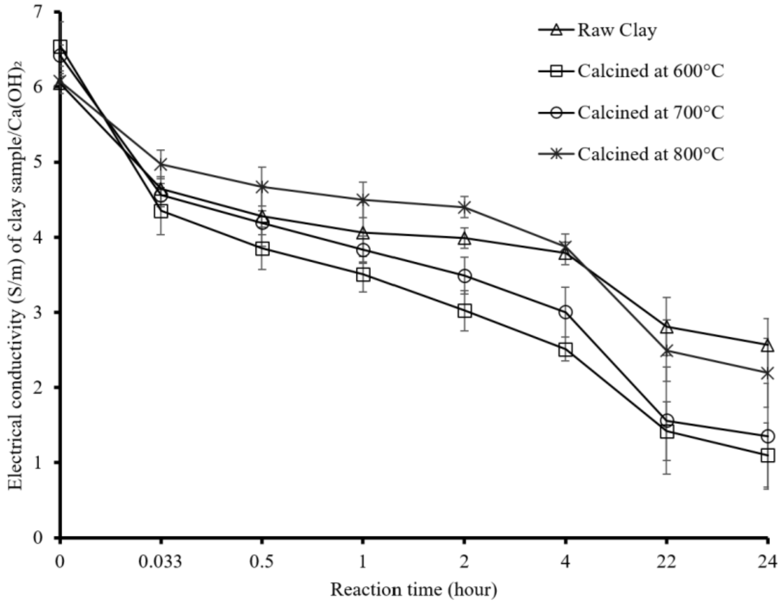

Appendix III.c: Electrical Conductivity (EC) of Aqueous Solutions of $Ca(OH)_2$ after the Addition of Clay from Gakoigo (Raw Clay and Clay Calcined at 600°C, 700°C, and 800°C)

Appendix 1V: ANOVA of the Pozzolanic Activity of Calcined Clay

Appendix IV.a: Analysis of Variance Results of the Electrical Conductivity Results

	Df	Sum Sq	Mean Sq	F value	Pr(>F)	
Location	2	1.7	0.83	11.321	2.25e-05	***
Temperature	3	48.7	16.23	220.636	< 2e-16	***
Duration	7	500.8	71.55	972.886	< 2e-16	***
Location:Temperature	6	6.0	1.00	13.572	8.05e-13	***
Location:Duration	14	0.9	0.06	0.835	0.630	
Temperature:Duration	21	21.2	1.01	13.724	< 2e-16	***
Location:Temperature:Duration	42	1.7	0.04	0.536	0.991	
Residuals	192	14.1	0.07			

Signif. codes: 0 ‘***’ 0.001 ‘**’ 0.01 ‘*’ 0.05 ‘.’ 0.1 ‘ ’ 1

Appendix IV.b: Analysis of Variance Results of the Frattini Results

	Df	Sum Sq	Mean Sq	F value	Pr(>F)	
Location	2	19.0	9.51	3.887	0.02725	*
Temperature	3	531.0	177.00	72.311	< 2e-16	***
Duration	1	110.1	110.07	44.969	2.08e-08	***
Location:Temperature	6	18.6	3.11	1.269	0.28951	
Location:Duration	2	1.0	0.51	0.209	0.81239	
Temperature:Duration	3	38.6	12.87	5.256	0.00323	**
Location:Temperature:Duration	6	5.4	0.90	0.368	0.89583	
Residuals	48	117.5	2.45			

Signif. codes: 0 '***' 0.001 '**' 0.01 '*' 0.05 '.' 0.1 ' ' 1

Appendix IV.c: Analysis of Variance of Compressive Strength Test Results for Cement-Calcined Clay Mortars

	Df	Sum Sq	Mean Sq	F value	Pr(>F)	
Location	2	285.5	142.7	12.535	2.13e-05	***
Temperature	3	1084.4	361.5	31.742	3.49e-13	***
Curing_Time	2	920.8	460.4	40.432	1.69e-12	***
Location:Temperature	6	420.4	70.1	6.152	3.03e-05	***
Location:Curing_Time	4	50.4	12.6	1.107	0.3600	
Temperature:Curing_Time	6	180.8	30.1	2.647	0.0224	*
Location:Temperature:Curing_Time	12	141.2	11.8	1.033	0.4286	
Residuals	72	819.9	11.4			

Signif. codes: 0 '***' 0.001 '**' 0.01 '*' 0.05 '.' 0.1 ' ' 1

Appendix V: Characterization Results of the Experimental Soils

Appendix V.a: Compaction Test Results for Murrum Soil

Test No	**1**	**2**	**3**	**4**	**5**	**6**
Weight of mould (g)	4506.5	4506.5	4506.5	4506.5	4506.5	4506.5
Mould + Sample ((g)	6059	6177	6395	6455	6415	5920
Tin No	4	18	15	29	2	9
Tin Weight (g)	9.52	9.38	9.34	9.52	9.38	9.4
Tin + Wet Soil (g)	77.26	74.54	107.2	87.26	98.84	87.54
Tin + Dry Soil (g)	70.14	65.2	89.84	70.88	78.36	85.66
Volume of Mould (m^3)	0.001021	0.001021	0.001021	0.001021	0.001021	0.001021
Weight of Sample (g)	1552.5	1670.5	1888.5	1948.5	1908.5	1413.5
Wet density (kg/m^3)	1520.54	1636.11	1849.63	1908.39	1869.21	1384.40
Weight of water (g)	7.12	9.34	17.36	16.38	20.48	1.88
Weight of Dry Soil (g)	60.62	55.82	80.5	61.36	68.98	76.26
Moisture Content (g)	9.28	14.27	19.10	24.23	27.22	2.47
Dry density (kg/m^3)	1391.42	1431.83	1553.00	1536.18	1469.22	1351.10

Appendix V.b: Compaction Test Results for Black Cotton Soil

Weight of mould	4506.5	4506.5	4506.5	4506.5	4506.5
Weight of mould + Sample	5924	6100	6253	6288	6234
Tin No	24	4	28	38	32
Tin Weight	9.44	9.56	9.44	30.36	36.1
Tin + Wet Soil	72.9	74.78	94.14	102.4	128.8
Tin + Dry Soil	64.86	63.4	75.9	84.4	103.7
Volume of Mould	0.001021	0.001021	0.001021	0.001021	0.001021
Weight of Sample	1417.5	1593.5	1746.5	1781.5	1727.5
Wet density	1388.32	1560.69	1710.55	1744.83	1691.94
Weight of water	8.04	11.38	18.24	18	25.1
Weight of Dry Soil	55.42	53.84	66.46	54.04	67.6
Moisture Content	14.51	21.14	27.45	33.31	37.13
Dry density	1212.43	1288.38	1342.18	1308.86	1233.82

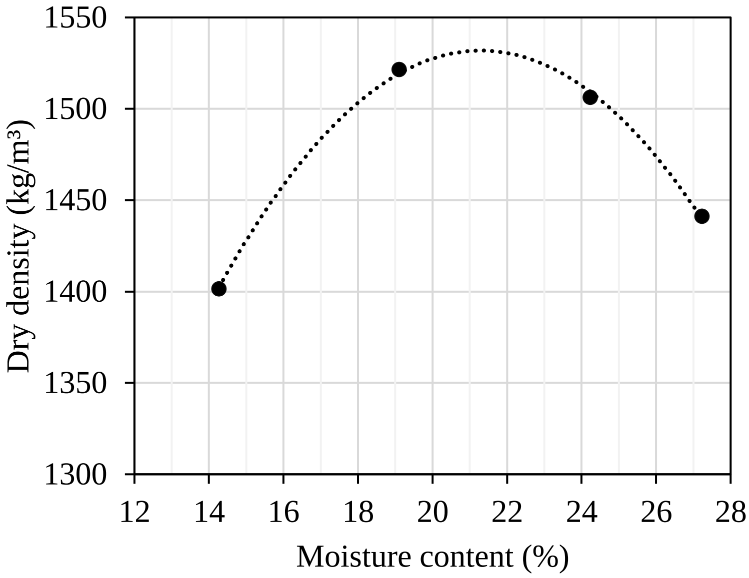

Appendix V.c: Optimum Moisture Content and Maximum Dry Density Graph for Natural Murrum Soil

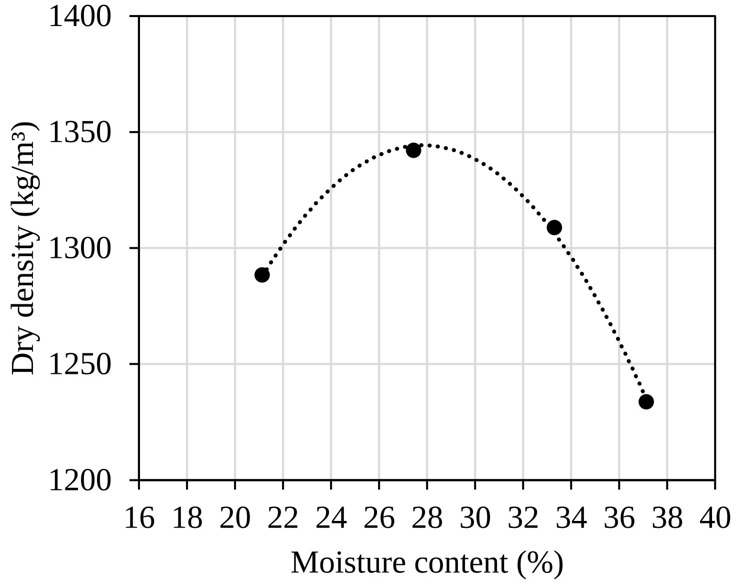

Appendix V.d: Optimum Moisture Content and Maximum Dry Density Graphs for Black Cotton Soil

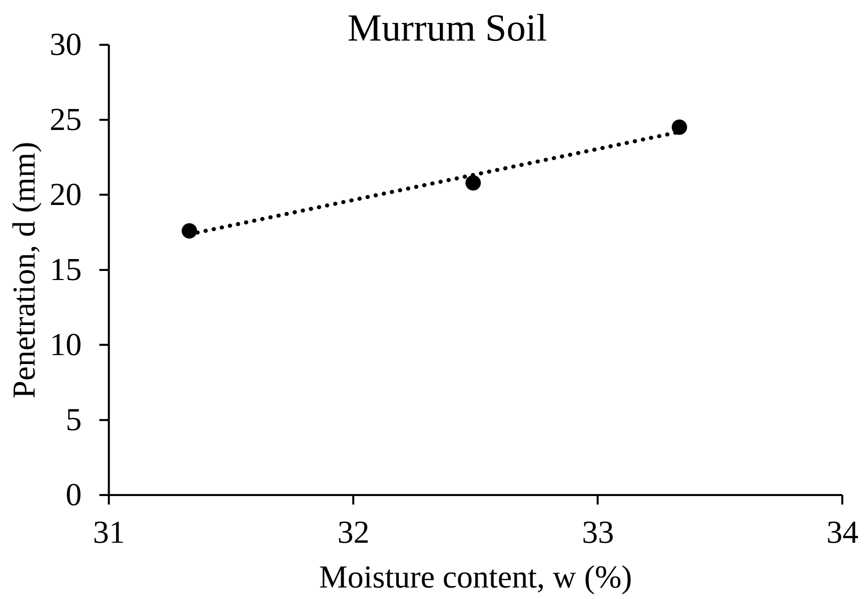

Appendix V.e: Liquid limit for Murrum Soil

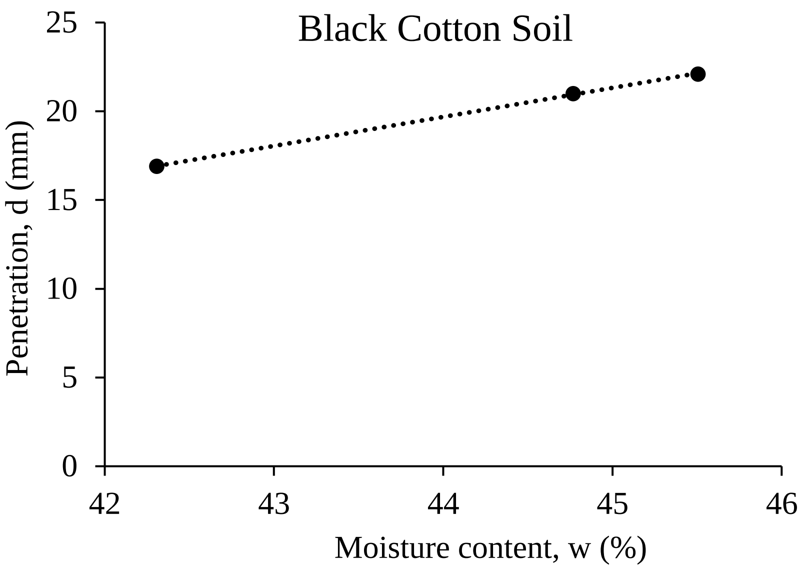

Appendix V.f: Liquid Limit for Black Cotton Soil

Appendix V.g: Atteberg Limits Results for Murrum Soil

	Liquid Limit				**Plastic Limit**		**Plasticity Index**
Penetration (mm)	15.5	17.6	20.8	24.5	-	-	
Tin No	11A	4A	10A	1A	9A	5	
Weight of Tin (g)	5.52	5.5	5.3	5.28	5.42	9.54	
Weight of Tin + Wet Soil (g)	8.7	11.82	10.04	11.04	10.46	15.44	
Weight of Tin + Dry Soil (g)	7.74	9.84	8.5	9.12	9.34	14.16	
Moisture Content (%)	30.19	31.33	32.49	33.33	22.22	21.69	
LL. PL. PI (%)	32				22		10

Appendix V.h: Atterberg Limits for Black Cotton Soil

	Liquid Limit				Plastic Limit		Plasticity Index
Pen (mm)	14.1	16.9	21	22.1	-	-	
Tin No	7A	3A	12A	8A	11	12	
Weight of Tin (g)	5.32	5.32	5.26	5.44	9.34	9.36	
Weight of Tin + Wet Soil (g)	8.88	10	8.7	9	16.04	16.58	
Weight of Tin + Dry Soil (g)	7.4	8.02	7.16	7.38	14.5	15.04	
Moisture content (%)	41.57	42.31	44.77	45.51	22.99	21.33	
LL. PL. PI (%)	44				22		22

Appendix V.i: Linear Shrinkage of Murrum and Black Cotton Soils

Sample	Murrum	Black cotton
Label	2	A2
Length A	139.8	140.25
Length B	129.6	120
Linear Shrinkage (%)	7.29	14.44

Appendix VI: Capillary Water Absorption Results of Stabilized Rammed Earth (Kg Water /Kg Soil Block)

Appendix VI.a: Capillary Water Absorption (Kg Water /Kg Soil Block) for Stabilized Rammed Murrum after a Curing Period of 14 Days

Binder Content (%)	**Replacement Rate (%)**	**Water Absorption (kg water/kg)**											
		1 hour			**2 hours**			**4 hours**			**24 hours**		
		Test 1	Test 2	Test 3	Test 1	Test 2	Test 3	Test 1	Test 2	Test 3	Test 1	Test 2	Test 3
0%	0	0.14	0.14	0.13	0.15	0.17	0.16	0.22	0.22	0.20	0.26	0.27	0.26
5%	0	0.08	0.08	0.08	0.11	0.11	0.10	0.14	0.15	0.13	0.23	0.23	0.23
5%	25%	0.10	0.10	0.09	0.11	0.11	0.12	0.14	0.14	0.14	0.21	0.21	0.21
5%	50%	0.10	0.08	0.10	0.13	0.12	0.14	0.15	0.13	0.16	0.22	0.22	0.23
5%	75%	0.11	0.11	0.10	0.13	0.14	0.12	0.19	0.19	0.17	0.26	0.25	0.25
10%	0%	0.05	0.05	0.04	0.05	0.08	0.06	0.07	0.08	0.06	0.15	0.14	0.16
10%	25%	0.06	0.04	0.05	0.05	0.04	0.07	0.09	0.07	0.08	0.18	0.18	0.17
10%	50%	0.09	0.09	0.07	0.14	0.11	0.10	0.14	0.13	0.12	0.24	0.24	0.24
10%	75%	0.08	0.08	0.08	0.08	0.09	0.10	0.12	0.11	0.12	0.25	0.25	0.25
15%	0%	0.04	0.05	0.04	0.06	0.05	0.05	0.07	0.08	0.06	0.10	0.12	0.09
15%	25%	0.03	0.05	0.04	0.05	0.05	0.05	0.05	0.07	0.07	0.11	0.13	0.11
15%	50%	0.06	0.06	0.06	0.07	0.08	0.07	0.09	0.10	0.09	0.19	0.20	0.18
15%	75%	0.11	0.09	0.11	0.13	0.12	0.13	0.18	0.15	0.17	0.26	0.25	0.25

Appendix VI.b: Capillary Water Absorption (Kg Water/Kg Soil Block) for Black Cotton Soil Stabilized Blocks after a Curing Period of 14 Days

Binder Content (%)	Replacement Rate (%)	Water Absorption (kg water/kg soil block)											
		1 hour			2 hours			4 hours			24 hours		
		Test 1	Test 2	Test 3	Test 1	Test 2	Test 3	Test 1	Test 2	Test 3	Test 1	Test 2	Test 3
0%	0	0.23	0.21	0.20	0.24	0.23	0.21	0.28	0.27	0.23	0.40	0.38	0.38
5%	0	0.20	0.20	0.21	0.22	0.21	0.23	0.25	0.25	0.26	0.35	0.36	0.35
5%	25%	0.12	0.09	0.10	0.15	0.13	0.13	0.16	0.16	0.16	0.23	0.26	0.25
5%	50%	0.11	0.14	0.16	0.19	0.22	0.23	0.23	0.26	0.27	0.34	0.39	0.41
5%	75%	0.16	0.17	0.16	0.19	0.20	0.19	0.23	0.26	0.24	0.35	0.38	0.38
10%	0%	0.10	0.10	0.09	0.14	0.14	0.12	0.19	0.20	0.18	0.28	0.27	0.28
10%	25%	0.09	0.11	0.08	0.10	0.11	0.09	0.13	0.14	0.11	0.26	0.24	0.23
10%	50%	0.12	0.11	0.11	0.12	0.12	0.12	0.15	0.14	0.13	0.24	0.23	0.23
10%	75%	0.14	0.14	0.14	0.17	0.15	0.14	0.18	0.19	0.20	0.29	0.27	0.26
15%	0%	0.10	0.09	0.09	0.13	0.13	0.12	0.17	0.16	0.15	0.25	0.25	0.25
15%	25%	0.05	0.06	0.04	0.07	0.09	0.06	0.10	0.12	0.08	0.19	0.21	0.17
15%	50%	0.08	0.05	0.04	0.10	0.08	0.07	0.13	0.13	0.09	0.22	0.23	0.19
15%	75%	0.09	0.11	0.10	0.10	0.12	0.11	0.13	0.14	0.13	0.25	0.25	0.23

Appendix VI.c: Capillary Water Absorption (Kg Water /Kg Soil Block) for Murrum Soil Stabilized Blocks after a Curing Period of 28 Days

Binder Content (%)	Replacement Rate (%)	Water Absorption (kg water/kg)											
		1 hour			2 hours			4 hours			24 hours		
		Test 1	Test 2	Test 3	Test 1	Test 2	Test 3	Test 1	Test 2	Test 3	Test 1	Test 2	Test 3
0%	0	0.12	0.14	0.13	0.14	0.15	0.16	0.22	0.20	0.21	0.23	0.23	0.22
5%	0	0.08	0.07	0.09	0.10	0.08	0.12	0.14	0.13	0.14	0.20	0.20	0.19
5%	25%	0.10	0.10	0.10	0.11	0.12	0.12	0.14	0.15	0.15	0.24	0.20	0.23
5%	50%	0.10	0.11	0.11	0.13	0.13	0.13	0.15	0.16	0.16	0.23	0.23	0.23
5%	75%	0.10	0.10	0.09	0.13	0.13	0.11	0.17	0.18	0.15	0.23	0.24	0.24
10%	0%	0.04	0.04	0.04	0.04	0.05	0.05	0.06	0.06	0.06	0.12	0.12	0.13
10%	25%	0.03	0.05	0.06	0.08	0.07	0.07	0.06	0.08	0.09	0.16	0.18	0.18
10%	50%	0.08	0.08	0.07	0.09	0.10	0.09	0.12	0.12	0.12	0.25	0.25	0.25
10%	75%	0.10	0.09	0.09	0.11	0.10	0.11	0.14	0.14	0.14	0.26	0.26	0.26
15%	0%	0.03	0.05	0.03	0.03	0.06	0.03	0.05	0.07	0.04	0.08	0.09	0.07
15%	25%	0.04	0.04	0.05	0.07	0.08	0.07	0.07	0.08	0.08	0.12	0.13	0.13
15%	50%	0.04	0.04	0.04	0.05	0.05	0.06	0.08	0.08	0.07	0.16	0.16	0.15
15%	75%	0.11	0.10	0.12	0.15	0.16	0.16	0.19	0.18	0.20	0.26	0.26	0.27

Appendix VI.d: Capillary Water Absorption (Kg Water/Kg Soil Block) for Black Cotton Soil Stabilized Blocks after a Curing Period of 28 Days

Binder Content (%)	**Replacement Rate (%)**	**Water Absorption (kg water/kg)**											
		1 hour			2 hours			4 hours			24 hours		
		Test 1	Test 2	Test 3	Test 1	Test 2	Test 3	Test 1	Test 2	Test 3	Test 1	Test 2	Test 3
0%	0	0.20	0.22	0.21	0.21	0.23	0.23	0.23	0.25	0.26	0.33	0.34	0.36
5%	0	0.17	0.15	0.14	0.18	0.17	0.17	0.20	0.19	0.19	0.30	0.27	0.28
5%	25%	0.10	0.06	0.06	0.15	0.14	0.15	0.15	0.15	0.15	0.22	0.19	0.23
5%	50%	0.13	0.14	0.14	0.16	0.17	0.16	0.17	0.18	0.18	0.29	0.30	0.30
5%	75%	0.14	0.20	0.17	0.21	0.21	0.21	0.22	0.23	0.23	0.36	0.37	0.36
10%	0%	0.14	0.16	0.14	0.15	0.17	0.15	0.16	0.18	0.16	0.30	0.32	0.28
10%	25%	0.09	0.09	0.06	0.13	0.09	0.11	0.15	0.13	0.11	0.25	0.26	0.23
10%	50%	0.10	0.09	0.09	0.12	0.10	0.13	0.14	0.12	0.14	0.22	0.23	0.21
10%	75%	0.12	0.12	0.13	0.14	0.13	0.15	0.16	0.15	0.17	0.30	0.29	0.30
15%	0%	0.09	0.10	0.10	0.10	0.08	0.11	0.12	0.12	0.14	0.22	0.19	0.22
15%	25%	0.07	0.04	0.04	0.09	0.06	0.06	0.11	0.08	0.08	0.20	0.17	0.18
15%	50%	0.08	0.09	0.06	0.12	0.12	0.09	0.14	0.14	0.10	0.22	0.20	0.21
15%	75%	0.09	0.09	0.09	0.10	0.13	0.10	0.12	0.14	0.11	0.26	0.27	0.25

Appendix VII: Compressive Strength Results of Stabilized Rammed Earth

Appendix VII.a: Compressive Strength Results of Murrum Stabilized Blocks after a Curing Period of 14 Days

Binder Content (%)	**Replacement Rate (%)**	**Curing Time (days)**	**Maximum Load (kN)**			**Compressive Strength (MPa)**			**Average Maximum Load (kN)**	**Average compressive Strength (MPa)**	**Std. dev.**
			Test 1	Test 2	Test 3	Test 1	Test 2	Test 3			
0%	0%	14	2.97	3.59	3.31	0.35	0.43	0.39	3.29	0.39	0.04
5%	0%	14	4.82	4.57	4.82	0.57	0.54	0.57	4.74	0.56	0.02
5%	25%	14	6.17	5.49	3.76	0.73	0.65	0.45	5.14	0.61	0.15
5%	50%	14	3.67	3.14	3.53	0.44	0.37	0.42	3.45	0.41	0.03
5%	75%	14	0.33	2.72	3.34	0.04	0.32	0.40	2.13	0.25	0.19
10%	0%	14	19.87	20.49	21.02	2.36	2.43	2.49	20.46	2.43	0.07
10%	25%	14	18.64	17.91	19.34	2.21	2.13	2.29	18.63	2.21	0.08
10%	50%	14	6.70	7.32	5.30	0.79	0.87	0.63	6.44	0.76	0.12
10%	75%	14	2.11	3.36	2.66	0.25	0.40	0.32	2.71	0.32	0.07
15%	0%	14	33.55	23.54	35.73	3.98	2.79	4.24	30.94	3.67	0.77
15%	25%	14	29.51	24.02	27.58	3.50	2.85	3.27	27.04	3.21	0.33
15%	50%	14	17.08	22.73	20.68	2.03	2.70	2.45	20.16	2.39	0.34
15%	75%	14	6.31	6.05	5.75	0.75	0.72	0.68	6.04	0.72	0.03

Appendix VII.b: Compressive Strength Results of Murrum Stabilized Blocks after a Curing Period of 28 Days

Binder Content (%)	Replacement Rate (%)	Curing Time (days)	Maximum Load (kN)			Compressive Strength (MPa)			Average Maximum Load (kN)	Average Compressive Strength (MPa)	Std. dev.
			Test 1	Test 2	Test 2	Test 1	Test 2	Test 3			
0%	0%	28	0.72	2.16	1.76	0.09	0.26	0.21	1.54	0.18	0.09
5%	0%	28	7.04	6.28	6.42	0.83	0.74	0.76	6.58	0.78	0.05
5%	25%	28	7.60	6.75	8.66	0.90	0.80	1.03	7.67	0.91	0.11
5%	50%	28	6.19	6.87	6.49	0.74	0.81	0.77	6.52	0.77	0.04
5%	75%	28	3.25	3.64	3.84	0.39	0.43	0.46	3.58	0.42	0.04
10%	0%	28	21.55	21.08	24.75	2.56	2.50	2.94	22.46	2.67	0.24
10%	25%	28	27.21	26.23	25.11	3.23	3.11	2.98	26.19	3.11	0.12
10%	50%	28	9.42	9.02	8.52	1.12	1.07	1.01	8.99	1.07	0.05
10%	75%	28	4.48	3.22	3.46	0.53	0.38	0.41	3.72	0.44	0.08
15%	0%	28	38.52	36.77	36.47	4.57	4.36	4.33	37.25	4.42	0.13
15%	25%	28	38.03	37.08	34.67	4.51	4.40	4.11	36.59	4.34	0.21
15%	50%	28	27.55	28.65	29.12	3.27	3.40	3.46	28.44	3.37	0.10
15%	75%	28	6.33	6.64	6.59	0.75	0.79	0.78	6.52	0.77	0.02

Appendix VII.c: Compressive Strength Results of Black Cotton Stabilized Blocks after a Curing Period of 14 Days

Binder Content (%)	Replacement Rate (%)	Curing Time (days)	Maximum Load (kN)			Compressive Strength (MPa)			Average Maximum Load (kN)	Average Compressive Strength (MPa)	Std. dev.
			Test 1	Test 2	Test 3	Test 1	Test 2	Test 3			
0%	0%	14	2.51	2.31	2.66	0.30	0.27	0.32	2.49	0.30	0.02
5%	0%	14	5.24	4.71	5.27	0.62	0.56	0.63	5.07	0.60	0.04
5%	25%	14	4.91	5.89	8.24	0.58	0.70	0.98	6.34	0.75	0.20
5%	50%	14	5.45	8.00	7.04	0.65	0.95	0.83	6.83	0.81	0.15
5%	75%	14	2.31	2.78	2.75	0.27	0.33	0.33	2.61	0.31	0.03
10%	0%	14	10.29	11.80	9.50	1.22	1.40	1.13	10.53	1.25	0.14
10%	25%	14	9.06	7.22	7.79	1.08	0.86	0.92	8.03	0.95	0.11
10%	50%	14	4.49	4.51	4.54	0.53	0.54	0.54	4.52	0.54	0.00
10%	75%	14	5.33	4.85	3.70	0.63	0.58	0.44	4.62	0.55	0.10
15%	0%	14	14.88	14.13	15.41	1.77	1.68	1.83	14.81	1.76	0.08
15%	25%	14	13.34	13.90	14.71	1.58	1.65	1.75	13.98	1.66	0.08
15%	50%	14	12.39	11.30	12.30	1.47	1.34	1.46	12.00	1.42	0.07
15%	75%	14	4.40	5.70	0.39	0.52	0.68	0.05	3.50	0.41	0.33

Appendix VII.d: Compressive Strength Results of Black Cotton Stabilized Blocks after a Curing Period of 14 Days

Binder Content (%)	Replacement Rate (%)	Curing Time (d)	Maximum Load (kN)			Compressive Strength (MPa)			Average Load (kN)	Average Compressive Strength (MPa)	Std. dev.
			Test 1	Test 2	Test 3	Test 1	Test 2	Test 3			
0%	0%	28	2.21	2.52	3.90	0.26	0.30	0.46	2.88	0.34	0.11
5%	0%	28	6.56	5.83	6.00	0.78	0.69	0.71	6.13	0.73	0.05
5%	25%	28	3.81	5.72	8.21	0.45	0.68	0.97	5.91	0.70	0.26
5%	50%	28	8.16	6.36	7.75	0.97	0.75	0.92	7.42	0.88	0.11
5%	75%	28	3.17	3.06	3.28	0.38	0.36	0.39	3.17	0.38	0.01
10%	0%	28	12.02	11.21	10.45	1.43	1.33	1.24	11.23	1.33	0.09
10%	25%	28	9.08	10.73	11.77	1.08	1.27	1.40	10.53	1.25	0.16
10%	50%	28	6.05	5.21	5.21	0.72	0.62	0.62	5.49	0.65	0.06
10%	75%	28	5.16	5.97	4.71	0.61	0.71	0.56	5.28	0.63	0.08
15%	0%	28	16.84	21.53	20.94	2.00	2.55	2.48	19.77	2.35	0.30
15%	25%	28	15.05	15.19	16.14	1.79	1.80	1.92	15.46	1.83	0.07
15%	50%	28	9.95	12.11	11.88	1.18	1.44	1.41	11.31	1.34	0.14
15%	75%	28	6.17	5.75	5.89	0.73	0.68	0.70	5.93	0.70	0.03

Appendix VIII: ANOVA Results of the Stabilization Experiments

Appendix VIII.a: Analysis of Variance for Compressive Strength Results of Stabilized Rammed Earth

	Df	Sum Sq	Mean Sq	F value	Pr(>F)	
stype	1	17.72	17.72	240.678	< 2e-16	***
ctime	1	3.32	3.32	45.118	7.44e-10	***
bcontent	1	56.27	56.27	764.274	< 2e-16	***
rrate	3	44.43	14.81	201.130	< 2e-16	***
stype:ctime	1	0.89	0.89	12.109	0.00071	***
stype:bcontent	1	13.18	13.18	178.991	< 2e-16	***
stype:rrate	3	8.44	2.81	38.217	< 2e-16	***
ctime:bcontent	1	0.65	0.65	8.800	0.00366	**
ctime:rrate	3	0.50	0.17	2.246	0.08668	.
bcontent:rrate	3	14.76	4.92	66.812	< 2e-16	***
stype:ctime:bcontent	1	0.11	0.11	1.557	0.21459	
stype:ctime:rrate	3	0.66	0.22	2.983	0.03425	*
ctime:bcontent:rrate	3	0.23	0.08	1.040	0.37769	
stype:ctime:bcontent:rrate	3	3.53	1.18	15.990	9.38e-09	***
Residuals	115	8.47	0.07			

Signif. codes: 0 ‘***’ 0.001 ‘**’ 0.01 ‘*’ 0.05 ‘.’ 0.1 ‘ ’ 1

Appendix VIII.b: Analysis of Variance for Water Absorption Results of Stabilized Rammed Earth

	Df	Sum Sq	Mean Sq	F value	Pr(>F)	
stype	1	4255	4255	287.570	< 2e-16	***
ctime	1	109	109	7.373	0.006836	**
bcontent	1	12846	12846	868.239	< 2e-16	***
rrate	3	4996	1665	112.557	< 2e-16	***
mtime	1	52034	52034	3516.869	< 2e-16	***
stype:ctime	1	36	36	2.458	0.117516	
stype:bcontent	1	99	99	6.712	0.009838	**
stype:rrate	3	4252	1417	95.798	< 2e-16	***
stype:mtime	1	93	93	6.299	0.012379	*
ctime:bcontent	1	13	13	0.855	0.355692	
ctime:rrate	3	99	33	2.230	0.083798	.
ctime:mtime	1	45	45	3.056	0.081013	.
bcontent:rrate	3	1006	335	22.661	8.09e-14	***
bcontent:mtime	1	200	200	13.502	0.000262	***
rrate:mtime	3	629	210	14.181	6.66e-09	***
stype:ctime:bcontent	1	31	31	2.116	0.146310	
stype:ctime:rrate	3	77	26	1.737	0.158362	
stype:ctime:mtime	1	0	0	0.012	0.913075	
ctime:bcontent:rrate	3	113	38	2.553	0.054732	.
ctime:bcontent:mtime	1	6	6	0.380	0.537994	
bcontent:rrate:mtime	3	78	26	1.749	0.155879	
stype:ctime:bcontent:rrate	3	1090	363	24.559	6.79e-15	***
stype:ctime:bcontent:mtime	1	52	52	3.488	0.062356	.
ctime:bcontent:rrate:mtime	3	65	22	1.464	0.223469	
Residuals	531	7856	15			

Signif. codes: 0 ‘***’ 0.001 ‘**’ 0.01 ‘*’ 0.05 ‘.’ 0.1 ‘ ’ 1